Heliyon 8 (2022) e10612

Contents lists available at ScienceDirect

Heliyon

journal homepage: www.cell.com/heliyon

Research article

Analysis of the role of m6A and lncRNAs in prognosis and immunotherapy of hepatocellular carcinoma

Yan Xu, Rong Liu *

Department of Hepatopancreatobiliary Surgical Oncology, Chinese People's Liberation Army (PLA) General Hospital, Beijing, 100853, China

ARTICLE INFO

Keywords:
NRAV
AL031985.3
Hepatocellular carcinoma
Risk score
m6A
Immune function

ABSTRACT

Objective: To study the role of m6A and lncRNAs in the prognosis and immunotherapy of hepatocellular carcinoma, construct the risk score of overall survival of hepatocellular carcinoma, and search for new therapeutic targets and drugs.

Methods: The data used in this study are obtained from The Cancer Genome Atlas (TCGA) database. A total of 424 HCC samples were included. The co-expression of lncRNAs and M6A-related genes in HCC was analyzed, COX regression analysis was conducted to construct the risk score for HCC prognosis, and the model's validity was further verified in different clinical trials subtypes and principal component analysis. GO enrichment analysis and immune function analysis were performed for the differential genes in the high-risk group and the low-risk group divided by risk score and analyzed the prognostic effect of TMB on the two groups. Based on the results, potential therapeutic agents for HCC were screened.

Results: The risk score can better predict the prognosis of HCC, the area under the ROC curve is 0.727. Differential genes were mainly located in the extracellular matrix and chromosomal regions and may play regulatory roles in binding sites and catalytic enzymes, thereby affecting the chromosome division and cell proliferation of cells. Type II IFN response, type I IFN response and MHC class I were the three most different functions in terms of immune function between the high-risk group and the low-risk group. Type II IFN response, type I IFN response was significantly down-regulated in the high-risk group, while MHC class I was up-regulated. 14 potential therapeutic drugs were screened out.

Conclusions: The risk score constructed with NRAV and AL031985.3 had a good predictive effect on the prognosis of HCC. Differences in genes and immune function between high-risk and low-risk groups promoted the occurrence and progression of HCC.

1. Introduction

Hepatocellular carcinoma (HCC) is one of the most common cancers in the world and the second leading cause of cancer-related deaths [1]. There are approximately 841,000 new cases and 782,000 deaths of HCC each year [2]. There are many methods to treat HCC, including surgery, radiofrequency ablation, transarterial chemoembolization (TACE), hepatic arterial infusion chemotherapy (HAIC), and drug therapy [3, 4, 5]. But the current treatment results of these methods are not satisfactory. The 3-year survival rate of HCC was only 12.7% and the median survival was 9 months [6].

Sorafenib is the first targeted drug used in the treatment of advanced HCC. It is a blocker of vascular endothelial growth factor receptors (VEGFRs). Although Sorafenib was established as a first-line drug for advanced HCC in 2017, it only prolonged the median overall survival of patients by 2.8 months [7]. After sorafenib, there are many clinical trials aimed at the treatment of advanced liver cancer, including Sunitinib [8], Brivanib [9], Linifanib [10], Lenvatinib [11]. It is worth noting that even lenvatinib (which has been approved for advanced HCC) did not show an advantage in the efficacy comparison with sorafenib [12]. Therefore, we need to develop better therapeutic targets and drugs for HCC.

N6-methyladenosine (m6A) is the most extensive and abundant transcription modification among eukaryotic messenger RNAs (mRNAs) [13], microRNAs (miRNAs) [14], and long non-coding RNAs (lncRNAs) [15]. M6A is mainly divided into three parts: “writers”, “erasers”, and “readers”. The main role of “writers” is to catalyze the production of m6A, including Methyltransferase-like 3 (METTL3) [16],

* Corresponding author.
E-mail address: liurong@301hospital.com.cn (R. Liu).

https://doi.org/10.1016/j.heliyon.2022.e10612
Received 16 January 2022; Received in revised form 14 May 2022; Accepted 7 September 2022

Table 1. Co-expression of m6A and lncRNA.

m6A	lncRNA	Cor	pvalue	Regulation
YTHDF2	AL031985.3	0.51148	2.54E-26	positive
YTHDF1	NORAD	0.550622	4.93E-31	positive
YTHDF1	AC091057.1	0.547303	1.31E-30	positive
YTHDF1	PTOV1-AS1	0.531677	1.12E-28	positive
YTHDF1	AC125257.1	0.526077	5.24E-28	positive
YTHDF1	AL035461.2	0.525615	5.94E-28	positive
YTHDF1	RNF216P1	0.523227	1.13E-27	positive
YTHDF1	AC099850.3	0.522158	1.51E-27	positive
YTHDF1	LINC00205	0.521027	2.05E-27	positive
YTHDF1	HCG18	0.519164	3.37E-27	positive
YTHDF1	AC093227.1	0.517472	5.28E-27	positive
YTHDF1	AL078644.1	0.5164	7.02E-27	positive
YTHDF1	BACE1-AS	0.514815	1.06E-26	positive
YTHDF1	SREBF2-AS1	0.514512	1.15E-26	positive
YTHDF1	WAC-AS1	0.508586	5.37E-26	positive
YTHDF1	AC005288.1	0.505018	1.34E-25	positive
YTHDF1	AC145207.5	0.504318	1.60E-25	positive
YTHDF1	MCM3AP-AS1	0.50412	1.68E-25	positive
YTHDF1	NRAV	0.500804	3.87E-25	positive
YTHDF1	SNHG1	0.500649	4.03E-25	positive
YTHDF1	AC102953.2	0.500525	4.15E-25	positive
YTHDC2	AC005288.1	0.594952	3.52E-37	positive
YTHDC2	PAXIP1-AS2	0.590209	1.78E-36	positive
YTHDC2	Z68871.1	0.590141	1.82E-36	positive
YTHDC2	EBLN3P	0.589931	1.96E-36	positive
YTHDC2	AC008906.1	0.560293	2.69E-32	positive
YTHDC2	AC005034.5	0.558154	5.16E-32	positive
YTHDC2	FGD5-AS1	0.539001	1.43E-29	positive
YTHDC2	AC108010.1	0.537957	1.93E-29	positive
YTHDC2	AC024075.1	0.535953	3.40E-29	positive
YTHDC2	AC104532.2	0.527398	3.65E-28	positive
YTHDC2	AC025917.1	0.525789	5.67E-28	positive
YTHDC2	AC073046.1	0.523695	1.00E-27	positive
YTHDC2	OIP5-AS1	0.523133	1.16E-27	positive
YTHDC2	AC010834.3	0.514932	1.03E-26	positive
YTHDC2	AL109614.1	0.51457	1.14E-26	positive
YTHDC2	LINC00630	0.510046	3.69E-26	positive
YTHDC2	AC021078.1	0.509839	3.89E-26	positive
YTHDC2	Z83843.1	0.508917	4.93E-26	positive
YTHDC2	AL031846.2	0.501408	3.33E-25	positive
YTHDC1	AC005288.1	0.742167	1.25E-66	positive
YTHDC1	AC007406.4	0.722877	1.09E-61	positive
YTHDC1	AC010834.3	0.6921	1.28E-54	positive
YTHDC1	LINC00630	0.683689	7.69E-53	positive
YTHDC1	ZNF32-AS2	0.664701	4.91E-49	positive
YTHDC1	EBLN3P	0.656172	2.05E-47	positive
YTHDC1	FAM111A-DT	0.643089	4.96E-45	positive
YTHDC1	ANKRD10-IT1	0.642009	7.71E-45	positive
YTHDC1	LINC02035	0.636429	7.33E-44	positive
YTHDC1	CR936218.1	0.631009	6.26E-43	positive
YTHDC1	THAP9-AS1	0.625603	5.09E-42	positive
YTHDC1	MCM3AP-AS1	0.625419	5.46E-42	positive
YTHDC1	LINC01560	0.621005	2.93E-41	positive
YTHDC1	AL031714.1	0.62024	3.91E-41	positive
YTHDC1	FGD5-AS1	0.618292	8.13E-41	positive
YTHDC1	AL157392.3	0.617146	1.25E-40	positive
YTHDC1	EIF3J-DT	0.615715	2.12E-40	positive
YTHDC1	ABALON	0.615207	2.56E-40	positive
YTHDC1	AC004771.2	0.611763	9.08E-40	positive

Table 1 (*continued*)

m6A	lncRNA	Cor	pvalue	Regulation
YTHDC1	AC073046.1	0.605194	9.73E-39	positive
YTHDC1	HCG18	0.601879	3.15E-38	positive
YTHDC1	AC093227.1	0.600514	5.10E-38	positive
YTHDC1	AC091057.1	0.599273	7.87E-38	positive
YTHDC1	AC037459.2	0.598336	1.09E-37	positive
YTHDC1	WARS2-AS1	0.595721	2.70E-37	positive
YTHDC1	AC009120.3	0.595252	3.18E-37	positive
YTHDC1	LINC00909	0.594674	3.88E-37	positive
YTHDC1	NORAD	0.594225	4.52E-37	positive
YTHDC1	AC129510.1	0.592677	7.69E-37	positive
YTHDC1	AC109460.2	0.591656	1.09E-36	positive
YTHDC1	AC091185.1	0.588817	2.85E-36	positive
YTHDC1	AC008124.1	0.588412	3.26E-36	positive
YTHDC1	LINC00265	0.586132	7.01E-36	positive
YTHDC1	Z68871.1	0.580921	3.93E-35	positive
YTHDC1	AL132989.1	0.578257	9.37E-35	positive
YTHDC1	PSMA3-AS1	0.575882	2.02E-34	positive
YTHDC1	AL133355.1	0.570903	9.92E-34	positive
YTHDC1	AC092614.1	0.569092	1.76E-33	positive
YTHDC1	AC092910.3	0.568975	1.82E-33	positive
YTHDC1	AP005899.1	0.566982	3.41E-33	positive
YTHDC1	C2orf49-DT	0.566697	3.72E-33	positive
YTHDC1	TAPT1-AS1	0.560589	2.46E-32	positive
YTHDC1	LENG8-AS1	0.560318	2.67E-32	positive
YTHDC1	AC138028.4	0.559864	3.07E-32	positive
YTHDC1	MIR4453HG	0.557289	6.71E-32	positive
YTHDC1	AC112220.2	0.557286	6.72E-32	positive
YTHDC1	ZEB1-AS1	0.556724	7.96E-32	positive
YTHDC1	CTBP1-DT	0.5535	2.10E-31	positive
YTHDC1	NFYC-AS1	0.552178	3.11E-31	positive
YTHDC1	AC004067.1	0.551588	3.70E-31	positive
YTHDC1	UBA6-AS1	0.550578	4.99E-31	positive
YTHDC1	INE1	0.548871	8.26E-31	positive
YTHDC1	NRAV	0.54811	1.03E-30	positive
YTHDC1	UBE2Q1-AS1	0.547881	1.10E-30	positive
YTHDC1	AC106037.2	0.54751	1.23E-30	positive
YTHDC1	AF131215.5	0.546567	1.62E-30	positive
YTHDC1	LINC00641	0.545955	1.94E-30	positive
YTHDC1	MAP3K14-AS1	0.543844	3.58E-30	positive
YTHDC1	AC008969.1	0.543399	4.07E-30	positive
YTHDC1	AC107027.3	0.542611	5.10E-30	positive
YTHDC1	AC008760.1	0.539962	1.09E-29	positive
YTHDC1	AC005104.1	0.539632	1.20E-29	positive
YTHDC1	AC096586.2	0.53862	1.60E-29	positive
YTHDC1	HMGN3-AS1	0.537345	2.29E-29	positive
YTHDC1	ASH1L-AS1	0.537236	2.37E-29	positive
YTHDC1	SEC24B-AS1	0.536885	2.61E-29	positive
YTHDC1	AC004076.2	0.535602	3.75E-29	positive
YTHDC1	AL031670.1	0.534471	5.15E-29	positive
YTHDC1	OIP5-AS1	0.533589	6.59E-29	positive
YTHDC1	AL078644.1	0.533381	6.99E-29	positive
YTHDC1	AC005253.1	0.530689	1.48E-28	positive
YTHDC1	AC022150.2	0.530433	1.58E-28	positive
YTHDC1	AP003392.1	0.529425	2.09E-28	positive
YTHDC1	AC087289.5	0.528915	2.41E-28	positive
YTHDC1	FBXL19-AS1	0.528801	2.49E-28	positive
YTHDC1	TRAPPC12-AS1	0.527675	3.39E-28	positive
YTHDC1	XPC-AS1	0.525204	6.64E-28	positive
YTHDC1	AC026412.3	0.52382	9.67E-28	positive

(*continued on next page*)

Table 1 (*continued*)

m6A	lncRNA	Cor	pvalue	Regulation
YTHDC1	PKD1P6-NPIPP1	0.52277	1.28E-27	positive
YTHDC1	AL049840.4	0.5219	1.62E-27	positive
YTHDC1	LINC01521	0.520677	2.25E-27	positive
YTHDC1	AL049840.3	0.520507	2.36E-27	positive
YTHDC1	LINC00342	0.520418	2.41E-27	positive
YTHDC1	AP001469.2	0.518913	3.60E-27	positive
YTHDC1	AC232271.1	0.51881	3.70E-27	positive
YTHDC1	WAC-AS1	0.518746	3.77E-27	positive
YTHDC1	AC004596.1	0.518099	4.48E-27	positive
YTHDC1	N4BP2L2-IT2	0.516555	6.73E-27	positive
YTHDC1	AC108010.1	0.51638	7.05E-27	positive
YTHDC1	ADNP-AS1	0.516281	7.24E-27	positive
YTHDC1	PTOV1-AS1	0.51493	1.03E-26	positive
YTHDC1	AL031282.2	0.514642	1.11E-26	positive
YTHDC1	AL355102.4	0.514274	1.23E-26	positive
YTHDC1	AC004908.1	0.514027	1.31E-26	positive
YTHDC1	AC015849.3	0.510056	3.68E-26	positive
YTHDC1	KANSL1L-AS1	0.509829	3.90E-26	positive
YTHDC1	AC245060.2	0.507945	6.33E-26	positive
YTHDC1	NIFK-AS1	0.507335	7.40E-26	positive
YTHDC1	CTBP1-AS	0.506378	9.46E-26	positive
YTHDC1	THBS3-AS1	0.504239	1.63E-25	positive
YTHDC1	LAMC1-AS1	0.503713	1.86E-25	positive
YTHDC1	AC067852.3	0.503548	1.94E-25	positive
YTHDC1	AC099850.3	0.502613	2.46E-25	positive
YTHDC1	AC127024.4	0.502497	2.53E-25	positive
YTHDC1	AC114956.2	0.501877	2.96E-25	positive
YTHDC1	AC025287.3	0.501436	3.30E-25	positive
WTAP	AC026356.1	0.582071	2.69E-35	positive
WTAP	TRAF3IP2-AS1	0.569147	1.73E-33	positive
WTAP	AC099850.3	0.554761	1.44E-31	positive
WTAP	AC091057.1	0.527277	3.78E-28	positive
WTAP	AL031714.1	0.521811	1.66E-27	positive
VIRMA	OTUD6B-AS1	0.645582	1.78E-45	positive
VIRMA	UBR5-AS1	0.586982	5.27E-36	positive
VIRMA	AF117829.1	0.53939	1.28E-29	positive
VIRMA	AC064807.1	0.511552	2.50E-26	positive
RBMX	HCG18	0.698662	4.73E-56	positive
RBMX	AC091057.1	0.668986	7.20E-50	positive
RBMX	AC099850.3	0.66859	8.61E-50	positive
RBMX	PTOV1-AS1	0.611412	1.03E-39	positive
RBMX	AC007406.4	0.602737	2.33E-38	positive
RBMX	LINC00630	0.595027	3.43E-37	positive
RBMX	MCM3AP-AS1	0.593656	5.50E-37	positive
RBMX	SNHG1	0.589773	2.06E-36	positive
RBMX	WAC-AS1	0.586376	6.46E-36	positive
RBMX	AC005288.1	0.584444	1.23E-35	positive
RBMX	LINC00909	0.582578	2.28E-35	positive
RBMX	TRAF3IP2-AS1	0.579985	5.34E-35	positive
RBMX	NIFK-AS1	0.57686	1.47E-34	positive
RBMX	ASH1L-AS1	0.572963	5.15E-34	positive
RBMX	ZNF32-AS2	0.572703	5.60E-34	positive
RBMX	AC093227.1	0.570616	1.09E-33	positive
RBMX	WARS2-AS1	0.568393	2.19E-33	positive
RBMX	EIF3J-DT	0.566846	3.55E-33	positive
RBMX	AL078644.1	0.562215	1.49E-32	positive
RBMX	NRAV	0.560055	2.90E-32	positive
RBMX	DNAJC9-AS1	0.559791	3.14E-32	positive
RBMX	LINC00205	0.558976	4.02E-32	positive
RBMX	MIR600HG	0.54688	1.48E-30	positive

Table 1 (*continued*)

m6A	lncRNA	Cor	pvalue	Regulation
RBMX	NUTM2A-AS1	0.546598	1.61E-30	positive
RBMX	LINC02035	0.545136	2.46E-30	positive
RBMX	LENG8-AS1	0.545093	2.49E-30	positive
RBMX	LINC00641	0.539012	1.43E-29	positive
RBMX	AC025176.1	0.536152	3.21E-29	positive
RBMX	SBF2-AS1	0.534498	5.11E-29	positive
RBMX	LINC00665	0.532905	7.98E-29	positive
RBMX	AC107027.3	0.531993	1.03E-28	positive
RBMX	FAM111A-DT	0.530129	1.72E-28	positive
RBMX	AL050341.2	0.529013	2.34E-28	positive
RBMX	AL157392.3	0.526427	4.76E-28	positive
RBMX	AC004076.2	0.525023	6.98E-28	positive
RBMX	AL008729.1	0.524459	8.13E-28	positive
RBMX	SNHG32	0.523448	1.07E-27	positive
RBMX	AL592148.3	0.518266	4.28E-27	positive
RBMX	DDX11-AS1	0.51823	4.32E-27	positive
RBMX	TMEM147-AS1	0.517423	5.35E-27	positive
RBMX	AC008969.1	0.515879	8.05E-27	positive
RBMX	AC007066.2	0.514552	1.14E-26	positive
RBMX	AC232271.1	0.514447	1.17E-26	positive
RBMX	AC099850.1	0.512819	1.79E-26	positive
RBMX	PSMA3-AS1	0.509336	4.43E-26	positive
RBMX	AL356481.1	0.509116	4.69E-26	positive
RBMX	AC127024.5	0.508843	5.03E-26	positive
RBMX	SNHG4	0.508719	5.19E-26	positive
RBMX	TMCO1-AS1	0.507927	6.36E-26	positive
RBMX	LINC01560	0.507793	6.58E-26	positive
RBMX	ZNF529-AS1	0.507117	7.83E-26	positive
RBMX	SEC24B-AS1	0.505458	1.20E-25	positive
RBMX	AC125257.1	0.505072	1.32E-25	positive
RBMX	CAPN10-DT	0.50388	1.78E-25	positive
RBMX	AL121772.3	0.50385	1.80E-25	positive
RBMX	AP000873.1	0.503369	2.03E-25	positive
RBMX	SNHG20	0.502945	2.26E-25	positive
RBMX	LINC00653	0.502135	2.77E-25	positive
RBMX	AC018690.1	0.500309	4.38E-25	positive
RBM15B	AC091057.1	0.560355	2.64E-32	positive
RBM15B	FGD5-AS1	0.553376	2.17E-31	positive
RBM15B	HCG18	0.552725	2.64E-31	positive
RBM15B	BACE1-AS	0.546771	1.53E-30	positive
RBM15B	LINC00205	0.540933	8.26E-30	positive
RBM15B	AC099850.3	0.530714	1.47E-28	positive
RBM15B	CTBP1-DT	0.530306	1.64E-28	positive
RBM15B	AC125257.1	0.52832	2.84E-28	positive
RBM15B	AC005288.1	0.527695	3.37E-28	positive
RBM15B	SREBF2-AS1	0.522054	1.56E-27	positive
RBM15B	MCM3AP-AS1	0.520187	2.57E-27	positive
RBM15B	PTOV1-AS1	0.519661	2.95E-27	positive
RBM15B	AL078644.1	0.510507	3.27E-26	positive
RBM15B	NRAV	0.50048	4.20E-25	positive
RBM15	AC125257.1	0.505343	1.23E-25	positive
METTL3	AC007406.4	0.574483	3.17E-34	positive
METTL3	TMEM147-AS1	0.573369	4.53E-34	positive
METTL3	LINC00641	0.559358	3.58E-32	positive
METTL3	AC007066.2	0.556181	9.38E-32	positive
METTL3	PTOV1-AS2	0.555605	1.12E-31	positive
METTL3	MCM3AP-AS1	0.552766	2.61E-31	positive
METTL3	AC093227.1	0.542113	5.89E-30	positive
METTL3	PKD1P6-NPIPP1	0.541276	7.49E-30	positive

(*continued on next page*)

Table 1 (*continued*)

m6A	lncRNA	Cor	pvalue	Regulation
METTL3	AL512770.1	0.53459	4.98E-29	positive
METTL3	AC091057.1	0.531741	1.10E-28	positive
METTL3	TRAF3IP2-AS1	0.531243	1.27E-28	positive
METTL3	AC107068.1	0.530405	1.60E-28	positive
METTL3	AC127024.4	0.526424	4.77E-28	positive
METTL3	AC027601.1	0.52485	7.31E-28	positive
METTL3	DNAJC9-AS1	0.522	1.58E-27	positive
METTL3	AC084018.1	0.521196	1.96E-27	positive
METTL3	AL355075.2	0.521169	1.97E-27	positive
METTL3	AL049840.4	0.521	2.07E-27	positive
METTL3	LENG8-AS1	0.520857	2.15E-27	positive
METTL3	AC008735.2	0.51703	5.94E-27	positive
METTL3	AC124045.1	0.511815	2.33E-26	positive
METTL3	AC018690.1	0.511586	2.47E-26	positive
METTL3	HCG18	0.509198	4.59E-26	positive
METTL3	SEMA3F-AS1	0.508958	4.88E-26	positive
METTL3	AL161452.1	0.507631	6.86E-26	positive
METTL3	AL008729.1	0.506437	9.31E-26	positive
METTL3	KDM4A-AS1	0.504539	1.51E-25	positive
METTL3	AL157392.3	0.503974	1.74E-25	positive
METTL3	AL031670.1	0.5036	1.92E-25	positive
METTL3	AC074117.1	0.501311	3.41E-25	positive
METTL3	AC037459.2	0.501077	3.62E-25	positive
METTL3	AC073575.2	0.500937	3.75E-25	positive
METTL3	C2orf49-DT	0.500632	4.04E-25	positive
METTL3	MED8-AS1	0.500274	4.42E-25	positive
METTL16	STARD7-AS1	0.565025	6.27E-33	positive
METTL16	AC020915.1	0.500863	3.82E-25	positive
METTL14	FGD5-AS1	0.534167	5.61E-29	positive
METTL14	EBLN3P	0.521662	1.73E-27	positive
LRPPRC	AC005288.1	0.566461	4.01E-33	positive
LRPPRC	AC092614.1	0.544749	2.75E-30	positive
LRPPRC	MCM3AP-AS1	0.537938	1.94E-29	positive
LRPPRC	HCG18	0.532317	9.40E-29	positive
LRPPRC	AL133243.2	0.51537	9.20E-27	positive
LRPPRC	AC016747.1	0.50876	5.14E-26	positive
LRPPRC	FGD5-AS1	0.5064	9.40E-26	positive
LRPPRC	SNHG16	0.503641	1.90E-25	positive
LRPPRC	AC099850.3	0.50047	4.21E-25	positive
HNRNPC	HCG18	0.627855	2.14E-42	positive
HNRNPC	AC091057.1	0.585151	9.72E-36	positive
HNRNPC	SNHG1	0.564401	7.61E-33	positive
HNRNPC	AC099850.3	0.559551	3.38E-32	positive
HNRNPC	LINC00909	0.554289	1.66E-31	positive
HNRNPC	AC007406.4	0.539936	1.10E-29	positive
HNRNPC	AC005288.1	0.529579	2.01E-28	positive
HNRNPC	LINC00205	0.526993	4.08E-28	positive
HNRNPC	MCM3AP-AS1	0.526508	4.66E-28	positive
HNRNPC	NRAV	0.525897	5.50E-28	positive
HNRNPC	TRAF3IP2-AS1	0.512055	2.19E-26	positive
HNRNPC	LINC00641	0.507041	7.98E-26	positive
HNRNPC	AL078644.1	0.502616	2.46E-25	positive
HNRNPC	PTOV1-AS1	0.502459	2.55E-25	positive
HNRNPC	AC093227.1	0.500813	3.86E-25	positive
HNRNPC	WARS2-AS1	0.500654	4.02E-25	positive
HNRNPA2B1	AC091057.1	0.697174	1.01E-55	positive
HNRNPA2B1	AC099850.3	0.641693	8.77E-45	positive
HNRNPA2B1	MCM3AP-AS1	0.610744	1.32E-39	positive
HNRNPA2B1	TRAF3IP2-AS1	0.5818	2.94E-35	positive
HNRNPA2B1	LINC00205	0.576077	1.90E-34	positive

Table 1 (*continued*)

m6A	lncRNA	Cor	pvalue	Regulation
HNRNPA2B1	AL355488.1	0.571513	8.18E-34	positive
HNRNPA2B1	PTOV1-AS1	0.567864	2.59E-33	positive
HNRNPA2B1	LINC00909	0.565523	5.37E-33	positive
HNRNPA2B1	ZNF32-AS2	0.561768	1.71E-32	positive
HNRNPA2B1	C2orf49-DT	0.559212	3.74E-32	positive
HNRNPA2B1	AC005288.1	0.558661	4.43E-32	positive
HNRNPA2B1	AC007406.4	0.55855	4.58E-32	positive
HNRNPA2B1	HCG18	0.558452	4.72E-32	positive
HNRNPA2B1	NCK1-DT	0.554035	1.79E-31	positive
HNRNPA2B1	AC018690.1	0.547897	1.10E-30	positive
HNRNPA2B1	WARS2-AS1	0.539057	1.41E-29	positive
HNRNPA2B1	LENG8-AS1	0.535455	3.91E-29	positive
HNRNPA2B1	AC025176.1	0.53232	9.39E-29	positive
HNRNPA2B1	LINC00630	0.530991	1.36E-28	positive
HNRNPA2B1	TMCO1-AS1	0.529289	2.17E-28	positive
HNRNPA2B1	SNHG21	0.527344	3.71E-28	positive
HNRNPA2B1	WAC-AS1	0.526861	4.23E-28	positive
HNRNPA2B1	AL050341.2	0.526771	4.33E-28	positive
HNRNPA2B1	SNHG1	0.526728	4.39E-28	positive
HNRNPA2B1	FAM111A-DT	0.52572	5.77E-28	positive
HNRNPA2B1	RNF216P1	0.521357	1.88E-27	positive
HNRNPA2B1	AC125257.1	0.520696	2.24E-27	positive
HNRNPA2B1	AC102953.2	0.520271	2.51E-27	positive
HNRNPA2B1	SNHG4	0.517178	5.71E-27	positive
HNRNPA2B1	CAPN10-DT	0.516675	6.52E-27	positive
HNRNPA2B1	AL031714.1	0.516285	7.23E-27	positive
HNRNPA2B1	DDX11-AS1	0.51562	8.62E-27	positive
HNRNPA2B1	AC093227.1	0.514662	1.11E-26	positive
HNRNPA2B1	AC012467.2	0.513989	1.32E-26	positive
HNRNPA2B1	THAP9-AS1	0.512563	1.92E-26	positive
HNRNPA2B1	ADNP-AS1	0.51172	2.39E-26	positive
HNRNPA2B1	LINC00294	0.5112	2.73E-26	positive
HNRNPA2B1	PTOV1-AS2	0.510187	3.55E-26	positive
HNRNPA2B1	UBE2Q1-AS1	0.508405	5.63E-26	positive
HNRNPA2B1	DLEU2	0.50722	7.63E-26	positive
HNRNPA2B1	AC073842.2	0.506719	8.67E-26	positive
HNRNPA2B1	AP005136.3	0.506053	1.03E-25	positive
HNRNPA2B1	AL031985.3	0.504822	1.41E-25	positive
HNRNPA2B1	AC092910.3	0.500986	3.70E-25	positive
FTO	AC005288.1	0.536076	3.28E-29	positive
FMR1	FMR1-IT1	0.553239	2.27E-31	positive

KIAA1429 [17], METTL14 [18], RBM15/15B [19] and Wilms tumor 1-associated protein (WTAP) [20]. The core function of "erasers" is to remove the methyl code from mRNA, including alkB homologue 5 (ALKBH5) [21] and fat mass and obesity-associated protein (FTO) [22]. "Reader" is responsible for decoding m6A methylation, including nuclear ribonucleoprotein (HNRNP) protein [23], IGF2 mRNA binding proteins (IGF2BP) [24], eukaryotic initiation factor (eIF) 3[25] and YT521-B homology (YTH) domain-containing protein [26]. Studies have found that m6A modification plays an important role in tumor proliferation, differentiation, invasion, and metastasis, and can also be used as a tumor oncogene or anti-oncogene [27, 28, 29]. M6A regulates many aspects of the development of HCC. METTL3 is related to the poor prognosis of HCC patients and promotes the proliferation, migration, and colony formation of HCC cells [30]. In addition, METTL14 is an anti-metastatic factor, and its down-regulation will also promote the progression and metastasis of HCC [31]. Therefore, it is of great significance to study the regulation of m6A in liver cancer, to identify new therapeutic targets and potential therapeutic drugs, and to improve the prognosis of patients with liver cancer.

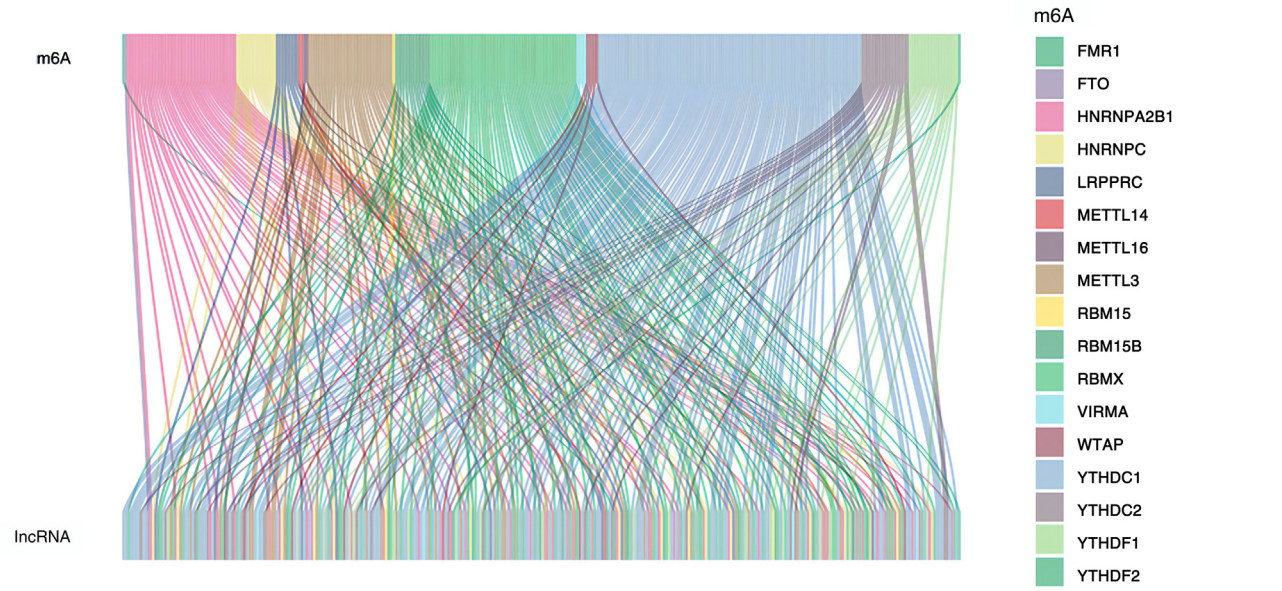

Figure 1. Sankey diagram of m6A and lncRNA. All m6A genes are shown above, and all m6a-related lncRNAs in HCC are shown below. The line indicates that there is the correlation between the two.

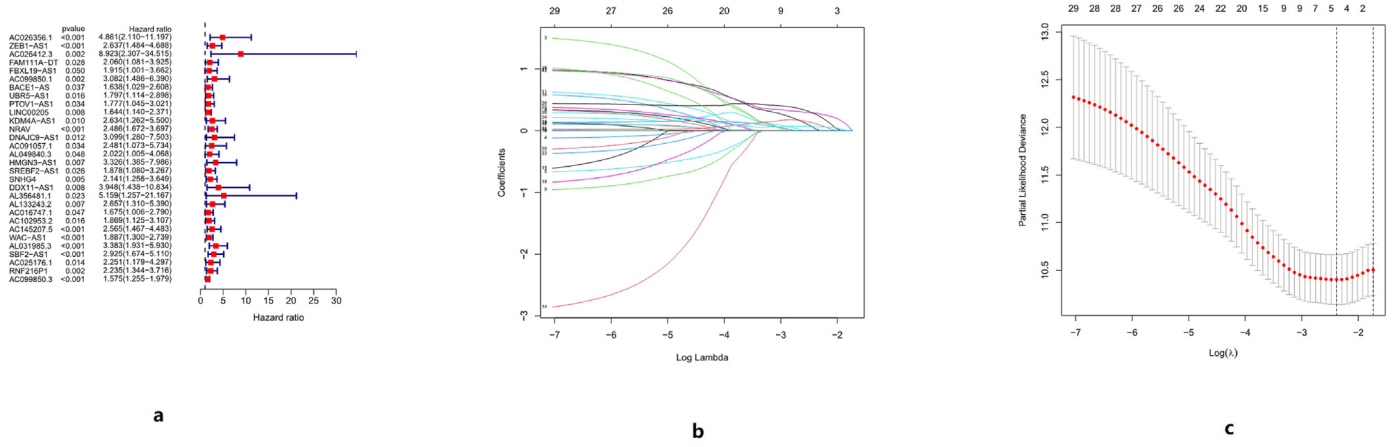

Figure 2. a: COX regression analysis was performed on the influence of m6A-related lncRNAs on HCC. b: Lasso regression of m6A-related lncRNAs. c: Cross-validation results of prediction models.

LncRNAs contain more than 200 nucleotides, interacts with DNA, RNA, or protein, regulate gene expression at the transcription or post-transcription level, and are closely related to the progression of gastric cancer, HCC, and colon cancer [32, 33, 34, 35]. Studies have shown that many lncRNAs, including MIAT [36], CDKN2BAS [37], and PCNAP1 [38], promote the proliferation and invasion of HCC cells, and lncRNA-D16366 can be used as a biological marker for the diagnosis and prognosis of HCC [39]. Therefore, studying the interaction between lncRNA and m6A in the occurrence and development of HCC can further discover its influence on the development of HCC, find potential therapeutic targets and drugs, and improve the prognosis of HCC patients.

2. Methods

2.1. Data of the research

The data used in this study are obtained from The Cancer Genome Atlas (TCGA) database (https://tcga-data.nci.nih.gov/tcga/). A total of 424 HCC samples were included, including 50 normal samples and 374 tumor samples. Clinical data mainly included age, survival status, TMN stage, tumor stage, grade, and gender.

2.2. Co-expression analysis of m6A and lncRNA

mRNAs and lncRNAs were screened from TCGA transcriptome data. Subsequently, m6A gene expression was extracted from transcriptome data. A total of 23 m6A genes were used in this paper. (Writers: METTL3, METTL14, METTL16, WTAP, VIRMA, ZC3H13, RBM15, RBM15B. Readers: YTHDC1, YTHDC2, YTHDF1, YTHDF2, YTHDF3, HNRNPC, FMR1, LRPPRC, HNRNPA2B1, IGFBP1, IGFBP2, IGFBP3, RBMX. Erasers: FTO, ALKBH5.) In the analysis of co-expression of the m6A genes and lncRNAs, the correlation test was adopted. The filter criterion for the correlation coefficient was set as corFilter = 0.4, and the filter criterion for the p-value of the correlation test was set as pvalueFilter = 0.001. Drawing the Sankey diagram based on the co-expression relationship of m6A and lncRNAs.

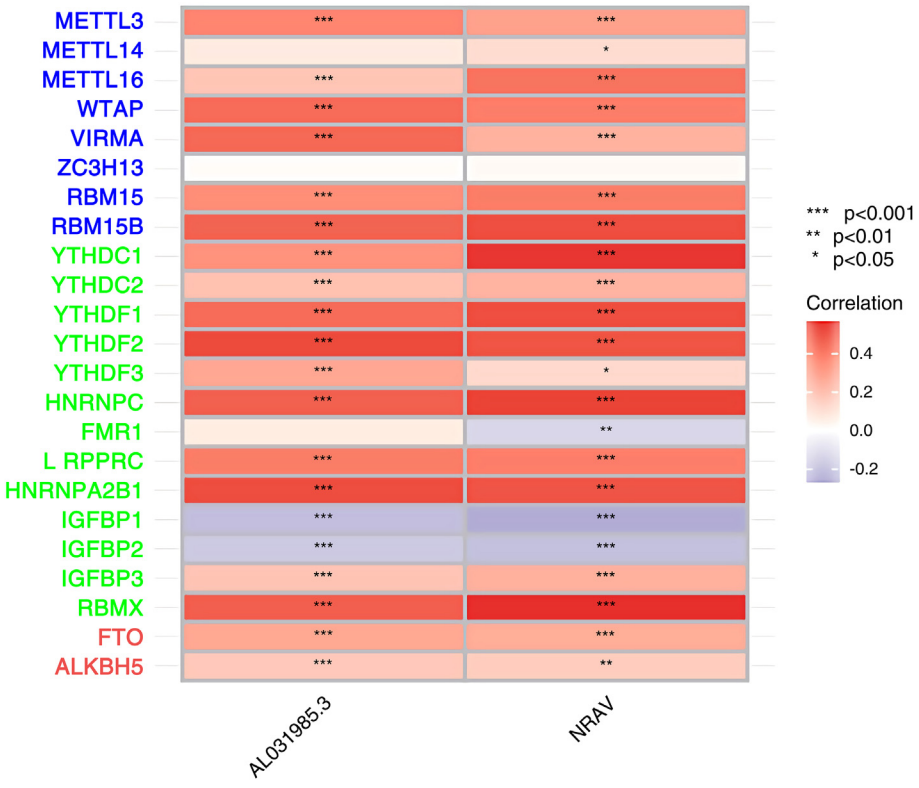

Figure 3. Heatmap of correlations between lncRNAs (NRAV, AL031985.3) and m6A-related genes in HCC. Among the m6A-related genes, blue represents "writers", green represents "Reader", and red represents "erasers". In the correlation heatmap, red represents a positive correlation between lncRNAs and m6A-related genes, and blue represents a negative correlation. The darker the color, the stronger the correlation. "*" means Pvalue < 0.05, "**" means Pvalue < 0.01, "***" means Pvalue < 0.001.

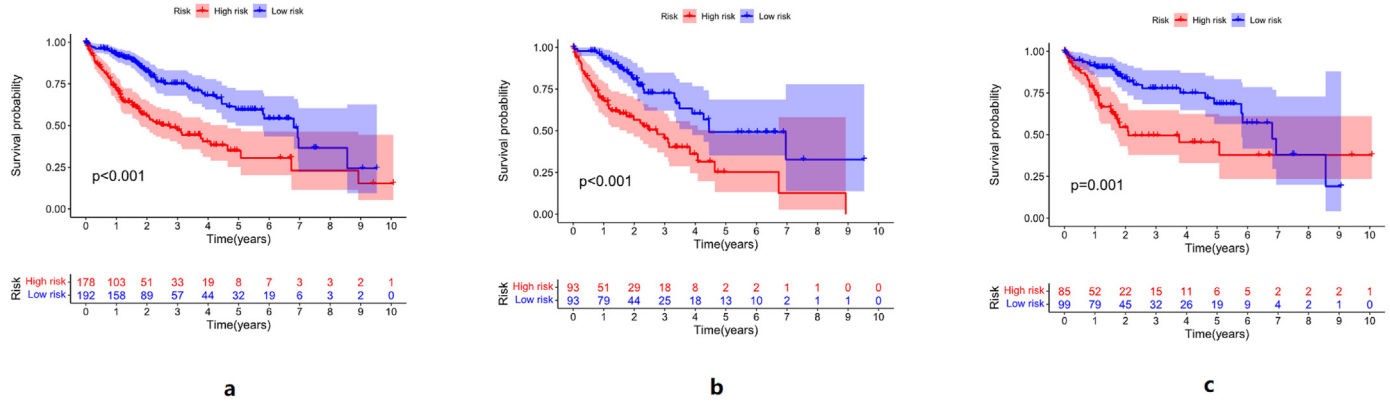

Figure 4. a: the survival curve of the whole sample group, b: the survival curve of the training group, c: the survival curve of the text group. The high-risk group and the low-risk group are divided by the median value of the risk score, with red representing the survival curve of the high-risk group and blue representing the survival curve of the low-risk group. Among the three groups, the high-risk group had a worse prognosis than the low-risk group.

2.3. Construct a prognostic model

Clinical data of the samples were combined with m6A-related lncRNA data, then divided into a training group and test group by 1:1. The training group is used to build the model, and the text group is used to validate the model. Construct predictive models using the "survival", "caret", "glmnet", "survminer", and "timeROC" packages. When constructing the prediction model, univariate COX regression was adopted, coxPfilter was set to 0.05, and then the forest map was drawn. Univariate COX regression was performed for the training group, followed by Lasso regression and cross-validation. Then the COX model is constructed. The text group works the same way as the training group. The samples of the two groups were divided into the high-risk group and the low-risk group with the median risk score as the boundary, and the ROC curves of the high-risk group and the low-risk group were plotted.

Used the "pheatmap" package to draw the risk curve, sorted the samples according to the patient risk score, and then drew the risk curve, survival status map, and risk heat map of the overall sample, the training group, and the text group, respectively. Univariate COX analysis and multivariate COX analysis were performed for the risk score, followed by independent prognostic analysis to obtain the forest map of the risk score. The predictive function of the model was calculated by the area under the ROC curve. The validity of the model was evaluated by the c-index curve. Used the "survival", "regplot", and "rms" packages to draw a nomogram of the risk score.

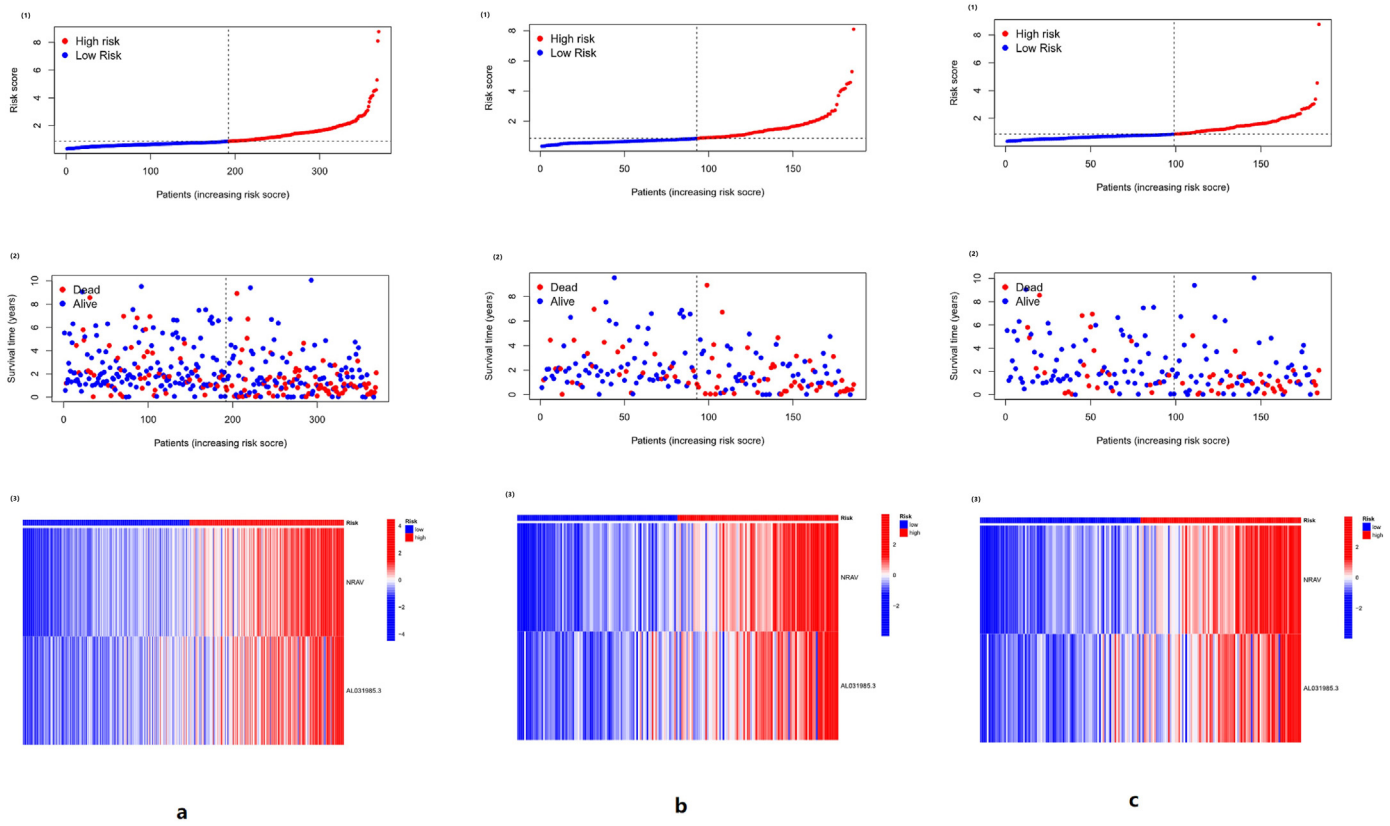

Figure 5. The risk curve of the three groups. In Figures 5a, (1) and (2) are the same in abscissa. They are the samples arranged according to the risk score from small to large, and the ordinate is the risk score of the samples. The patient risk score increases from left to right, with the median risk score dividing patients into high-risk (red) and low-risk (blue) groups. (2) The far point in red represents the death of the patient, the blue represents the survival of the patient, and the ordinate represents the survival time of the patient. As the patient's risk score increases, the number of patients who died increases. (3) Red represents the high expression of lncRNA, and blue represents low expression. In the high-risk group, both NRAV and AL031985.3 were highly expressed. The same trend as Figure 5a can be seen in Figure 5b and Figure 5c. As the risk score increased, the number of deaths increased, and NRAV and AL031985.3 were highly expressed in the high-risk group.

2.4. Model validation for clinical grouping

Used the "survival" and "survminer" packages to plot the survival curves of the high-risk group and the low-risk group in subgroups of age, sex, and tumor stage, respectively, to verify the validity of the risk score.

2.5. Principal component analysis

Principal component analysis was performed using the "limma" and "scatterplot3d" packages, and PCA plots of all gene expression levels, m6A-related gene expression levels, m6A-related lncRNA expression levels, and model-related lncRNA expression levels were plotted.

2.6. Risk differential analysis and GO enrichment analysis

The wilcoxon test was used to analyze the genes that differ between the high-risk and low-risk groups, and the filter conditions were set as logFCfilter = 1 and fdrFilter = 0.05. GO enrichment analysis of differential genes in high-risk group and low-risk group was performed using "clusterProfiler", "org.Hs.eg.db", "enrichplot", "ggplot2", "ggpubr", and "dplyr" packages. (pvalueFilter = 0.05, qvalueFilter = 0.05).

2.7. Immune function analysis

Used "limma", "GSVA", "GSEABase", "pheatmap", and "reshape2" to perform differential analysis of immune function between the high-risk group and low-risk group, and drew a heat map. The mutation dataset of HCC was divided into the high-risk group and low-risk group by risk score, and then drew the waterfall chart of gene mutations in the high-risk group and low-risk group, respectively.

2.8. Tumor mutational burden (TMB)

Get TMB data from the TCGA database and selected the results of varscan for analysis. TMB data for each sample was extracted using Strawberry Perl software. Using the "limma" and "ggpubr" packages in R software to merge TMB data with high-risk group data and low-risk group data, and draw a violin plot. Then use the "survival" and "survminer" packages to draw the survival curves of TMB and TMB combined with the risk score.

2.9. Screening for potential drugs

The "pRRophetic" package was used to predict potential therapeutic drugs for HCC. Combined the data of drug sensitivity with the data of the high-risk group and low-risk group, calculated the IC50 value of the drug in the high-risk group and low-risk group, and then drew the box plot.

3. Statistics

Analysis was performed using R 4.1.2 and Strawberry Perl.

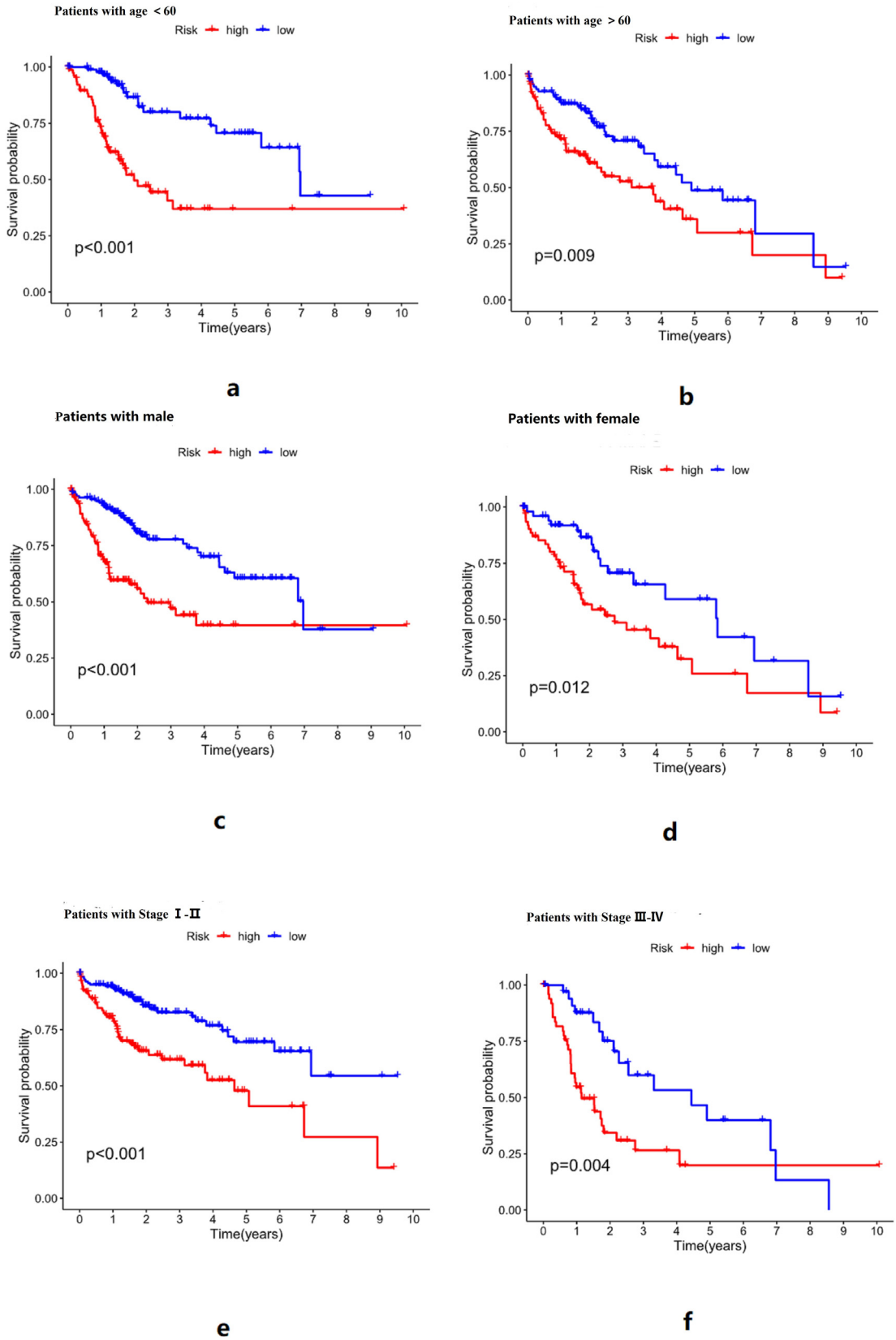

Figure 6. a: Survival curves of the high-risk and low-risk groups in the age group <60 years, b: Survival curves of the high-risk and low-risk groups in the age group > 60 years, c: Survival curves of the high-risk and low-risk groups in the male group, d: Survival curves of the high-risk and low-risk groups in the female group, e: Survival curves of the high-risk and low-risk groups in the stage I-II group, f: Survival curves of the high-risk and low-risk groups in the stage III-IV group. It can be seen from the above survival curve results of different groups that the risk score has a good predictive effect on the survival of HCC patients of different genders, ages, tumor stages, and grades.

Table 2. The comparison of clinical data between train group and text group.

Covariates	Type	Total	Test	Train	Pvalue
Age	≤65	232(62.7%)	116(63.04%)	116(62.37%)	0.9782
Age	>65	138(37.3%)	68(36.96%)	70(37.63%)	
Gender	FEMALE	121(32.7%)	69(37.5%)	52(27.96%)	0.065
Gender	MALE	249(67.3%)	115(62.5%)	134(72.04%)	
Grade	G1	55(14.86%)	21(11.41%)	34(18.28%)	0.3224
Grade	G2	177(47.84%)	91(49.46%)	86(46.24%)	
Grade	G3	121(32.7%)	61(33.15%)	60(32.26%)	
Grade	G4	12(3.24%)	7(3.8%)	5(2.69%)	
Grade	unknown	5(1.35%)	4(2.17%)	1(0.54%)	
Stage	Stage I	171(46.22%)	86(46.74%)	85(45.7%)	0.9747
Stage	Stage II	85(22.97%)	42(22.83%)	43(23.12%)	
Stage	Stage III	85(22.97%)	43(23.37%)	42(22.58%)	
Stage	Stage IV	5(1.35%)	3(1.63%)	2(1.08%)	
Stage	unknown	24(6.49%)	10(5.43%)	14(7.53%)	
T	T1	181(48.92%)	91(49.46%)	90(48.39%)	0.7669
T	T2	93(25.14%)	44(23.91%)	49(26.34%)	
T	T3	80(21.62%)	42(22.83%)	38(20.43%)	
T	T4	13(3.51%)	5(2.72%)	8(4.3%)	
T	unknown	3(0.81%)	2(1.09%)	1(0.54%)	
M	M0	266(71.89%)	136(73.91%)	130(69.89%)	1
M	M1	4(1.08%)	2(1.09%)	2(1.08%)	
M	unknown	100(27.03%)	46(25%)	54(29.03%)	
N	N0	252(68.11%)	124(67.39%)	128(68.82%)	0.6033
N	N1	4(1.08%)	3(1.63%)	1(0.54%)	
N	unknown	114(30.81%)	57(30.98%)	57(30.65%)	

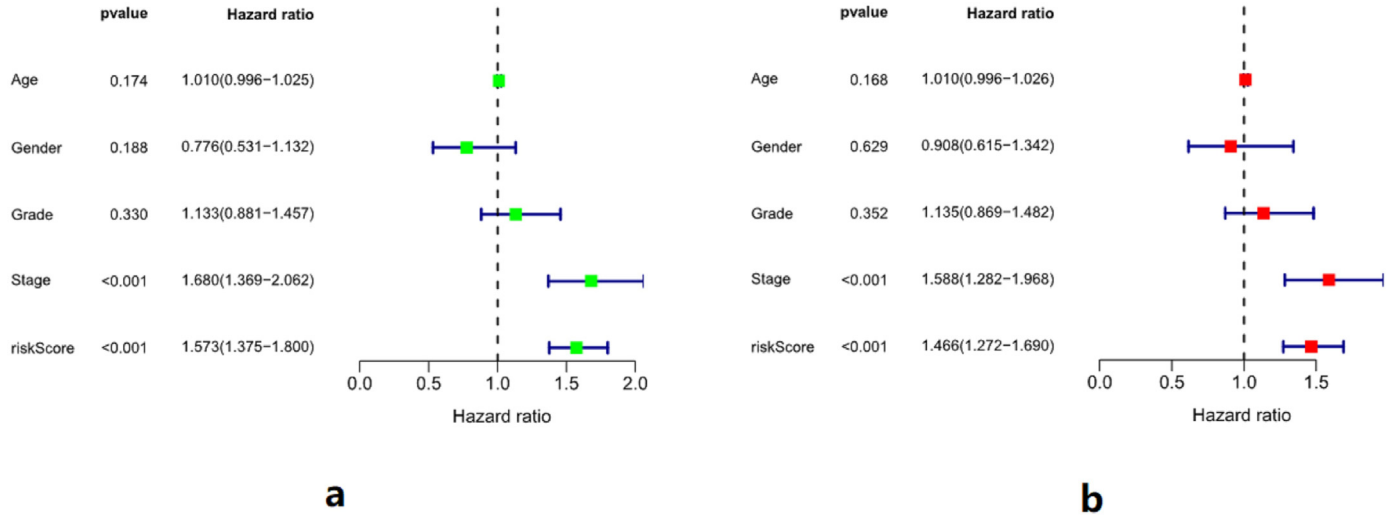

Figure 7. Independent prognostic analysis of risk scores. a: In univariate analysis, Hazard ratio (HR) of the prediction model was 1.573, 95%IC [1.375,1.8], $P < 0.001$. b: In multivariate analysis, HR of the prediction model was 1.466, 95%IC: [1.272,1.169], $P < 0.001$. Therefore, the risk score is an independent predictor of prognosis in HCC patients.

4. Results

4.1. Co-expression analysis of m6A and lncRNA

A total of 424 HCC samples were included, including 50 normal samples and 374 tumor samples. The co-expression of the m6A genes and lncRNAs can be seen in Table 1. LncRNAs were positively regulated by the m6A genes in HCC samples. YTHDC1 is involved in the most extensive regulation of lncRNAs in HCC. The correlation between the m6A genes and lncRNAs can be seen in Figure 1.

4.2. Construct a prognostic model

Cox regression analysis was performed on the m6A-related lncRNA on HCC, and the results were shown in Figure 2. Univariate Cox regression analysis of m6A-related lncRNAs showed that the HR of AL031985.3 was 3.383 [1.931, 5.930], and the HR of NRAV was 2.468, [1.672, 3.697]. After univariate Cox regression-related lncRNAs were incorporated into the prognostic model and optimized, the included lncRNAs were NRAV and AL031985.3. The correlation between m6A-related genes and two lncRNAs was shown in Figure 3. ZC3H13 had no correlation with the two

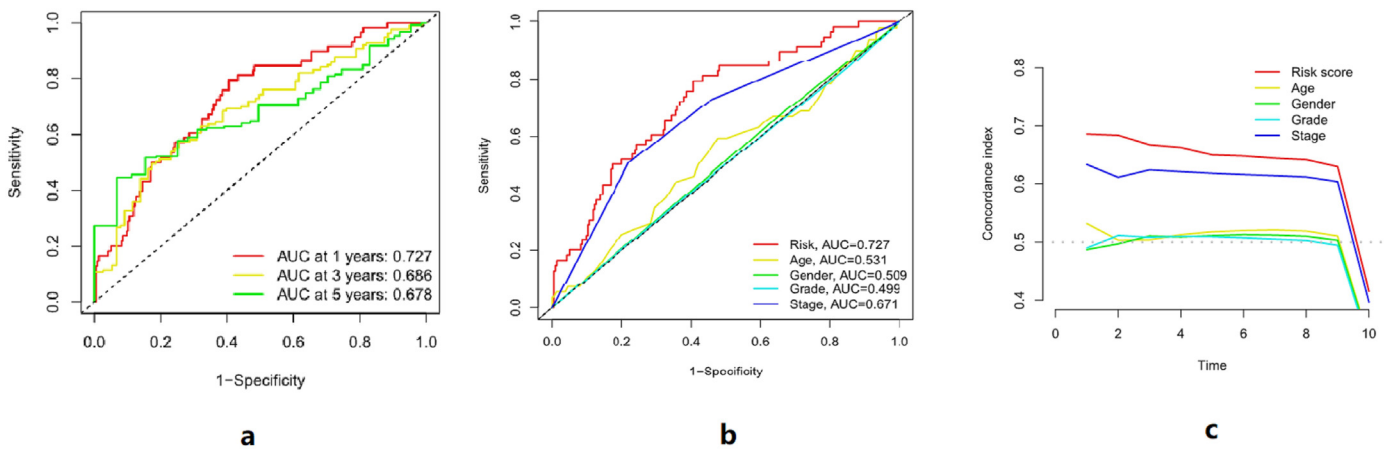

Figure 8. a: The area under the ROC curve of 1 year, 3 years, and 5 years. The area under the ROC curve of the risk score for predicting 1-year survival of HCC patients was 0.727, that for predicting 3-year survival was 0.686, and that for predicting 5-year survival was 0.678. b: The area under the ROC curve of the risk score, age, gender, grade, and stage, c: The C-index curve of risk score, age, gender, grade, and stage. As can be seen from Figure 8b and Figure 8c, the risk score can better predict the prognosis of HCC patients.

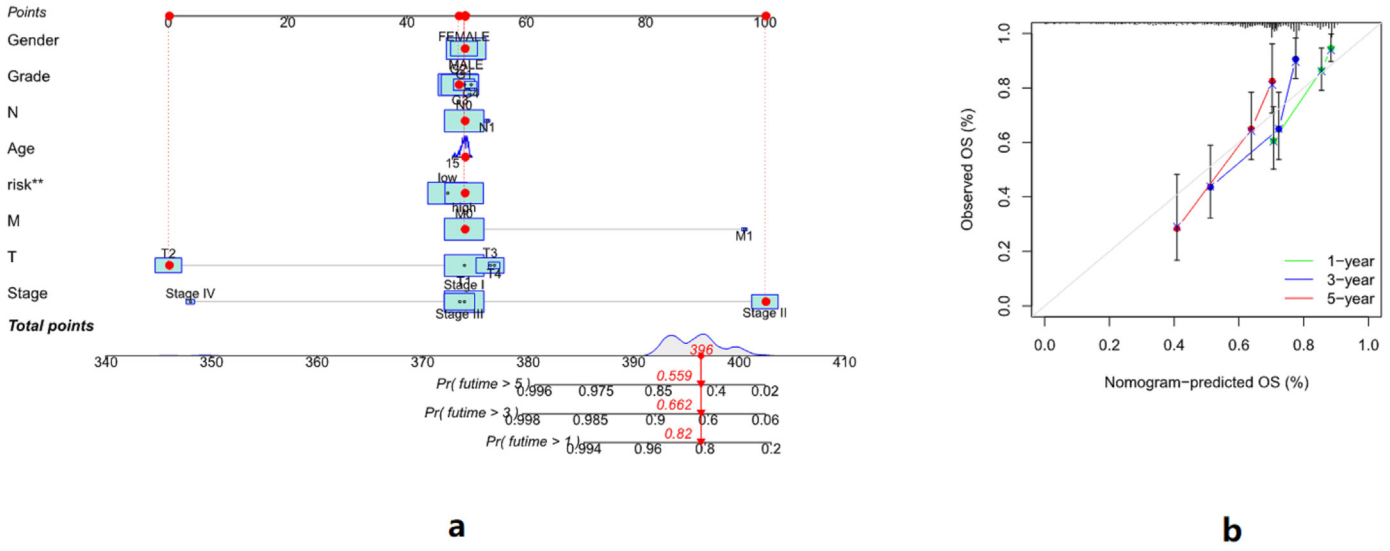

Figure 9. a: The nomogram of the risk score. We take the 15th sample as an example, with a total score of 396 points for each item. Therefore, the probability of his survival over 1 year is 82%, the probability of his survival over 3 years is 66.2%, and the probability of his survival over 5 years is 55.9%. b: Calibration curves for risk scores predicting patients at 1, 3, and 5 years.

lncRNAs, FMR1 had no correlation with AL031985.3, and was negatively correlated with NRAV. IGFBP1 and IGFBP2 were negatively correlated with the two lncRNAs, while the remaining genes showed positive correlations. The risk score of HCC prognosis constructed by m6A-related lncRNA was: Risk score = 0.706559118591986* NRAV+ 0.766983203593444* AL031985.3.

In the survival curves of all sample group, training group and text group, the overall survival time of the low-risk group was longer than that of the high-risk group, as shown in Figure 4. The risk curve of the prediction model can be seen in Figure 5. No matter in the whole sample group, training group, or text group, with the increase in risk score, the death of patients increased, and the expression of NRAV and AL031985.3 increased.

In subgroups of age, gender, and tumor stage, overall survival was longer in the low-risk group than in the high-risk group, as shown in Figure 6. The chi-square test of clinical data between groups can be seen in Table 2, Pvalue >0.05 in each group, so there is no difference in age, gender, grade, and stage among all groups.

In univariate analysis, Hazard ratio (HR) of the risk score was 1.573, 95%IC [1.375,1.8], $P < 0.001$, and in multivariate analysis, HR of the risk score was 1.466, 95%IC: [1.272,1.169], $P < 0.001$. Univariate and multivariate analyses of the risk score showed that the risk score was an independent predictor of HCC prognosis (Figure 7).

The areas under the ROC curve for predicting 1-year, 3-year, and 5-year survival of patients with HCC by risk score were 0.727, 0.686, and 0.678, respectively. This shows that the risk score we constructed has a better prediction effect on the survival of HCC patients. To further verify the prediction effect of the risk score, we compared the prediction effect of the risk score with age, gender, tumor stage, and grade. The results showed that the area under the ROC curve of the risk score was 0.727, which was significantly better than age, sex, tumor stage, and grade. Besides that, the C-index of risk score was also significantly better than age, sex, tumor stage, and grade (Figure 8). The above results indicate that risk score can be used as an effective method for prognosis prediction of HCC patients.

Based on the risk score constructed by lncRNAs, we drew the nomogram (Figure 9a). We took the 15th sample as an example. The patient had a total score of 396 for all items, and the probability of survival over 1 year was 82%, the probability of survival over 3 years was 66.2%, and the probability of survival over 5 years was 55.9%. The

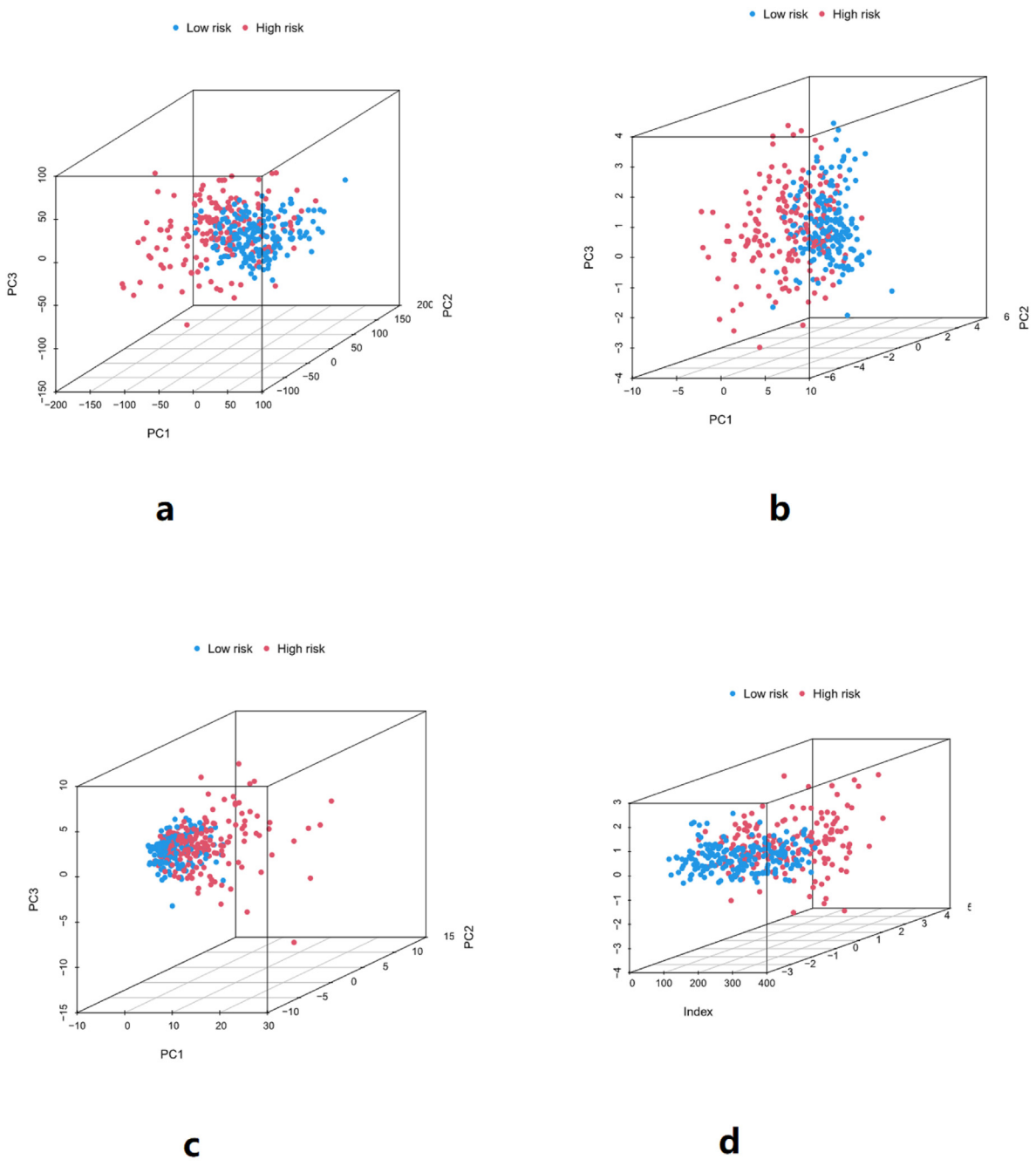

Figure 10. a: PCA of the whole gene, b: PCA of m6A genes, c: PCA of m6A-related lncRNAs, d: PCA of lncRNAs used for risk scores construction. The results showed that compared with m6A genes, m6A-related lncRNAs, and other genes, the lncRNAs used for risk score construction had the best discrimination between high-risk group and low-risk group samples. This means that the lncRNAs used to construct the risk score can well distinguish samples from the high-risk group and the low-risk group.

results of the correction curve of the nomogram also showed that the nomogram had a better prediction effect on the 1-, 3-, and 5-year survival rates of HCC patients (Figure 9b).

4.3. Principal component analysis

Principal component analysis (PCA) was performed on the whole gene, m6A genes, m6A-related lncRNAs, and lncRNAs used for risk scores construction, respectively, as shown in Figure 10. The results showed that compared with m6A genes, m6A-related lncRNAs, and other genes, the lncRNAs used for risk score construction had the best discrimination between high-risk group and low-risk group samples. This means that the lncRNAs used to construct the risk score can well distinguish samples from the high-risk group and the low-risk group.

4.4. Risk differential analysis and GO enrichment analysis

Genes that differ between high-risk and low-risk groups were shown in Table 3. Differential genes were highly expressed in the high-risk group (Figure 11a). The GO enrichment analysis of the differential genes showed that the differential genes were mainly located in the extracellular matrix and chromosomal regions, and may play regulatory roles in binding sites and catalytic enzymes, thereby affecting the chromosome division and cell proliferation of cells (Figure 11b).

Table 3. Genes that differ between high-risk and low-risk groups.

gene	lowMean	highMean	logFC	pValue	fdr
SOGA1	0.762441385	1.824778388	1.259022929	4.72E-23	1.93E-21
CYS1	0.278046091	2.053921639	2.88498518	0.033887537	0.0408347
CTNND2	0.577150807	3.06400425	2.408398055	1.86E-07	4.03E-07
C4orf48	2.310128195	5.155930001	1.158259764	0.00010396	0.0001662
SOX12	4.084522532	8.348446134	1.031340257	1.47E-15	1.01E-14
AL662795.2	0.748358071	1.565414701	1.064744264	6.32E-17	5.75E-16
FTCD	115.976255	54.82683524	-1.08087535	1.10E-19	1.81E-18
RHOV	0.146416731	2.746931604	4.229668667	1.41E-11	5.17E-11
CDCA8	1.959628819	6.02557972	1.620519636	3.72E-25	3.14E-23
CYP4F2	39.10312697	18.70670726	-1.06372834	1.73E-15	1.18E-14
NPTX2	2.192038303	8.332143897	1.926414747	6.22E-05	0.0001019
OLFML3	2.444922906	6.730261952	1.460873683	1.82E-06	3.55E-06
AC137723.1	1.625261897	0.633187447	-1.35996766	1.47E-10	4.68E-10
RNF157	1.597150798	3.241197133	1.021026235	1.96E-07	4.24E-07
RMI2	1.863554698	3.761635296	1.013302816	1.82E-16	1.49E-15
RHNO1	3.221034348	6.507791967	1.014644089	2.18E-27	4.63E-25
IFT57	1.434889536	3.045737501	1.085851931	6.87E-13	3.02E-12
DYRK2	1.242583961	2.579993887	1.05402431	3.39E-23	1.45E-21
IL2RG	4.706857184	10.81368313	1.200022002	2.51E-06	4.82E-06
AP000769.1	0.909100227	2.172440052	1.256805103	6.69E-10	1.95E-09
SCRN1	0.910306529	3.704860497	2.024994888	1.23E-10	3.95E-10
CD24	25.24229194	71.66716996	1.505469476	9.37E-14	4.73E-13
CSGALNACT1	0.841990382	2.007520658	1.253539175	0.002754124	0.0037626
FZD7	0.475086959	1.868792166	1.975842621	2.95E-14	1.62E-13
CSPP1	1.310948933	2.81857042	1.104352125	1.15E-14	6.76E-14
PPP1R14D	0.713302608	1.799713889	1.335181418	4.72E-07	9.79E-07
FAM133A	0.608962332	1.742805546	1.516986712	1.77E-06	3.45E-06
SOX9	5.212905911	15.20305852	1.544201866	1.09E-12	4.68E-12
MRC2	1.545081071	4.085646627	1.40288189	8.57E-05	0.0001382
CD44	3.564727589	8.493284304	1.252530711	1.77E-05	3.07E-05
TUBA1A	5.82656021	11.92201192	1.032911396	1.03E-05	1.84E-05
SPATS2	1.658761467	3.811684859	1.200322406	3.07E-34	9.14E-31
CXCL5	0.367517406	6.772840097	4.20387645	1.71E-09	4.74E-09
P3H4	2.466147173	5.80461829	1.234942301	1.13E-15	7.96E-15
BACE2	1.650550936	7.986519449	2.274619248	3.95E-08	9.24E-08
ANKRD10-IT1	1.49081584	3.09610523	1.054352454	3.62E-11	1.26E-10
ABCC1	1.061173667	3.843910247	1.85691387	5.95E-18	6.73E-17
CYP4A11	99.73993045	43.74599058	-1.1890204	7.55E-18	8.26E-17
IDO1	0.807892825	1.62669382	1.009706906	0.012429087	0.0158238
RHPN1	1.13536993	2.778093943	1.290932949	1.94E-11	7.01E-11
PDCD1	0.654982552	1.966524444	1.586119738	1.11E-05	1.97E-05
CFTR	0.231759152	3.99978452	4.109224061	6.93E-05	0.000113
NDC80	1.421201834	3.521709558	1.309164477	1.97E-17	1.98E-16
CRYAB	4.817038411	11.36279722	1.238099699	0.017037426	0.0213031
IER5L	2.234043739	5.44235659	1.284574055	1.57E-12	6.59E-12
CYP2C8	141.833323	57.30456804	-1.30747447	7.27E-12	2.77E-11
SPRED1	0.931632471	2.361691086	1.34198744	1.33E-18	1.74E-17
CBX2	0.509733628	1.663612838	1.706504287	1.58E-16	1.31E-15
EPO	0.988229782	4.975480087	2.331917299	8.62E-11	2.83E-10
PITX1	0.654483775	2.906078947	2.150644563	6.62E-12	2.53E-11
ALOX5	1.094513511	3.41969985	1.64357994	1.02E-09	2.91E-09
MCUB	0.732285309	1.841648823	1.330520227	1.52E-10	4.82E-10
ANG	369.2250878	177.8023201	-1.05422643	4.14E-17	3.87E-16
MUC13	27.40074782	56.08700444	1.033451264	0.001610715	0.0022677
FXYD2	1.912891571	7.283101564	1.928797865	9.30E-06	1.67E-05
AC009005.1	0.92748876	1.906386183	1.039438697	2.24E-11	8.00E-11
COL1A2	14.90655905	38.58812017	1.372209492	8.31E-06	1.50E-05
AC016885.3	0.741704892	1.667776384	1.169008675	0.004262725	0.0057043

(*continued on next page*)

Table 3 (*continued*)

gene	lowMean	highMean	logFC	pValue	fdr
PLXNA3	0.876452565	2.027489136	1.209946268	1.43E-14	8.30E-14
MMP7	2.727885941	13.34629389	2.290583949	2.27E-06	4.37E-06
CXCL8	4.109531976	11.95328047	1.540360604	4.06E-08	9.48E-08
TTC22	0.908201636	1.863023412	1.036561264	2.19E-10	6.81E-10
TINAG	1.619376624	3.379565451	1.061399197	0.001255914	0.0017894
NAA40	1.5047136	3.323470003	1.143201415	1.23E-30	1.04E-27
ZDHHC1	0.945212521	2.14730752	1.183818171	0.000907024	0.0013155
ANTXR1	1.504406927	3.163700235	1.072418054	0.001112216	0.0015963
NBL1	1.214368075	3.352736791	1.465133459	0.000275858	0.0004226
NCEH1	1.048580674	4.761677062	2.183031918	2.95E-16	2.30E-15
CRYBB1	0.292442019	4.467851366	3.933358669	7.81E-05	0.0001265
BCL9L	1.49257711	3.124001458	1.065589661	3.02E-12	1.22E-11
ITGAM	0.98673375	2.654476031	1.427694354	4.33E-11	1.49E-10
KCNE4	0.711908812	1.936080485	1.443374564	2.13E-05	3.67E-05
CDKN2A	2.503256906	5.829550124	1.219578192	3.16E-09	8.50E-09
S100A11	52.02634995	186.4531412	1.841498703	5.05E-13	2.27E-12
BHMT	123.112429	54.03195865	-1.18809153	4.22E-13	1.92E-12
MGAT5	1.844473089	4.07332581	1.142998475	2.42E-15	1.60E-14
MARCKSL1	28.67798548	59.56908508	1.054620117	5.20E-13	2.33E-12
LAMP5	0.118305757	2.825986048	4.578162157	7.16E-10	2.08E-09
CSF1	3.897025635	9.406648984	1.271307448	2.89E-14	1.58E-13
PAGE2	5.166092308	11.79718005	1.191296718	5.74E-05	9.44E-05
PNMA1	3.142605462	7.946675346	1.338390245	1.26E-22	4.40E-21
MUC1	0.364885758	3.933870129	3.430432585	2.49E-08	5.98E-08
ARL4C	3.434925189	9.020185591	1.392878439	1.38E-12	5.86E-12
LAMA5	2.996030302	7.651097661	1.352614523	4.52E-15	2.84E-14
ADGRD1	0.680772244	1.551612724	1.188524389	0.000222974	0.0003445
CEACAM6	0.130061269	3.876690804	4.897562362	0.017010877	0.0212766
NFE2L3	1.010001383	3.307987133	1.711596354	1.47E-19	2.33E-18
TREM2	3.421131511	7.52300552	1.136835585	7.00E-09	1.80E-08
PTAFR	0.837020261	2.100965963	1.32771834	6.78E-08	1.55E-07
RBL1	0.622736543	1.509901489	1.277760579	1.21E-25	1.28E-23
CASC9	1.504257938	3.267509472	1.119139448	9.73E-05	0.0001561
SPINT1-AS1	0.63408306	1.656854973	1.385703588	9.38E-07	1.88E-06
SLC2A5	0.92351958	2.20700133	1.256873045	9.24E-09	2.34E-08
AC245100.3	7.308543701	23.46461986	1.68283122	0.002155181	0.0029865
NCAPH	1.031887546	3.132277879	1.60192645	2.58E-23	1.16E-21
MAEL	0.564197602	1.752532919	1.635169104	1.59E-05	2.79E-05
MEX3A	0.58633949	1.927560044	1.71696767	8.36E-16	6.01E-15
PCSK1	1.106614147	3.651671457	1.722404699	0.000384745	0.0005807
SUSD1	0.849965003	1.765125976	1.054295805	1.31E-17	1.35E-16
TMIE	0.76224025	1.703827402	1.1604615	0.000149059	0.0002345
SFRP2	0.37720339	1.833153558	2.280913092	0.01709177	0.0213688
TNC	1.319199686	4.249673981	1.687689207	0.000101086	0.0001619
UPP2	5.137791942	1.85707062	-1.46811979	2.80E-10	8.57E-10
LMNB1	4.297094176	10.30835286	1.262380526	1.08E-21	2.90E-20
TPPP3	1.600259314	3.705888837	1.211513901	0.000532583	0.0007916
MARCKS	14.25561745	30.13037156	1.079687936	3.34E-17	3.18E-16
PRAME	1.078533735	5.188271469	2.266182665	5.72E-09	1.49E-08
PLBD1	1.535586868	5.514195996	1.84436042	1.27E-13	6.26E-13
HAUS6	0.956745937	2.05700371	1.104336621	1.10E-25	1.21E-23
STK39	1.675403225	4.629913925	1.466477017	1.33E-14	7.77E-14
ETNPPL	30.70566778	11.90737614	-1.36664944	3.93E-12	1.55E-11
DCAF16	1.776379287	4.022862323	1.17928271	3.87E-29	1.92E-26
PLAUR	0.893045845	2.909205969	1.703819297	1.77E-14	1.01E-13
CYBB	2.457813617	6.034106715	1.295764695	7.56E-07	1.53E-06
CIDEC	1.535843994	3.402754763	1.1476715	0.000369288	0.0005584
COL6A3	2.651730971	6.612948247	1.318359196	8.01E-06	1.45E-05
TMC4	3.739501577	10.23691171	1.452862649	0.034143993	0.0411229

(*continued on next page*)

Table 3 (*continued*)

gene	lowMean	highMean	logFC	pValue	fdr
TUBA3C	0.724125494	4.895085467	2.757022399	0.000280582	0.0004295
CHST3	0.524242128	1.60205389	1.611617479	0.000114407	0.0001821
MIR3189	0.994954027	2.066691879	1.054621544	0.000623817	0.0009199
INAVA	0.825246571	2.279663829	1.465923949	9.64E-14	4.85E-13
LINC02768	1.996761296	0.867513644	-1.20270352	1.30E-10	4.16E-10
LINC00665	0.694312631	2.17954562	1.650370079	2.12E-11	7.60E-11
BCL2A1	1.017610078	2.493149564	1.29278457	5.87E-06	1.08E-05
SPRING1	1.580663752	4.16176875	1.396666302	8.52E-28	2.20E-25
AC079466.1	2.161833365	7.295315891	1.754715125	0.000148131	0.0002331
CCNF	0.91008703	2.105970381	1.210408727	4.70E-21	1.07E-19
RASA3	1.355274983	2.96174721	1.127862908	8.30E-10	2.39E-09
RAI1	1.063265537	2.377915615	1.161195582	1.36E-20	2.78E-19
MKI67	1.452944653	4.246575351	1.547320101	1.15E-22	4.04E-21
NUMBL	0.818716157	1.699158373	1.053385056	1.85E-14	1.05E-13
FUT4	0.540782043	1.868107848	1.788458595	3.53E-11	1.23E-10
PPP1R13L	2.168525724	4.342274085	1.001736235	9.24E-09	2.34E-08
ZIC2	1.055950719	2.802653293	1.408250778	9.73E-12	3.65E-11
DUOXA2	0.476067745	5.096430155	3.420248261	0.000178726	0.0002787
CNTRL	0.68093086	1.466969208	1.107258366	2.84E-20	5.27E-19
UGT1A3	2.816408087	1.363620684	-1.046414	6.52E-06	1.19E-05
OIP5	1.163328888	2.771809111	1.252568882	3.39E-18	4.05E-17
CHRNA4	1.883688122	0.853278197	-1.14247203	0.000495952	0.0007397
SEC14L2	34.52708866	14.4776505	-1.2539012	4.56E-14	2.42E-13
WFDC2	2.651178178	9.450155931	1.833704502	0.003609464	0.004869
ARHGAP11A	0.792833721	2.136166767	1.429934051	4.58E-23	1.88E-21
ADH4	310.2887243	141.4941644	-1.13286872	4.65E-10	1.38E-09
TM6SF2	8.636530557	3.986073897	-1.11548342	1.95E-14	1.10E-13
ARL6IP6	1.271372429	2.647399558	1.058189242	2.24E-20	4.25E-19
HMOX1	17.90904514	38.61737129	1.108561543	5.95E-08	1.36E-07
NCS1	1.222775519	2.729887382	1.158681863	3.71E-10	1.12E-09
DBN1	2.909053687	9.760042116	1.746337451	5.23E-11	1.78E-10
CRMP1	0.683845294	1.519211912	1.151581237	7.41E-07	1.50E-06
APOBEC3C	2.104884297	5.059488479	1.265250602	4.97E-06	9.20E-06
CD109	1.041496609	2.100820995	1.012295097	4.92E-06	9.12E-06
PROM1	0.120128762	2.130148215	4.1483003	1.05E-05	1.86E-05
ADGRE5	4.623528453	9.496789304	1.038445579	3.35E-09	9.00E-09
BIRC5	4.133098801	10.09889651	1.288901904	4.19E-18	4.90E-17
UNC13D	0.649607581	2.235198362	1.782762495	1.08E-07	2.40E-07
VSIG4	2.76585398	5.558859787	1.007064	0.010291586	0.0132128
SLC39A10	1.058144507	2.22103423	1.069694963	1.37E-19	2.19E-18
SLC13A5	36.30341246	18.11451919	-1.00295865	2.37E-13	1.12E-12
CENPA	0.921740335	2.795630206	1.600741251	2.97E-22	9.00E-21
RPP25	1.779760066	3.746931907	1.074026999	7.52E-10	2.18E-09
DCXR-DT	7.275206925	2.981725281	-1.28684094	7.55E-09	1.94E-08
SERPINH1	14.20940324	31.42917225	1.14525831	7.96E-14	4.06E-13
ZFPM2-AS1	0.812098673	2.215064465	1.44762175	1.75E-06	3.42E-06
CCND2	0.932096126	2.460944945	1.400661731	4.40E-05	7.34E-05
GOLM1	14.02535343	33.26803878	1.246099693	2.01E-11	7.24E-11
SLC1A5	3.42422531	14.68339004	2.100335552	3.93E-20	7.06E-19
ABR	0.843665592	2.314316583	1.455843059	3.80E-08	8.90E-08
TLCD3A	1.185360493	2.649798278	1.160556656	1.19E-15	8.39E-15
FMO1	0.939561762	2.382556155	1.342450313	4.47E-06	8.31E-06
SERPINE2	1.577624798	5.286019533	1.744427622	2.88E-08	6.85E-08
TUBB4A	1.985751636	5.669002405	1.51340969	4.82E-07	9.98E-07
CDK1	2.366377086	6.398031135	1.434948025	7.39E-21	1.62E-19
KCNK5	2.741613018	5.834185055	1.0895062	0.001668011	0.0023409
DDR1	2.138462895	8.647424744	2.015696379	2.03E-16	1.66E-15
C16orf89	0.123468345	4.583089729	5.214107418	4.67E-06	8.67E-06
TMEM132A	0.703676427	4.720306382	2.745896414	1.67E-13	8.11E-13

(*continued on next page*)

Table 3 (*continued*)

gene	lowMean	highMean	logFC	pValue	fdr
CLDN10	0.55626587	3.604859095	2.696096374	0.01675755	0.0209862
MT2A	516.2996407	182.6353283	-1.49924273	0.00096892	0.0014013
EZH2	1.794428018	4.16935424	1.216299901	4.12E-24	2.54E-22
DTX3	1.161957788	2.609732906	1.167344502	1.34E-05	2.36E-05
HLA-DQB2	2.056099011	5.136764138	1.320950093	8.73E-07	1.76E-06
SLC22A1	120.2348974	40.55850728	-1.56777923	1.91E-14	1.08E-13
TTC36	19.99192077	4.091237301	-2.28880796	3.50E-15	2.25E-14
MEP1A	1.748810821	5.45922804	1.642322729	5.88E-05	9.65E-05
ARHGAP33	0.822655609	1.659503558	1.01239122	5.85E-18	6.62E-17
F13A1	1.586746125	3.747369646	1.239806975	4.84E-05	8.04E-05
UCA1	0.123690551	4.733081744	5.257972637	0.001110218	0.0015942
XXYLT1	0.792611213	1.718810911	1.116725558	8.22E-20	1.39E-18
TPX2	4.990859927	13.74896077	1.461962256	1.24E-21	3.29E-20
SFRP4	1.044703012	2.192162494	1.069261871	0.001205296	0.0017214
TMEM165	2.67775801	5.379646751	1.006485853	4.93E-24	2.91E-22
ADORA2BP1	2.808905036	1.136344822	-1.30560717	1.48E-10	4.71E-10
GPX8	0.711548147	2.086803637	1.552261568	2.19E-08	5.30E-08
ARL14	0.399767559	3.439272032	3.104869924	3.23E-06	6.10E-06
MAD2L1	0.899762746	2.295468521	1.351172108	4.70E-25	3.83E-23
LINC00844	32.59893743	9.371669622	-1.79844694	9.62E-11	3.14E-10
HAVCR2	1.188691923	2.846952538	1.260043585	4.58E-08	1.06E-07
PAFAH1B3	8.039837001	20.44194487	1.346294305	1.42E-16	1.20E-15
PLEK	2.419877075	5.401234999	1.158355556	5.21E-07	1.07E-06
ITGB1-DT	0.724568839	2.476247098	1.772960618	1.05E-07	2.35E-07
CHD3	2.249726351	4.678443698	1.056279164	1.29E-08	3.22E-08
APOC3	5547.85486	2292.035526	-1.27530064	2.99E-26	4.14E-24
AC016735.1	1.04813775	3.512311889	1.744592626	1.38E-05	2.42E-05
COL5A1	3.409245622	7.861512209	1.205354307	3.22E-05	5.45E-05
NCAPD2	2.895043205	7.395360895	1.353035674	7.07E-26	8.95E-24
LTO1	1.83379779	3.955177724	1.108907959	2.95E-13	1.37E-12
CHIT1	0.345042837	1.808129652	2.389650743	0.010714597	0.0137263
CDK19	1.389641153	2.794193882	1.007719745	5.74E-15	3.55E-14
ITGAV	5.403178116	13.06780039	1.274136177	6.33E-14	3.27E-13
CREB3L1	0.784379864	3.775772772	2.26714754	0.000176272	0.0002751
SLC6A8	2.690748065	10.15256803	1.915765471	5.00E-11	1.70E-10
LRFN4	0.525042518	1.6547338	1.656092986	6.32E-06	1.15E-05
HAPLN3	0.668856601	1.465169161	1.131298396	9.79E-07	1.96E-06
LIF	0.657630788	3.1636277	2.266230084	6.43E-12	2.47E-11
MCM6	5.159295547	11.57631843	1.165930514	9.02E-23	3.24E-21
RUNX1	0.882099282	1.802243529	1.030781021	1.21E-14	7.10E-14
FCGBP	0.362939615	2.05203354	2.49925287	3.62E-12	1.44E-11
SLC9A1	1.079368145	2.523309628	1.225130231	5.45E-14	2.85E-13
AGR2	3.323233751	21.98725652	2.726007924	1.94E-05	3.37E-05
B3GNT7	0.510409195	2.072584878	2.021704959	2.20E-07	4.73E-07
VGLL4	1.245002262	2.64819166	1.088859176	7.99E-19	1.09E-17
SKA1	1.069656551	3.039736972	1.506798847	4.40E-19	6.34E-18
EMB	0.703305378	1.571828733	1.160220876	6.36E-05	0.0001042
MTF2	1.252107445	2.566799125	1.035612029	1.10E-27	2.67E-25
PLEKHB1	0.421965603	3.052130447	2.854619319	2.36E-10	7.31E-10
MEIS2	0.973616928	2.209390183	1.182222067	2.15E-10	6.69E-10
AC111000.4	0.747461623	1.531562105	1.034932457	9.30E-06	1.67E-05
AC012065.2	15.7593154	5.453554886	-1.53093601	1.09E-10	3.52E-10
GTSE1	0.66432363	2.251478484	1.760914554	1.58E-24	1.10E-22
HOXB7	0.60623601	1.80197447	1.571627116	0.012395001	0.0157821
PRKX	0.77749003	1.775889247	1.19164553	2.54E-05	4.35E-05
DBF4	0.886852256	1.828913225	1.044220941	7.76E-26	9.42E-24
POF1B	0.475416688	1.867725013	1.97401761	3.84E-08	9.00E-08
PI3	3.283544345	10.34227382	1.655227563	0.000123462	0.000196
RBPJL	0.009656708	2.504139394	8.018567731	0.028012913	0.0340769

(*continued on next page*)

Table 3 (*continued*)

gene	lowMean	highMean	logFC	pValue	fdr
WFDC21P	1.176705498	3.051879881	1.374944887	0.001878844	0.0026247
COL3A1	30.50422594	80.12475329	1.393238887	0.000138341	0.0002184
ZWINT	4.728890567	11.31832343	1.259086608	5.92E-21	1.33E-19
MNDA	0.932901964	2.035911039	1.125877138	8.15E-07	1.65E-06
BIRC3	5.986421013	12.3721305	1.047328307	8.73E-06	1.57E-05
KRT19	2.549848708	27.2336082	3.416904585	0.000147873	0.0002327
OSMR	2.290136699	6.325041649	1.465641264	2.55E-13	1.20E-12
GNMT	104.497557	31.77421135	-1.71754099	3.06E-15	2.00E-14
NPAS2	1.10908399	2.23704005	1.012222461	5.51E-18	6.29E-17
AL161668.4	3.406264282	1.575286954	-1.11257572	4.45E-10	1.33E-09
INCENP	1.454755728	3.060517683	1.072998777	2.41E-20	4.55E-19
THSD4	0.726220464	1.721366867	1.245075115	0.0368668	0.0442275
MACROH2A2	5.94819219	12.54651326	1.07676332	1.29E-08	3.20E-08
ISLR	3.242726836	8.936778116	1.462547307	0.003171214	0.0043047
CYP2C9	169.0238079	61.62565952	-1.45562339	2.11E-17	2.10E-16
PLK1	1.351478327	4.276531245	1.661902704	2.45E-24	1.65E-22
CPA2	0.070217762	7.424496107	6.724313295	1.54E-05	2.69E-05
ETV4	4.298901441	8.963634751	1.060115829	5.70E-10	1.68E-09
TPM4	12.02328621	27.20711003	1.178152451	9.64E-16	6.87E-15
UHRF1	0.671316103	2.179420344	1.698880321	5.72E-24	3.27E-22
MFAP2	0.396864444	1.983989389	2.321686092	4.10E-10	1.23E-09
FAM83A-AS1	9.962472875	3.514503289	-1.50318309	1.82E-06	3.55E-06
LINC01702	19.91832353	8.678032009	-1.19865641	2.76E-09	7.49E-09
HPX	778.5962644	333.4381475	-1.22345626	1.64E-24	1.14E-22
TMEM54	6.767982511	14.28154917	1.077354737	3.21E-09	8.64E-09
CD7	2.233613534	6.610223724	1.565319513	0.000327866	0.0004982
PTGES	1.674796239	4.911651864	1.552222723	6.65E-08	1.52E-07
CDCA5	2.15583613	4.998936444	1.213373665	2.91E-20	5.39E-19
MCM4	4.788695019	10.68098397	1.157340097	3.66E-21	8.67E-20
CDKN3	3.519248945	7.104568951	1.01347955	2.73E-11	9.66E-11
LINC02041	0.464983671	1.793959412	1.947895292	2.09E-09	5.71E-09
PTGFRN	4.511081522	9.843033793	1.12562969	4.85E-19	6.90E-18
CCL25	39.60654341	9.669980021	-2.03415398	0.000379945	0.0005739
AC092868.1	0.61648605	1.647775301	1.418379368	1.04E-07	2.33E-07
SLC6A9	0.650626829	1.655263859	1.347158991	3.18E-11	1.11E-10
PKP3	0.227095297	2.365755751	3.3809314	1.30E-09	3.66E-09
ZNF667-AS1	0.814833609	1.650936259	1.018707028	0.000794076	0.0011587
CYP2B6	40.07238038	16.38337363	-1.29037575	7.16E-10	2.08E-09
TUBA1C	5.847423549	12.45277656	1.090594452	9.52E-22	2.60E-20
SOX4	3.115068136	11.65990706	1.904220665	2.14E-16	1.73E-15
MIR210HG	0.716541838	2.191159641	1.612571748	5.14E-14	2.70E-13
PTTG1	5.895142943	12.51997581	1.086633074	2.76E-14	1.52E-13
MXRA8	2.734894077	7.063376206	1.36887298	0.000599797	0.0008862
CTSC	4.691214305	10.49160455	1.161202023	4.53E-14	2.41E-13
SEPTIN5	0.985285361	2.031347338	1.043823418	5.82E-09	1.51E-08
SPP1	153.2336432	540.8368222	1.819460297	5.13E-13	2.30E-12
ZNF468	1.022169514	2.38293582	1.221105627	1.32E-14	7.72E-14
FDCSP	3.459184914	20.2190758	2.547213013	2.73E-06	5.22E-06
MTHFD2	0.788328273	1.754005683	1.153785	1.18E-08	2.95E-08
MIR4292	1.233677587	2.892175406	1.229189646	2.75E-12	1.11E-11
FZD1	0.624029408	2.314887724	1.891256298	1.28E-15	8.93E-15
LOXL1	1.113627139	3.64806161	1.711863819	0.009350889	0.0120624
PFKP	1.71667649	8.33828591	2.280132654	1.93E-09	5.30E-09
PYCR1	4.428659467	12.20195983	1.462170913	8.35E-11	2.75E-10
TMEM237	0.632782778	1.437310358	1.183589375	3.20E-27	6.44E-25
ADH1B	297.5167939	137.0766887	-1.11798786	2.27E-14	1.27E-13
TROAP	1.445574533	3.829598929	1.405550313	3.45E-18	4.11E-17
SPINT2	4.184393182	13.52231457	1.69225179	8.03E-05	0.0001299
UNC5B	1.511955959	3.208337924	1.085409987	1.50E-11	5.48E-11

(*continued on next page*)

Table 3 (*continued*)

gene	lowMean	highMean	logFC	pValue	fdr
FCER1G	13.91700924	32.3845239	1.218455324	5.40E-07	1.11E-06
ZNF731P	2.459721675	5.387506402	1.131122599	8.03E-13	3.50E-12
CCNB2	2.228830605	6.025262183	1.434737047	2.39E-20	4.52E-19
AQP8	4.407179136	2.053486558	-1.10178003	0.004686372	0.0062396
PLEKHA2	1.241028914	2.676129269	1.108611078	2.35E-12	9.67E-12
SLC27A5	71.47095298	25.40754009	-1.49210032	1.60E-23	7.77E-22
SCD5	0.408239527	3.937443364	3.269771393	0.000628381	0.0009265
RASSF8	0.637071654	1.892830877	1.57101796	2.52E-15	1.66E-14
AC239800.2	1.95778209	0.873779435	-1.16387914	1.24E-08	3.09E-08
AREG	0.465910787	1.879882018	2.012516482	3.13E-08	7.42E-08
HKDC1	5.914846344	15.38335481	1.378957565	1.48E-13	7.24E-13
HSPA7	1.184613434	3.233501269	1.448680824	1.03E-05	1.83E-05
DMPK	1.626946658	3.329891578	1.033308253	1.99E-13	9.52E-13
TMEM45A	4.17081155	8.446351048	1.018000081	0.000825351	0.0012017
ENDOD1	1.760182053	3.928093454	1.158104601	0.008271441	0.0107223
KRT17	0.667611179	3.502840055	2.391445096	3.65E-07	7.65E-07
HROB	0.715209502	1.584664979	1.147740058	1.19E-16	1.01E-15
REN	2.234571773	0.813463765	-1.4578484	4.46E-07	9.28E-07
FBXO32	1.239771322	2.565231763	1.049015139	9.48E-05	0.0001522
MAFA-AS1	1.109634022	2.502862876	1.173495325	0.000416811	0.0006266
LINC00205	0.905113996	1.950869348	1.107945751	4.93E-17	4.56E-16
CTSK	3.828560333	26.39328678	2.785297124	1.85E-07	4.01E-07
RNF145	3.368278279	7.377983449	1.131215218	1.20E-20	2.51E-19
FNBP1L	3.591897529	7.279042871	1.019002569	1.15E-21	3.06E-20
ETV5	1.797391551	3.917106949	1.123883793	7.19E-16	5.21E-15
TMEM65	1.360242305	3.014335169	1.147976175	1.90E-18	2.38E-17
ENAH	3.672603915	7.464534635	1.023249009	1.61E-20	3.23E-19
FAM241B	2.252294427	4.662047976	1.049568418	1.22E-11	4.50E-11
RAVER2	0.697204228	1.725333272	1.307221843	7.80E-10	2.25E-09
LPCAT4	0.865316614	2.535079796	1.550731152	6.65E-19	9.26E-18
GCA	1.886367828	3.819348327	1.017715482	2.18E-14	1.22E-13
SLC1A7	1.023863046	3.269039488	1.674844053	0.015564277	0.0195764
AL355102.4	1.118981906	4.06460321	1.860927815	1.28E-08	3.18E-08
TREH	1.783453595	0.764504452	-1.22207687	0.000175586	0.0002741
OGFRL1	0.794115329	1.679971825	1.081016588	6.01E-15	3.70E-14
APOF	46.53064897	21.40930421	-1.1199434	2.78E-11	9.83E-11
PFKFB3	3.064625998	11.21052113	1.871070419	1.42E-10	4.55E-10
NRAV	1.233467892	3.036729337	1.299798165	8.40E-51	9.99E-47
KNTC1	0.711345288	1.821579742	1.356568232	3.56E-21	8.46E-20
ASF1B	2.412406435	6.83208781	1.501853529	2.72E-22	8.45E-21
CERCAM	0.802464496	2.835374465	1.821029815	1.64E-08	4.04E-08
DAB2	3.771358863	9.221588854	1.289930908	1.66E-11	6.02E-11
SCAMP5	2.675680505	5.500549563	1.039669908	2.48E-08	5.95E-08
LINC01287	1.928090352	4.042614187	1.068115865	0.001065955	0.0015336
CAPN6	0.18805603	3.042621037	4.016080186	2.21E-06	4.26E-06
E2F5	0.623995665	1.416791808	1.183019865	7.82E-17	6.97E-16
CENPO	0.772177198	1.841970922	1.25424643	4.35E-26	5.75E-24
BHLHE41	0.441232288	1.944560294	2.139833696	5.78E-09	1.50E-08
HAGLR	0.69150872	2.365820164	1.774521065	2.14E-05	3.69E-05
HK2	0.861592875	3.200526229	1.893230907	1.16E-15	8.15E-15
RHOQ	2.994419086	6.038657933	1.011951803	1.10E-19	1.81E-18
HIF1A	8.477794192	19.55008276	1.205413866	3.31E-14	1.80E-13
IGLV7-46	1.081626254	6.857903535	2.664565535	0.020645467	0.0255246
CDC6	1.549584904	4.410060847	1.508916757	4.59E-22	1.34E-20
IGHV3-43	1.017299232	3.943423848	1.954704682	0.033009359	0.0398168
ABHD17C	1.875160062	3.870855413	1.045638672	5.49E-14	2.87E-13
PDX1	1.322156688	2.701541097	1.030889469	0.002337012	0.0032231
JAG1	2.656742436	6.910552942	1.379142782	3.06E-07	6.47E-07
CLIC3	0.544309931	2.109142272	1.954156151	3.42E-05	5.77E-05

(*continued on next page*)

Table 3 (*continued*)

gene	lowMean	highMean	logFC	pValue	fdr
KCTD17	2.675743383	7.491394807	1.485294595	1.84E-14	1.04E-13
MSC	2.94283375	15.84409574	2.428667376	8.72E-09	2.22E-08
TRAIP	0.791321916	1.811085785	1.194518264	1.44E-18	1.85E-17
FBXO5	0.668359075	1.560230311	1.223063703	1.31E-21	3.47E-20
LPCAT1	3.778173822	10.43563396	1.465757263	6.83E-24	3.81E-22
TOP2A	3.801539376	12.12654655	1.673513113	2.63E-23	1.18E-21
F2RL1	3.863199674	7.853850723	1.02360393	6.52E-06	1.19E-05
NR1I3	23.37646096	11.41336266	-1.03433262	1.85E-13	8.90E-13
SGPP2	0.221575467	2.275127088	3.360077076	2.76E-17	2.65E-16
IGFBP6	1.958618775	4.670783839	1.25382806	0.006633178	0.0086876
EIF5A2	0.765778534	1.950869134	1.349117879	2.59E-13	1.21E-12
PPT1	12.18349134	25.06045081	1.040484752	9.57E-27	1.65E-24
WASF1	2.028930168	4.23232839	1.060732361	1.25E-15	8.73E-15
MAP3K21	0.708193477	1.774574936	1.325258036	1.85E-09	5.09E-09
SLC6A6	0.759756697	2.541676118	1.74217081	7.10E-11	2.36E-10
TSPAN15	3.776135856	11.74749267	1.637370292	4.48E-10	1.34E-09
ADAMTS9	0.741903753	1.807609999	1.284779499	6.33E-14	3.27E-13
PODXL2	3.384594712	6.854369822	1.018040945	0.001139223	0.0016327
CYP2A7	40.46244486	9.076428402	-2.15638688	4.31E-15	2.73E-14
P3H3	0.786514061	1.817629329	1.208513556	0.003830688	0.0051528
CHST11	0.997230043	2.936177505	1.557940936	1.43E-12	6.05E-12
DDX11	0.976846962	2.147816669	1.13666639	2.60E-17	2.52E-16
TNFRSF21	5.063633586	15.24614356	1.590199448	1.18E-15	8.27E-15
FXYD3	1.561314522	4.380903818	1.488467348	2.01E-05	3.47E-05
RELN	3.968348171	8.456546862	1.091530066	0.013975611	0.0176867
SPDEF	0.51150466	2.483619381	2.279624807	7.74E-07	1.57E-06
SLC7A7	1.196793773	3.020806203	1.335759059	2.93E-11	1.03E-10
ACTL8	0.637215731	1.909552709	1.583380954	0.000536226	0.0007968
HSD11B1	264.5586111	116.8643563	-1.1787524	4.29E-09	1.14E-08
INHA	0.585054368	2.433967081	2.056667053	0.001237089	0.0017642
TMEM51	1.740132714	6.118222507	1.813915236	1.91E-13	9.15E-13
DSG2	3.340466088	11.01479472	1.72132129	8.49E-17	7.48E-16
CDKN1C	1.977896239	4.953883486	1.324593194	0.03539813	0.0425472
PIGS	2.386049772	5.050667467	1.081849922	7.88E-23	2.93E-21
STK17B	1.011570412	2.183166292	1.10982528	2.42E-12	9.91E-12
NIBAN1	0.775779827	1.914655748	1.303365855	1.46E-05	2.57E-05
PLAU	2.025639526	6.142584033	1.600468228	3.86E-10	1.16E-09
CDH24	0.632456701	1.410050431	1.156708143	3.55E-09	9.53E-09
SMC4	1.452840056	3.436403043	1.24202337	1.33E-16	1.12E-15
GPLD1	9.629323296	3.773653209	-1.35147257	4.73E-12	1.85E-11
LAPTM4B	26.27050428	55.88174315	1.08893313	5.39E-13	2.40E-12
SH3BP1	0.882736976	1.96921352	1.157564014	7.18E-14	3.68E-13
CMTM3	3.580551011	7.364443496	1.040394889	1.62E-09	4.50E-09
LAMB1	6.199246528	15.89080979	1.358027863	4.57E-13	2.07E-12
PRR11	0.863673141	2.569425865	1.572888697	2.16E-23	9.96E-22
C1orf116	0.458835241	2.057567115	2.164891382	8.81E-08	1.98E-07
S100A6	51.13331181	155.5831539	1.605350483	4.34E-07	9.03E-07
BICC1	1.452105166	6.565477177	2.176753928	1.08E-08	2.72E-08
GUCY1A1	0.760898776	1.663912874	1.128803446	5.55E-05	9.15E-05
SHCBP1	0.480971595	1.630904685	1.761648868	7.62E-24	4.17E-22
PRC1	2.170466316	5.482352889	1.336790162	6.95E-23	2.66E-21
HILPDA	1.477722129	5.335455173	1.852236344	3.79E-33	9.01E-30
FABP5	2.112097388	5.085173787	1.267620721	1.23E-07	2.72E-07
LYPD1	1.57965677	4.807612278	1.60570943	2.53E-13	1.19E-12
UBE2T	5.85236276	12.49292856	1.094020607	1.08E-17	1.14E-16
GCNT3	0.342017791	2.639351582	2.948040262	1.10E-17	1.16E-16
QSOX1	7.578203387	16.89161111	1.156379172	2.89E-05	4.92E-05
SPINDOC	1.949850692	4.93780187	1.340505294	2.75E-26	3.94E-24
RBMS2	0.797283653	1.613397707	1.016937116	2.01E-07	4.34E-07

(*continued on next page*)

Table 3 (*continued*)

gene	lowMean	highMean	logFC	pValue	fdr
GAL3ST1	2.547079074	11.12100207	2.126371136	9.68E-14	4.87E-13
BASP1	2.538883647	8.526005185	1.747675653	0.00023612	0.000364
FLNC	1.806447809	3.872817031	1.10022777	5.55E-08	1.27E-07
SLC2A6	2.062849964	4.269082437	1.049287127	2.28E-11	8.15E-11
SLC29A4	2.999509087	6.814807271	1.183946455	1.62E-08	3.97E-08
C6orf223	0.712189866	2.834419486	1.992719476	4.98E-16	3.72E-15
IGFBP3	26.2782954	52.79217193	1.006452326	3.21E-12	1.29E-11
EXO1	0.728520841	1.900988693	1.383707802	1.60E-21	4.12E-20
NT5DC2	3.286921947	9.494195578	1.530308571	4.08E-15	2.60E-14
CHST1	0.797754158	1.997115784	1.323901848	1.08E-07	2.40E-07
GBP5	0.838743293	2.716871329	1.695645012	0.001154926	0.001654
MSI2	0.962184261	1.948493284	1.017973854	2.86E-19	4.28E-18
GLIS2	1.665136642	4.456675171	1.420327242	5.96E-13	2.64E-12
ALOX5AP	1.301505291	3.444493071	1.404110499	5.89E-08	1.35E-07
SLC10A1	98.8214734	26.99211934	-1.87228631	1.03E-22	3.68E-21
LIMCH1	0.726809375	2.058976565	1.502278475	6.18E-05	0.0001013
SYT13	0.238879736	3.691406439	3.94981421	1.99E-07	4.31E-07
DNASE1L3	6.674977871	2.728724008	-1.29053657	1.01E-16	8.71E-16
CFHR4	19.201294	6.714445828	-1.5158633	8.15E-17	7.23E-16
STC2	1.027600177	2.999976985	1.54567239	3.81E-09	1.02E-08
MT1XP1	2.108372892	0.801786848	-1.39483939	0.016011949	0.0201181
MT2P1	7.265677076	2.697948233	-1.42923458	0.008794561	0.0113744
CDT1	2.746364845	5.584856353	1.023996879	3.41E-19	5.01E-18
TTK	0.702914439	1.948516242	1.470954961	3.60E-18	4.27E-17
CSAG1	2.366426605	7.215651279	1.60841944	0.005598311	0.0073876
TMSB4XP8	4.098889837	9.007215102	1.135847899	5.37E-07	1.11E-06
FOXQ1	2.811327012	5.807802464	1.046741108	1.41E-06	2.78E-06
FOLR1	0.341645737	1.965899013	2.524616181	1.89E-07	4.10E-07
CHAF1B	0.767581926	2.142364005	1.480810981	1.61E-20	3.23E-19
SKA3	0.937692705	2.213072061	1.238863315	1.06E-17	1.12E-16
AC105118.1	0.542066191	2.562660512	2.241101436	0.000127205	0.0002017
BICDL1	1.634291292	3.540835597	1.115424711	2.39E-11	8.51E-11
NUF2	1.129605089	3.397835756	1.588797624	8.58E-22	2.38E-20
TUBB6	2.624976479	5.789401856	1.141109805	0.000251896	0.0003871
FKBP10	3.443701605	13.67520329	1.989530235	9.27E-07	1.86E-06
IGKV1OR2-108	0.523116924	1.950644777	1.898745729	0.019323313	0.0240043
B3GNT5	0.895881778	2.046474489	1.191760412	8.09E-09	2.07E-08
LINC02608	7.88758801	3.924100893	-1.00722206	1.29E-09	3.62E-09
SSX1	5.089912624	11.16378263	1.133113144	0.004417436	0.0058967
LTB	5.308374896	12.12050577	1.191107734	5.67E-05	9.34E-05
GNPDA1	4.780988847	10.08050943	1.076187603	8.79E-29	3.60E-26
LINC01436	0.50443838	2.997287506	2.570907525	4.15E-07	8.65E-07
DRAM1	2.327840645	5.4996557	1.240349003	1.09E-25	1.21E-23
PROK1	2.26710684	0.241616859	-3.23005935	0.003916045	0.0052617
ANKRD1	1.022082984	3.414624893	1.740214768	0.002065759	0.0028736
LPAR2	0.805586739	3.040008417	1.915963478	3.21E-12	1.29E-11
SYK	0.986857668	2.4754022	1.326749022	1.26E-08	3.13E-08
CYP3A43	1.967438733	0.817137699	-1.26766759	5.60E-10	1.65E-09
HID1	1.584045216	3.873319434	1.289956968	3.27E-07	6.90E-07
SLC25A47	79.97957502	30.58917863	-1.38661025	5.49E-10	1.62E-09
AC008549.1	14.71651529	7.208044496	-1.02975627	1.89E-07	4.09E-07
CYP1A2	34.46191091	14.87232956	-1.21237206	5.39E-06	9.93E-06
ST6GALNAC4	2.120431178	4.359233584	1.039716852	2.35E-17	2.31E-16
RCC2	7.16660893	18.16305531	1.341644371	6.22E-35	2.47E-31
VCAN	1.371602901	4.433431806	1.692561024	5.08E-07	1.05E-06
ZBTB12	1.060583481	2.910264461	1.456292075	2.04E-25	2.00E-23
FABP3	3.337262972	13.21956285	1.985937191	7.62E-05	0.0001237
LTBP1	2.222838595	4.583550257	1.044062297	8.73E-06	1.57E-05
MACIR	0.564333778	1.759011774	1.640144531	1.00E-13	5.02E-13

(*continued on next page*)

Table 3 (*continued*)

gene	lowMean	highMean	logFC	pValue	fdr
ENTPD2	1.054641704	2.972674928	1.495008756	5.55E-09	1.44E-08
ICAM1	10.77119825	23.22327694	1.108392807	3.78E-10	1.14E-09
S100A9	14.96286044	83.28613269	2.476690304	2.94E-07	6.23E-07
RNF144A	0.637643734	1.608392152	1.334796713	3.08E-12	1.24E-11
BAK1	4.75037241	10.38551153	1.128459752	3.76E-28	1.32E-25
TTR	1237.440583	569.8336548	-1.11874652	3.66E-17	3.46E-16
KCNQ1	1.201690312	4.120362121	1.777705988	3.88E-06	7.29E-06
LPA	4.817584386	2.202713641	-1.12902798	5.59E-13	2.49E-12
KIF2C	1.404464139	5.068041331	1.851408503	1.00E-25	1.15E-23
MT1A	49.06528349	16.44213568	-1.57730489	0.001249168	0.0017804
EMILIN2	0.740410435	1.686324541	1.187485082	2.54E-11	9.00E-11
CDK4	9.371139413	19.3549388	1.046405369	1.33E-26	2.16E-24
TFF1	2.645030417	9.198796543	1.798160816	3.65E-05	6.14E-05
ASNS	1.393188136	3.885504715	1.47971192	1.42E-10	4.55E-10
GMIP	1.796678182	3.603422519	1.004035806	2.24E-17	2.21E-16
CDCA3	0.878836856	2.134034631	1.279916309	2.34E-18	2.87E-17
AKR1B1	4.849224231	11.43499423	1.237629767	3.39E-09	9.10E-09
TTYH3	7.981481401	19.74955987	1.307092054	5.60E-24	3.22E-22
PRTFDC1	0.877559085	1.884147014	1.10234337	8.57E-11	2.82E-10
CACNG4	1.036746738	2.708186217	1.385263435	0.002743895	0.0037499
MAGEB2	0.965472535	3.63318247	1.9119267	0.000629794	0.0009285
ZNF28	0.726035997	1.655288186	1.188969429	3.21E-14	1.75E-13
PKDCC	3.60018815	7.667230256	1.090633201	4.09E-09	1.09E-08
ANKRD52	2.596645585	5.345578793	1.04169705	5.73E-28	1.70E-25
FANCE	1.060125881	2.281496357	1.105744768	7.45E-20	1.27E-18
MT1X	144.6116349	37.05118762	-1.96459194	1.19E-05	2.10E-05
FCN3	5.409702287	2.676969182	-1.01494867	0.005245222	0.0069432
KLF5	1.568159992	4.399675356	1.488324315	1.26E-05	2.23E-05
ITIH5	0.230960622	4.517544807	4.289820104	0.000273782	0.0004195
ITGA3	0.799281245	4.898168867	2.615467371	8.69E-08	1.96E-07
WWTR1	3.026242252	6.316116861	1.061510384	2.07E-08	5.03E-08
SLAMF8	1.63654421	3.507894613	1.099952829	3.14E-06	5.95E-06
MMP9	4.859248072	13.70751313	1.496161865	1.48E-09	4.12E-09
CRABP2	0.664487146	2.749148816	2.048671808	4.22E-05	7.06E-05
RRAD	1.249388208	2.769866115	1.148594425	0.000839941	0.0012222
ZNF385A	2.963170555	6.322763669	1.093413628	1.17E-14	6.91E-14
PIP4P2	1.271487559	3.080145728	1.276481263	2.57E-13	1.21E-12
HDAC7	2.112893945	4.33071494	1.035384859	4.36E-14	2.32E-13
LRRC8B	0.624000282	1.713877874	1.457645725	7.39E-21	1.62E-19
MFSD2A	14.19102219	6.46081198	-1.13519112	7.48E-06	1.36E-05
TM4SF20	1.988884468	7.675899268	1.948376305	4.93E-05	8.18E-05
WDR72	1.727965895	4.212267163	1.285522199	1.02E-06	2.03E-06
SOD3	5.242306863	13.87916483	1.404647047	0.003206348	0.0043499
PHF19	1.229207214	2.788758101	1.18189466	6.69E-23	2.57E-21
KITLG	0.859319545	1.937741894	1.173109804	1.79E-12	7.49E-12
FMNL2	1.240110466	3.433995297	1.469419426	5.35E-13	2.39E-12
SDS	232.0839493	89.69024365	-1.37162379	4.93E-07	1.02E-06
B4GALNT4	0.457747493	1.78229265	1.961110355	0.001170825	0.0016752
USH1C	1.767534462	5.144361071	1.541253562	1.19E-10	3.85E-10
ERP27	0.482055747	1.767366753	1.874329551	1.67E-06	3.26E-06
NEO1	2.488961833	5.298371337	1.090004851	3.94E-16	3.00E-15
MMD	3.618325947	8.585179747	1.246525965	5.15E-25	4.14E-23
DEPDC1B	0.690687808	2.805287347	2.022042892	2.68E-24	1.78E-22
CENPW	5.408123256	11.82020085	1.128054613	4.10E-13	1.87E-12
FJX1	1.059198484	2.55081584	1.267985783	0.000975658	0.0014105
GPD2	1.102896379	2.500662238	1.181012956	3.72E-28	1.32E-25
PLXNA1	1.221960775	3.168665164	1.374677242	5.05E-23	2.02E-21
TTLL4	2.166614368	4.564746725	1.075092421	4.49E-18	5.20E-17
S100A8	2.106548368	9.320217705	2.145482612	0.019527169	0.0242276

(*continued on next page*)

Table 3 (*continued*)

gene	lowMean	highMean	logFC	pValue	fdr
SIPA1L3	1.895670397	3.871331896	1.030121855	2.76E-17	2.65E-16
LRCOL1	3.937731949	1.951089028	-1.0130853	4.30E-08	1.00E-07
DTL	1.542127235	3.609069135	1.226704979	7.12E-20	1.22E-18
NDRG1	16.59639833	35.49800628	1.09686781	8.73E-11	2.87E-10
ALDH3B1	1.519818733	3.620674353	1.25235916	1.52E-12	6.38E-12
F9	92.97811661	39.03211419	-1.25222959	3.34E-13	1.54E-12
FZD6	1.905579786	4.059472293	1.091062184	7.07E-13	3.10E-12
PBK	1.783046926	4.470063561	1.325950674	2.32E-18	2.85E-17
RFLNA	0.256567352	2.10759909	3.038190955	0.000717646	0.0010524
CNDP1	1.579449578	0.392994687	-2.00684017	7.31E-06	1.33E-05
LILRB4	0.697499772	1.582921534	1.182325093	4.88E-07	1.01E-06
CKAP2L	0.555466718	1.59194536	1.519018443	3.16E-23	1.37E-21
OLFML2B	1.990150622	5.228052876	1.393396109	2.06E-10	6.42E-10
CCNE1	1.934778429	5.169430495	1.417836993	1.32E-20	2.71E-19
SLC7A10	0.193137123	1.905836106	3.302726665	4.56E-07	9.47E-07
COL16A1	0.725455629	1.923704397	1.406927844	3.45E-07	7.25E-07
BUB1B	0.740996211	2.573734703	1.79632528	9.57E-27	1.65E-24
MFSD10	5.157719532	13.39259871	1.376630701	1.42E-18	1.83E-17
MOGAT2	8.752677084	3.597652768	-1.2826684	4.59E-10	1.37E-09
VNN2	3.592147267	9.714258366	1.43525736	5.14E-08	1.18E-07
C11orf49	0.975349037	2.053108487	1.073819365	2.61E-16	2.06E-15
VLDLR	0.48867081	1.605026606	1.715662379	3.70E-08	8.68E-08
GUCA2A	0.691065352	2.027061682	1.552495936	0.00439018	0.0058643
ADAM8	0.889338739	1.922793208	1.112398678	2.77E-10	8.47E-10
PLP2	20.33237089	47.71337652	1.230615332	1.67E-10	5.27E-10
SERPINC1	2060.690685	870.9342536	-1.24249225	1.16E-24	8.33E-23
KIF18B	0.73166824	2.490500043	1.767173894	5.56E-23	2.19E-21
SMARCD3	0.997210312	2.683385754	1.428084759	9.58E-08	2.15E-07
SCTR	0.332201283	5.707567113	4.102746369	6.11E-07	1.25E-06
ZSWIM5	0.835310658	1.817199178	1.121331807	4.33E-14	2.31E-13
TACC3	2.812949903	6.858681152	1.28584733	9.16E-22	2.52E-20
ARNTL2	0.967987577	2.274592358	1.232547578	8.62E-13	3.74E-12
IQGAP3	1.785035749	3.958679343	1.149066245	4.58E-17	4.24E-16
HMMR	1.57945492	3.436153631	1.121367781	2.56E-14	1.42E-13
FCN2	2.739530247	1.211759733	-1.17682486	4.65E-05	7.74E-05
CYP39A1	6.301191961	2.664690707	-1.24165667	1.45E-06	2.86E-06
MCM8	0.720166923	1.698596868	1.237940251	2.60E-23	1.17E-21
CLEC11A	3.146621141	6.801555639	1.112061269	0.002205604	0.0030518
MCM2	4.158312021	11.37663222	1.452003625	3.04E-23	1.33E-21
ITPR3	0.473521954	2.804073392	2.566020889	1.74E-12	7.28E-12
CEP55	0.587135168	2.441350738	2.055914998	2.33E-26	3.42E-24
PHLDA2	5.626041107	11.54832276	1.037491335	6.11E-11	2.05E-10
ANXA13	4.260807834	13.0103642	1.610462457	3.93E-06	7.37E-06
APOC1P1	91.19091263	28.18276143	-1.69407709	3.77E-11	1.31E-10
TAT	223.4565137	75.14001954	-1.5723407	5.33E-18	6.09E-17
SFXN3	1.995151291	4.862679303	1.285253299	6.34E-12	2.44E-11
PTK7	1.046929201	2.718679801	1.376742361	2.37E-05	4.07E-05
MSLN	0.098129695	2.067691031	4.397187036	0.002421659	0.0033332
AMIGO2	0.888620182	2.040481341	1.199270705	3.05E-07	6.44E-07
WDR76	1.122815442	2.4677984	1.136103731	8.94E-18	9.61E-17
LECT2	47.76647012	21.56888241	-1.14704684	2.55E-14	1.41E-13
CHST2	0.640067169	1.550442578	1.27638488	2.91E-07	6.17E-07
LINC01093	6.373255501	1.988212938	-1.68055822	2.08E-06	4.03E-06
TNFRSF19	1.620055202	3.343278462	1.04522055	0.009350889	0.0120624
DES	0.465574583	2.325749673	2.32061162	0.029546129	0.0358467
GP2	1.294940026	4.281925162	1.725374298	0.026033356	0.0318055
IGSF23	17.62609313	6.446796873	-1.4510583	2.01E-15	1.35E-14
FMNL1	1.101697754	2.251410013	1.031100334	1.43E-09	4.01E-09
TYMS	5.91652986	12.02118158	1.022755543	1.13E-14	6.68E-14

(*continued on next page*)

Table 3 (*continued*)

gene	lowMean	highMean	logFC	pValue	fdr
MAGEA12	1.523400503	4.700922899	1.625648742	0.00070302	0.0010318
ATP1B3	7.881347234	17.07328873	1.115226814	2.02E-18	2.51E-17
FBXL19	1.413048145	2.952027617	1.062895597	5.61E-29	2.47E-26
NCDN	2.096088898	4.614817938	1.138573828	8.51E-30	5.17E-27
CYP4A22	28.20823886	10.86706028	-1.37615488	4.81E-18	5.54E-17
NXPH4	1.509634883	5.175257432	1.777430964	2.23E-14	1.25E-13
SLC25A24	0.492358443	1.694507411	1.783085044	1.19E-12	5.11E-12
RRM2	4.036027681	8.807663435	1.125823271	7.88E-18	8.56E-17
CTSV	0.312796228	2.603413233	3.057109303	2.24E-16	1.80E-15
FIBIN	0.78250499	2.111155555	1.431861027	6.01E-05	9.85E-05
MDFI	0.791218271	2.468964993	1.641758734	0.000408793	0.0006149
PAEP	2.00022586	21.18295082	3.404668753	1.78E-08	4.35E-08
SULF1	1.052563852	3.373377297	1.680285931	1.82E-08	4.45E-08
CPNE7	0.611433642	1.770428451	1.533830701	0.000359848	0.0005447
HJURP	1.263483256	3.616622101	1.517236314	2.85E-22	8.77E-21
SLC41A1	1.521060108	3.430553561	1.173364226	2.30E-16	1.83E-15
SFRP5	0.926727006	14.67491147	3.985063576	0.001647289	0.0023151
TMC6	1.556604492	4.145718321	1.413219671	5.56E-10	1.64E-09
AC136601.2	2.044484106	0.956327002	-1.09616093	3.21E-08	7.60E-08
PCK1	132.9858515	59.95370077	-1.14935205	4.78E-16	3.59E-15
NDN	2.604970436	7.091816795	1.444888268	0.00453586	0.0060466
AC006329.1	3.824379603	1.701556959	-1.16837028	3.47E-14	1.88E-13
CLDN4	4.698047234	14.42551328	1.61848953	8.52E-09	2.17E-08
KRT80	0.258642798	2.677350573	3.371773134	1.65E-08	4.04E-08
CDCA7L	0.890631231	2.707623911	1.604127254	1.02E-18	1.36E-17
LINC01554	28.87353625	9.929266032	-1.53998883	3.54E-08	8.32E-08
PDE4A	0.840183829	1.826735136	1.120490545	3.24E-08	7.66E-08
PCLAF	1.523515964	3.983511258	1.386636035	1.37E-21	3.60E-20
CYP2A13	3.943499094	0.583964867	-2.75552283	1.68E-13	8.14E-13
ARHGEF25	0.707096235	1.465638482	1.051550805	0.020144953	0.0249499
MT1E	166.8333022	49.87607975	-1.74198732	0.002981826	0.0040573
RCAN3	0.7005272	1.49896803	1.09745664	7.11E-18	7.85E-17
KIF20A	1.530817994	4.533725499	1.56639428	5.15E-22	1.49E-20
FOXJ1	0.356983704	2.571392036	2.848619458	5.00E-13	2.25E-12
LINC00942	0.496991553	2.732225945	2.458783558	9.20E-10	2.63E-09
MMP1	0.412451325	3.7161184	3.171500692	4.00E-10	1.20E-09
LINC01018	15.34634161	7.613101589	-1.01133854	1.00E-08	2.52E-08
DCLRE1B	0.9535369	1.924650921	1.01323613	1.52E-26	2.41E-24
RACGAP1	2.209263936	5.352581979	1.276669202	3.04E-23	1.33E-21
GPD1L	1.171834579	2.700198223	1.204296393	2.66E-15	1.75E-14
MAGEA3	3.555433908	8.36529844	1.234391373	3.78E-05	6.35E-05
SLCO3A1	0.974019948	2.01418321	1.048171692	2.16E-05	3.72E-05
PLPP2	1.677511591	6.26593044	1.901206019	2.15E-08	5.22E-08
LAMC2	0.236178135	3.093514326	3.711299399	6.11E-05	0.0001001
PLCD3	0.546386652	1.975646556	1.854330726	1.31E-13	6.48E-13
TES	3.750483569	7.941026307	1.082248853	1.26E-17	1.32E-16
SH3RF1	1.553139394	3.376483781	1.12033431	2.50E-11	8.89E-11
EPS8L3	3.392616651	8.23331938	1.279075769	3.32E-10	1.01E-09
AC011591.1	1.890094803	0.874295948	-1.11226498	1.35E-06	2.66E-06
TMPRSS3	0.980130858	2.911992123	1.57096017	1.00E-07	2.25E-07
GRAMD1B	0.610173215	1.550932638	1.34584527	1.04E-08	2.62E-08
PTPRS	1.048286382	2.389381331	1.188604216	0.010883469	0.0139351
UBE2C	6.927108672	20.73463099	1.58171716	6.99E-18	7.74E-17
CCL28	0.935982083	2.207016835	1.237544816	2.60E-08	6.24E-08
MOB3B	0.947041232	2.084490659	1.138195762	4.74E-05	7.88E-05
CXCL6	1.674757628	7.578877783	2.178031919	2.70E-05	4.61E-05
AC021146.9	14.29035041	5.917827812	-1.27190167	4.68E-14	2.48E-13
NKD2	0.650193205	1.445605359	1.152733376	0.012774443	0.0162202
BUB1	0.764343944	2.32884243	1.607319148	2.10E-25	2.03E-23

(*continued on next page*)

Table 3 (*continued*)

gene	lowMean	highMean	logFC	pValue	fdr
NUP210	5.049615177	10.26708442	1.0237812	1.65E-22	5.56E-21
DPYSL3	1.559520668	3.490608887	1.162376044	0.000357186	0.0005411
KIRREL2	0.025128506	2.93219843	6.866514004	2.00E-07	4.32E-07
CLSTN1	6.220024741	16.46536509	1.404442278	2.25E-19	3.44E-18
MISP	2.12081692	4.585267056	1.112385676	1.16E-06	2.31E-06
HHIPL2	0.988339826	2.294716056	1.215236567	0.001429814	0.0020255
MMP2	5.274654201	13.64490245	1.37121366	0.005437551	0.0071842
RAD51AP1	1.003933596	2.583212013	1.363502209	5.10E-22	1.48E-20
F3	0.693787034	1.755877666	1.33962755	3.62E-09	9.68E-09
SPDL1	0.994512957	2.09653461	1.075944574	2.14E-23	9.96E-22
TMEM201	1.088505532	2.250448196	1.047863615	4.02E-22	1.19E-20
RAVER1	0.943852648	2.169528648	1.200748085	1.21E-15	8.51E-15
ITGB4	1.384860979	5.987328837	2.112171351	1.13E-09	3.21E-09
GPC4	0.85659542	2.962596078	1.790176073	5.41E-07	1.11E-06
AC079360.1	2.022514021	0.765451872	-1.40176613	6.27E-09	1.62E-08
CABYR	1.411857791	2.931254374	1.05392339	8.69E-07	1.75E-06
RBP2	0.646034907	2.268796706	1.812243318	0.000203877	0.0003164
STK26	1.476139389	3.051054587	1.047479033	1.25E-12	5.35E-12
TPM2	8.232690345	16.61335424	1.012907515	0.000544256	0.000808
HSD17B13	71.23076279	33.13393212	-1.10419102	1.03E-05	1.84E-05
ARMCX1	0.984601774	2.47252248	1.328371394	7.08E-07	1.44E-06
APOA5	153.2167519	65.87362752	-1.21780114	1.19E-19	1.94E-18
ROBO1	4.40580932	9.360246935	1.087139533	1.77E-09	4.89E-09
FOXM1	2.083811788	6.028895847	1.532668828	2.75E-22	8.49E-21
VANGL1	0.837054277	1.71864552	1.037878932	3.77E-23	1.59E-21
LINC00221	0.663833377	1.600720846	1.269828661	0.000760651	0.0011127
KIF4A	1.380760899	4.345625012	1.654100173	1.74E-23	8.35E-22
FCGR2A	1.56101762	3.335676926	1.095492743	7.98E-11	2.64E-10
CA9	1.282150169	23.45336591	4.193157836	1.81E-23	8.65E-22
CENPM	2.479174913	6.138758827	1.308086931	6.40E-20	1.11E-18
TNFAIP2	8.003255848	16.92747011	1.080707436	1.63E-08	4.01E-08
NMB	3.154512179	6.961575132	1.141996847	9.81E-11	3.20E-10
RTL8B	1.020430338	2.433294122	1.253733019	0.000127846	0.0002026
WNK2	0.400754493	2.442022762	2.607286048	9.21E-10	2.63E-09
C2CD4A	0.76155848	2.833271858	1.895442307	1.66E-07	3.63E-07
RAB25	1.95969367	6.809745134	1.796972647	0.040143566	0.0479457
FLNA	11.72480016	33.15760393	1.499776424	5.30E-09	1.38E-08
KRT23	8.645093136	19.6694981	1.186006734	0.0102728	0.013193
FNDC5	14.71227059	4.727985832	-1.6377223	5.88E-09	1.53E-08
FAM117B	0.643434303	1.808957038	1.491293387	3.11E-22	9.39E-21
LAMC1	12.60036578	25.46800327	1.01522024	4.66E-15	2.92E-14
CLIP2	1.728641085	4.44493539	1.362524093	1.30E-14	7.62E-14
ANLN	1.047692443	3.69084861	1.816737296	1.14E-25	1.24E-23
IMPDH1	2.111284929	6.587299158	1.641565779	6.03E-16	4.42E-15
MAGEC2	3.156360583	7.207833834	1.191303724	0.018879587	0.0234805
SEL1L3	2.316729462	9.640088351	2.056956787	5.28E-12	2.05E-11
MXRA5	0.502759764	1.57650962	1.648792873	0.008176929	0.010609
TNFRSF11B	1.710386195	4.827479091	1.496947897	9.02E-07	1.81E-06
CXCL1	2.949650768	15.05914531	2.352023833	2.90E-08	6.89E-08
TMC5	0.597803931	3.238503614	2.437583066	1.62E-09	4.51E-09
PKM	7.984789813	44.22628061	2.469577581	6.18E-25	4.83E-23
AC010547.2	0.236780575	2.122033402	3.163824729	4.82E-05	8.00E-05
ANXA2P2	1.528443945	3.309747372	1.11465746	1.85E-14	1.05E-13
PAPLN	0.931573918	3.565689469	1.936438913	5.63E-10	1.66E-09
CYP8B1	97.75362979	37.21709778	-1.39318472	4.63E-14	2.46E-13
HPR	251.3515068	109.4280816	-1.19972333	1.02E-16	8.77E-16
CYBA	13.59713983	27.96502592	1.040320457	2.44E-07	5.23E-07
OSBPL3	0.715950317	1.726675022	1.270065198	2.33E-17	2.29E-16
CHGA	0.287707916	4.154755352	3.852086705	0.018491621	0.0230269

(*continued on next page*)

Table 3 (*continued*)

gene	lowMean	highMean	logFC	pValue	fdr
PRSS2	0.538876755	15.94776985	4.887255525	0.000363268	0.0005496
BCL9	2.319450868	4.807110684	1.051386736	2.76E-19	4.15E-18
LINGO1	1.178675923	2.422029641	1.039049417	1.30E-05	2.29E-05
GSTP1	12.8884454	35.15601786	1.447693408	0.004864141	0.0064603
LHFPL2	1.050698304	2.539885807	1.27341516	2.92E-15	1.91E-14
RASEF	0.900176454	2.296095758	1.350903076	1.99E-05	3.45E-05
PLTP	8.829201059	23.22371512	1.395243978	4.57E-06	8.50E-06
WDR54	1.007901789	2.342129897	1.216466023	1.13E-15	7.96E-15
EPCAM	13.33681586	31.0687255	1.220048794	0.000443177	0.0006641
BAMBI	11.02923	23.36579671	1.083066157	3.82E-12	1.52E-11
B4GALT5	6.859948313	13.8483172	1.013441064	7.79E-20	1.33E-18
GLYATL1	19.54299934	7.936262886	-1.30012018	2.94E-19	4.36E-18
H2AC7	0.667513986	1.373532488	1.041021064	1.05E-06	2.09E-06
CTH	39.35070407	19.42141986	-1.01874077	9.40E-08	2.11E-07
IL2RB	1.092382808	2.245721772	1.039700686	0.000432749	0.0006495
IGHV4-39	8.351142607	38.18702814	2.193037142	0.004321298	0.0057774
FMOD	3.08178588	6.409816996	1.05651654	0.00121976	0.0017408
ARHGEF2	2.154037406	4.863302612	1.174893061	7.94E-18	8.62E-17
MICAL1	1.536731073	3.258635083	1.084403085	1.57E-11	5.73E-11
MAGEA6	2.799655404	6.847895139	1.290411346	3.12E-06	5.91E-06
SAA1	1663.310761	770.2018143	-1.11074931	0.001199147	0.0017136
POSTN	2.178208668	6.68480026	1.617742285	1.58E-07	3.45E-07
AC007423.1	4.245302445	1.704951015	-1.31613705	0.009942972	0.0127943
LAD1	15.7104891	33.34500834	1.085742714	6.97E-05	0.0001135
COLCA2	0.814394139	2.419432075	1.570869353	2.28E-13	1.08E-12
RDH16	59.94166922	25.58666655	-1.22816706	1.38E-11	5.09E-11
SH3YL1	0.810711701	1.730102987	1.093597048	0.020513148	0.0253742
TC2N	1.123958654	3.005953506	1.419233729	1.64E-06	3.20E-06
FBLN1	3.63412805	12.14267568	1.740405199	0.000130913	0.0002071
C4orf46	0.667025478	1.497736314	1.166969876	2.66E-30	1.86E-27
FCGR3A	7.273749111	15.06410316	1.050343715	4.83E-06	8.96E-06
H2AW	1.795635376	4.387402185	1.288872537	8.14E-09	2.08E-08
ATP1A1	46.6862051	103.1068441	1.143071872	2.02E-17	2.02E-16
ELOVL7	0.973682531	4.064293195	2.061481117	1.54E-10	4.90E-10
ABCC4	1.187405293	2.499839498	1.074023021	1.35E-09	3.79E-09
YBX3	2.604403257	5.429675863	1.059913228	2.30E-05	3.95E-05
CCDC9B	0.818273985	2.134911924	1.383520661	1.51E-06	2.98E-06
PLEKHB2	3.75336848	8.093695736	1.108612684	2.12E-22	6.82E-21
GINS1	1.26835561	3.763457057	1.569099218	7.62E-24	4.17E-22
CTHRC1	2.414051697	7.689371655	1.67140914	1.18E-10	3.81E-10
KEL	0.251761452	2.067650333	3.037862918	0.001305337	0.0018569
AC022784.1	0.622474181	1.450136015	1.220102321	0.001565547	0.0022082
PLCB1	0.717044323	1.484963103	1.050292881	4.95E-13	2.23E-12
PTPRC	1.361791484	2.961287595	1.120718793	8.85E-05	0.0001425
SMIM10	0.62978046	1.581025873	1.327940076	8.96E-05	0.0001442
LAIR1	0.984054585	2.053134374	1.061017804	2.98E-08	7.07E-08
GPRIN1	0.586928024	1.569933652	1.419448091	3.59E-23	1.52E-21
CDC7	0.74194361	2.032728513	1.454036099	1.08E-23	5.52E-22
CTAG2	2.799859541	9.502421868	1.762940804	0.000225277	0.0003479
KIF11	1.045191944	2.934767775	1.489478439	1.19E-24	8.53E-23
E2F3	1.743441133	3.987426433	1.193520249	3.40E-27	6.75E-25
CPVL	5.127042703	10.76807662	1.070561761	6.80E-06	1.24E-05
WIPF1	1.49765821	3.041380319	1.022017819	2.64E-07	5.62E-07
TACSTD2	0.953710912	4.925605281	2.368677091	0.039960032	0.0477315
ZSWIM4	0.881326434	2.037882838	1.209322728	3.91E-16	2.98E-15
NAALADL1	1.118325344	2.583365381	1.207911748	0.000526834	0.0007837
HES4	2.219322947	5.055287297	1.187673466	4.31E-08	1.00E-07
NCK2	4.366113169	11.94082857	1.451481518	9.68E-11	3.16E-10
RAB31	1.740745591	3.681118936	1.080438994	7.21E-09	1.85E-08

(*continued on next page*)

Table 3 (*continued*)

gene	lowMean	highMean	logFC	pValue	fdr
MUC20	1.413744959	3.634206123	1.362118368	0.012225805	0.0155783
MUC6	1.907107271	6.704086244	1.813654714	0.007144751	0.0093289
PNMA5	0.482597189	2.123632912	2.137642989	0.012550677	0.0159683
MAMLD1	0.917466312	1.898412017	1.049066048	0.000172213	0.000269
CCNB1	5.434333107	13.71317493	1.335387723	5.11E-21	1.16E-19
MPZL1	6.789253276	13.8940544	1.03314284	6.42E-27	1.16E-24
MAB21L2	0.426217229	1.837552757	2.108124855	0.000552425	0.0008195
SINHCAF	1.236250555	3.471653739	1.489651892	7.95E-17	7.07E-16
FANCD2	0.567575161	1.495982576	1.398210014	1.14E-22	4.01E-21
LINC02506	1.496656197	3.105803053	1.053223495	0.005650716	0.0074518
B3GNT9	0.636420046	1.784470977	1.487445253	9.91E-15	5.93E-14
SLC12A2	1.394471138	3.188703158	1.193251726	2.20E-08	5.33E-08
LINC02362	3.358075462	1.561193037	-1.10498572	3.27E-09	8.80E-09
ADCY1	1.748204112	0.795043258	-1.13676837	2.92E-05	4.96E-05
HENMT1	0.752111543	1.587507419	1.07774479	5.58E-05	9.19E-05
LCAT	22.50708933	10.8917337	-1.04714588	1.67E-11	6.06E-11
YEATS2	1.096401926	2.369497615	1.11180444	2.45E-32	3.65E-29
STX3	2.37924109	5.626275861	1.241678822	1.42E-19	2.26E-18
PSRC1	1.194910053	2.85682236	1.257509308	2.15E-19	3.32E-18
TMED3	1.292560231	2.759378282	1.09411174	5.01E-10	1.49E-09
NEK2	1.674595172	4.318924313	1.366859663	3.59E-20	6.55E-19
LRRC1	1.523137968	3.355726648	1.139578572	7.45E-17	6.68E-16
MLLT11	1.104879783	2.352214517	1.090130232	0.000170216	0.000266
NCF2	2.595653199	5.659345768	1.124537644	2.06E-10	6.42E-10
ADAP1	0.616716472	1.444227626	1.22761886	6.65E-06	1.21E-05
GPRC5B	1.833202388	3.94750436	1.106574789	0.000388944	0.0005868
GRB7	2.840067986	6.42864761	1.178589805	4.34E-08	1.01E-07
NDST1-AS1	1.725319053	0.669094058	-1.36658224	6.41E-06	1.17E-05
SLC7A5	3.279134455	7.001072704	1.094260931	1.31E-08	3.25E-08
NDUFA4L2	5.702258116	16.26585042	1.512241002	8.28E-08	1.87E-07
MLANA	0.099599843	2.1071894	4.403032715	0.001127575	0.0016172
COMP	0.533316393	1.877355246	1.815638093	0.000992777	0.0014337
EGLN3	0.627488559	2.624802925	2.064548047	2.74E-12	1.11E-11
AGRN	10.6736508	24.00624289	1.169355914	3.55E-16	2.72E-15
PRR15L	3.394785974	8.342061606	1.297083345	1.77E-05	3.09E-05
PKMYT1	0.81171693	1.916572362	1.23947986	1.07E-20	2.26E-19
MFSD6	1.346386151	2.94100896	1.127218937	1.27E-09	3.59E-09
G6PC	206.8615047	91.6913541	-1.17380759	6.21E-18	7.00E-17
C15orf48	2.991941813	8.31304792	1.47429541	4.79E-10	1.43E-09
CDR2L	0.945959603	2.932599022	1.632329344	8.16E-05	0.0001319
RAD51	0.712902404	1.730822812	1.279681548	1.55E-20	3.13E-19
MARVELD1	1.79315935	3.693960055	1.042664566	4.47E-06	8.31E-06
TUSC3	1.226148474	3.827437505	1.642245136	6.60E-07	1.35E-06
UAP1L1	0.673683219	3.313172203	2.298070921	2.21E-15	1.47E-14
CTSE	0.634666395	3.1806548	2.325253443	7.12E-05	0.000116
FGFR1	0.623770525	2.147981462	1.783894255	2.69E-05	4.59E-05
SPC25	1.146117957	2.748988849	1.262145522	2.16E-20	4.15E-19
CAD	2.869295297	5.768452489	1.007487885	2.93E-23	1.29E-21
CYP1B1	3.815962219	8.364953503	1.132310633	1.40E-05	2.47E-05
ASRGL1	0.99002363	2.491745767	1.331622012	1.16E-14	6.86E-14
TEAD2	4.180454503	11.2695979	1.430704334	2.53E-19	3.81E-18
TMEM74B	1.256465766	3.072764865	1.290166009	1.26E-07	2.79E-07
ASAP1	2.077355391	4.688727234	1.174448301	5.83E-19	8.17E-18
LOX	0.921727427	2.839564836	1.623257767	7.79E-14	3.97E-13
RHBDF2	2.381643871	4.820602706	1.017255832	2.86E-15	1.87E-14
PAQR4	1.562690557	3.921793995	1.32748163	1.53E-20	3.09E-19
COL1A1	29.15642712	74.17811896	1.347179744	4.86E-06	9.00E-06
TRIM47	6.974430073	14.46114595	1.052034646	1.50E-13	7.33E-13
FERMT1	0.62857588	1.448159102	1.204061294	5.98E-10	1.75E-09

(*continued on next page*)

Table 3 (*continued*)

gene	lowMean	highMean	logFC	pValue	fdr
LGALS9	3.700400332	7.588280583	1.036091666	1.38E-07	3.05E-07
RGS2	4.732105562	16.64024542	1.814122549	6.17E-12	2.37E-11
ANO1	14.27514056	6.395939747	-1.1582767	5.48E-07	1.13E-06
LRIG3	1.703888369	3.675807637	1.109230449	1.53E-12	6.42E-12
NCAPG	1.190000376	3.372570629	1.502886627	1.45E-21	3.80E-20
GPNMB	5.659566511	17.62743106	1.639058777	1.96E-07	4.24E-07
KIFC1	2.720050313	7.784091467	1.516895325	8.35E-23	3.06E-21
RENBP	3.654499646	10.44566102	1.515157993	5.37E-07	1.11E-06
KIF23	0.541861042	1.903720198	1.812826622	1.91E-26	2.88E-24
SERPINI1	1.626982143	5.059861798	1.636899564	7.84E-12	2.98E-11
IFFO2	1.3613032	3.019617693	1.149377474	7.38E-20	1.26E-18
CMTM4	1.153109585	2.346418862	1.024930948	2.68E-10	8.24E-10
AGAP2-AS1	0.836322548	1.932401796	1.208263733	0.005806763	0.0076491
SAA2	204.587123	88.23878713	-1.21323048	0.007674173	0.0099851
HSD17B6	222.6620503	109.7435786	-1.02071916	1.99E-17	1.99E-16
TRIP13	0.832927506	2.876511885	1.78805759	5.87E-25	4.63E-23
B3GNT3	3.727614578	12.10245963	1.698975678	1.14E-06	2.28E-06
MELK	1.346911266	3.854865149	1.517025582	1.49E-23	7.32E-22
C19orf33	1.985111867	5.322886916	1.422988607	0.001078361	0.0015496
NCAPG2	1.236334073	2.707611675	1.130952212	3.49E-21	8.34E-20
SAA2-SAA4	54.9473459	22.76048135	-1.27151873	0.002650126	0.0036282
VSIG1	0.466795694	1.797176315	1.944868797	0.000233207	0.0003596
EVC	0.901327207	2.110008562	1.227126009	4.17E-06	7.80E-06
SMOX	2.473520881	6.197421545	1.325102024	4.21E-16	3.19E-15
IL4I1	0.786999433	3.097442826	1.976643151	9.42E-16	6.71E-15
HS1BP3-IT1	7.247961125	3.619053986	-1.00196259	1.30E-09	3.66E-09
ADAM17	1.031387723	2.336882693	1.179998537	1.30E-19	2.09E-18
KIF12	5.830518003	14.41629351	1.306004321	3.54E-08	8.32E-08
ZNF320	0.540765657	1.599266027	1.564334505	3.21E-13	1.49E-12
ISYNA1	5.448709107	13.60230977	1.319865276	0.004480861	0.0059773
SRPX2	1.043119518	4.068401825	1.963557709	1.08E-05	1.92E-05
BSPRY	1.146394303	2.448972624	1.095073301	4.45E-05	7.42E-05
KIRREL1	0.941752519	2.050654785	1.122664751	0.000105636	0.0001688
SCPEP1	8.146094589	18.24118771	1.163019197	2.30E-13	1.09E-12
NEURL3	1.145732917	4.634319647	2.01608678	5.40E-11	1.83E-10
POLA1	1.03262919	2.091070445	1.017919379	5.84E-23	2.28E-21
FANCI	1.054717903	2.662157584	1.335738789	8.83E-24	4.71E-22
TRIM16	2.111524299	4.641239387	1.136225261	1.69E-10	5.33E-10
AL162582.1	2.759466113	0.863154397	-1.67669862	2.01E-10	6.27E-10
UROC1	16.99271454	6.651649996	-1.35313218	1.66E-10	5.24E-10
TGFB1	7.96789167	17.65262929	1.147613145	8.56E-07	1.73E-06
CORO2A	1.336777309	2.797645122	1.065453821	1.29E-09	3.64E-09
CRYGS	0.719704798	2.51240403	1.803591308	7.08E-07	1.44E-06
STMN1	8.496105099	18.88927736	1.152693992	2.88E-19	4.30E-18
FBLIM1	3.801091089	8.680870279	1.191426085	2.08E-11	7.46E-11
HLA-DOA	1.89294888	4.26185117	1.170844762	0.004480861	0.0059773
ASPDH	33.6850447	13.46154716	-1.32326398	8.35E-19	1.14E-17
CDC20	5.026303415	16.60192642	1.723780988	7.66E-22	2.16E-20
PLA2G7	2.56551112	5.62623881	1.132924512	8.68E-05	0.0001398
OXCT1	0.933996781	2.122374893	1.184190032	1.19E-06	2.37E-06
PPP1R18	6.011572358	12.56742343	1.06387461	8.22E-17	7.28E-16
IGHV1-3	0.285192023	1.809460048	2.665553721	0.012611728	0.0160392
PLEKHG2	1.159788049	2.353208372	1.020767896	6.10E-18	6.89E-17
GBA3	12.16814765	5.822792763	-1.06332639	1.46E-09	4.08E-09
PAQR5	1.135232714	3.419658267	1.590864092	2.44E-12	9.97E-12
IGSF3	1.14125313	3.724290486	1.706346787	5.70E-14	2.97E-13
CDC45	1.365998489	3.430590333	1.328500967	1.26E-20	2.60E-19
AP001065.3	3.758197335	1.524818848	-1.30140296	2.13E-20	4.12E-19
AC026401.3	2.140118871	4.50124617	1.072633535	3.60E-18	4.27E-17

(*continued on next page*)

Table 3 (*continued*)

gene	lowMean	highMean	logFC	pValue	fdr
CRHBP	1.782535474	0.758628294	-1.2324657	1.63E-06	3.19E-06
ADRA2A	0.489887565	1.566905283	1.677395396	0.016156368	0.0202829
ACSS1	1.477464119	3.153910439	1.094018598	2.11E-08	5.11E-08
FAAP24	0.755043718	1.576218117	1.061835103	1.44E-27	3.29E-25
IGF2BP1	1.162457531	2.643876364	1.185476704	3.57E-05	6.01E-05
RTL6	0.870500541	2.124599395	1.287273739	4.21E-10	1.26E-09
TRNP1	7.150933275	16.21608864	1.181222433	1.64E-10	5.18E-10
ALPI	2.929743538	6.541219263	1.158785194	0.014656966	0.0184978
PDGFRA	0.891198114	1.874455561	1.072653538	0.02828746	0.0343933
DUSP9	6.33900341	16.2421334	1.357413194	1.84E-05	3.19E-05
NRM	4.260981681	10.52148478	1.304080557	7.06E-21	1.56E-19
PTGDS	25.39593323	160.2730313	2.657862293	0.021267179	0.0262441
FGD6	0.771487832	2.026793471	1.39348378	1.18E-17	1.24E-16
CHST4	0.358924084	2.882127743	3.005383644	8.84E-06	1.59E-05
CARMIL1	0.778902117	2.046160786	1.39340557	1.46E-18	1.87E-17
FYB1	0.909512257	2.030553265	1.158707886	1.06E-05	1.90E-05
TUBA1B	17.6856021	38.75260907	1.131718109	8.94E-23	3.23E-21
AC004832.5	1.519642013	0.745203306	-1.02802552	1.40E-11	5.15E-11
OLFM4	0.086887058	5.488698157	5.981178889	3.00E-06	5.70E-06
SLC7A1	0.734210594	2.208629055	1.588885297	2.09E-14	1.17E-13
SNAP25	0.570993076	3.221696416	2.496275396	4.63E-12	1.82E-11
LMNB2	3.051458072	8.258303365	1.436346649	1.19E-27	2.82E-25
IFT140	0.680126251	1.40148577	1.043082615	1.94E-14	1.09E-13
CHEK1	0.820907074	1.867953665	1.186167845	3.66E-21	8.67E-20
PTHLH	0.305860786	2.239110849	2.871978894	3.30E-10	1.00E-09
CLGN	2.730404033	6.690187163	1.292932121	1.64E-10	5.18E-10
ZG16	4.696420252	2.005288251	-1.22775188	6.94E-10	2.02E-09
ARMCX2	0.589872916	1.59124058	1.431675898	0.000112152	0.0001787
SLC34A2	0.181030529	11.21109249	5.952550049	4.66E-06	8.65E-06
PRSS22	0.093895989	2.033897269	4.437039466	3.49E-05	5.89E-05
EMP3	5.242534605	11.55796444	1.140550952	3.63E-07	7.61E-07
MMP14	10.96727525	36.33563819	1.728180103	1.95E-15	1.31E-14
SLC16A3	1.424356898	4.874028442	1.774803985	7.89E-17	7.02E-16
PAQR8	0.901493498	2.094754411	1.216392121	2.85E-10	8.72E-10
NUSAP1	5.323551476	12.35950914	1.215160517	7.32E-20	1.25E-18
MYBL2	4.239831113	14.78759023	1.802308268	7.96E-22	2.23E-20
ATP13A2	2.47524825	5.164071988	1.060935888	4.81E-23	1.95E-21
ACSM2A	30.11097873	14.20418415	-1.08397363	1.51E-19	2.38E-18
TMEM156	0.970716132	3.526115883	1.860958515	1.42E-06	2.79E-06
ADRA2C	1.875430502	4.194074256	1.161130603	0.001314404	0.0018682
PFN2	2.266865907	7.363058974	1.699606204	2.24E-08	5.41E-08
SLC36A1	0.925549816	1.852285086	1.000923614	3.10E-21	7.48E-20
KIF2A	1.135761441	2.413373677	1.087391475	1.23E-26	2.03E-24
SLC38A1	2.113447855	6.854965234	1.697550832	1.14E-16	9.71E-16
GLS	2.654380543	5.842100258	1.138111901	1.48E-15	1.02E-14
TGFB3	1.567622014	3.370268008	1.104285583	2.35E-05	4.04E-05
MAPK13	1.723350361	4.183423462	1.279468006	7.24E-11	2.41E-10
CASP2	1.413617896	3.171634216	1.165834186	9.04E-32	1.19E-28
ELF4	0.704116506	2.497068644	1.826349413	4.27E-13	1.94E-12
TCF19	3.558432533	7.971545823	1.163617632	2.88E-19	4.30E-18
SAMSN1	0.702023503	1.483688404	1.0795969	3.17E-07	6.70E-07
MIR23AHG	1.281877255	2.892952537	1.17428453	1.28E-06	2.53E-06
NEMP1	1.618112207	3.424529942	1.081594321	2.62E-22	8.18E-21
LINC02428	5.323676422	2.646121573	-1.00854354	0.00046413	0.0006941
COL4A5	0.600816094	1.558144136	1.374833332	8.08E-08	1.83E-07
PCSK1N	1.272454998	7.664120871	2.59050568	6.40E-05	0.0001047
ASPM	1.23064423	2.893469331	1.233386603	1.84E-15	1.25E-14
MCM3	13.61353202	29.09929594	1.095942826	8.41E-24	4.54E-22
MAPRE1	12.28492105	25.12339098	1.032142616	1.08E-25	1.21E-23

(*continued on next page*)

Table 3 (*continued*)

gene	lowMean	highMean	logFC	pValue	fdr
AL137798.1	2.65089651	1.123724114	-1.23819247	0.000102066	0.0001633
TEDC2	1.211170778	2.590696321	1.096937611	3.81E-17	3.59E-16
FOLH1B	1.51210468	0.519534122	-1.54126761	9.26E-06	1.66E-05
DCXR	420.4422837	176.9769336	-1.24834643	5.52E-16	4.08E-15
CENPH	1.383119342	2.893086643	1.064683886	3.95E-22	1.17E-20
NTS	12.25950821	151.6044749	3.628339327	1.02E-05	1.82E-05
TTC39A	0.615580321	2.424157396	1.977464356	7.45E-17	6.68E-16
MELTF	0.794933105	2.322944744	1.547049472	2.99E-09	8.08E-09
SNHG3	2.070233742	4.665190713	1.172142393	9.51E-14	4.79E-13
RAB3IL1	1.808474365	5.008448824	1.469590705	2.43E-14	1.35E-13
AACS	0.641124971	1.471496019	1.198606133	8.17E-26	9.72E-24
GSDME	0.741367747	1.563470906	1.076491116	1.89E-10	5.94E-10
DLGAP5	0.949460485	2.904900967	1.613309117	3.17E-22	9.52E-21
SLAMF7	0.990225748	2.32681696	1.232528357	0.00305824	0.004157
TYRO3	0.496302074	1.696488505	1.773261266	1.19E-16	1.01E-15
OPN1SW	0.945498194	1.956630942	1.049225054	9.37E-17	8.18E-16
TNFSF13B	0.931455232	1.911990728	1.03751719	1.22E-05	2.16E-05
NBEAL2	1.389860866	2.97761603	1.09921726	5.07E-19	7.19E-18
DNER	0.25232066	2.165143213	3.101132212	1.97E-05	3.42E-05
IQGAP1	2.23829944	5.397626494	1.269922095	1.78E-14	1.02E-13
AL035461.2	1.377707857	2.794791502	1.020470662	9.37E-11	3.07E-10
AC090204.1	0.849813445	1.952478921	1.200088899	8.62E-05	0.000139
DLG3	0.526990969	1.639386858	1.637306193	4.39E-10	1.31E-09
PLGLA	2.6846561	1.128560126	-1.25025401	1.18E-09	3.33E-09
CENPU	2.368273461	4.943545908	1.061710554	3.12E-19	4.63E-18
MAFG-DT	0.977759758	1.993344461	1.027639104	4.88E-13	2.20E-12
AZGP1	358.0799149	178.0887726	-1.00768503	3.88E-18	4.56E-17
SERPINA11	123.7130299	60.9909264	-1.02033092	5.55E-09	1.44E-08
HLA-U	1.128925814	2.280999276	1.014715304	0.000796251	0.0011617
STMN2	0.757125544	1.99702923	1.399251001	0.008113915	0.010533
KCNJ11	0.710805443	1.473555282	1.051774551	4.88E-10	1.45E-09
CHML	1.373440158	3.013111129	1.13345983	1.28E-16	1.08E-15
PDE7A	0.876612602	2.082644053	1.248404964	3.56E-23	1.51E-21
ALDOA	43.11331274	104.0724784	1.271383278	1.87E-20	3.69E-19
CA12	2.025027305	5.662726808	1.483555569	2.59E-06	4.95E-06
TRIM71	0.654816742	1.467037805	1.163742935	1.97E-06	3.82E-06
TMEM158	0.312584947	1.762651584	2.495427122	3.37E-05	5.69E-05
IGLV3-25	9.307933338	21.40672192	1.201531105	0.016811631	0.0210517
NRSN2	2.742072734	7.874632026	1.52194567	3.05E-11	1.07E-10
TLDC2	0.664686215	1.825084231	1.457217709	1.69E-10	5.33E-10
CDCA4	1.77069613	4.040684343	1.190283001	3.57E-25	3.06E-23
RARRES1	3.188856581	7.513007122	1.236351256	1.19E-05	2.11E-05
DUOX2	0.488749303	8.900316419	4.186690076	2.22E-05	3.82E-05
RGS1	2.742806529	7.831951537	1.513718976	2.13E-12	8.82E-12
DCDC2	3.190442217	13.25176194	2.054355882	1.98E-05	3.42E-05
PTGFR	0.996117187	2.621149451	1.395812233	0.008680876	0.0112384
MMP12	0.52384234	3.207957262	2.614450346	1.10E-11	4.09E-11
PGAP4	0.932536446	2.613944554	1.486996524	1.33E-10	4.25E-10
ARMCX6	0.855917116	1.999229272	1.223900927	2.84E-10	8.67E-10
IL18	1.294635487	3.332752122	1.364168064	3.88E-05	6.51E-05
ESPL1	0.868845948	1.897952231	1.127271376	2.72E-15	1.79E-14
EPHB6	0.699308739	2.443604652	1.805009452	6.28E-07	1.28E-06
CTTNBP2NL	0.810962945	1.812022794	1.159893202	2.40E-18	2.94E-17
CYRIB	2.725228925	5.489073259	1.01018517	2.72E-22	8.45E-21
NQO1	38.28129917	79.35985816	1.051769655	0.002567007	0.0035223
LINC01980	1.145185364	2.449194029	1.096725933	0.001180295	0.0016875
GLS2	2.477955915	0.991931943	-1.32083748	9.87E-05	0.0001582
ITGA2	0.677916555	2.031457956	1.583335899	4.95E-13	2.23E-12
ORC1	0.720348643	2.168108049	1.589669422	2.16E-23	9.96E-22

(*continued on next page*)

Table 3 (*continued*)

gene	lowMean	highMean	logFC	pValue	fdr
C12orf75	1.771335555	10.56879535	2.576901504	1.18E-20	2.47E-19
GCGR	14.58060975	5.691348639	-1.35720859	2.24E-08	5.41E-08
KIAA1522	9.070285966	18.32459229	1.014561158	9.03E-19	1.22E-17
TMEM159	0.654399043	2.050664581	1.647848992	7.87E-07	1.59E-06
SMIM22	0.168725358	2.560089008	3.923445252	1.02E-07	2.28E-07
HPD	718.9159057	332.6224488	-1.11193748	1.40E-12	5.93E-12
NDE1	0.741491839	1.532054301	1.046964712	1.14E-24	8.29E-23
APLP1	0.454625676	2.467908269	2.440537699	3.16E-09	8.50E-09
TUBB2B	0.849740475	1.943484681	1.193551547	6.77E-06	1.23E-05
CDC25A	0.653444546	1.628765261	1.317641983	5.83E-19	8.17E-18
CYP3A4	505.9259451	175.1266907	-1.53052725	1.78E-09	4.92E-09
ZNF213	0.782500225	1.66590578	1.090143735	2.22E-20	4.23E-19
HNF1B	2.227577062	6.283552799	1.496105166	1.28E-07	2.82E-07
TOR4A	1.102418897	3.054173494	1.470109494	3.06E-10	9.32E-10
HRG	550.9675112	241.5937742	-1.18938397	1.28E-15	8.93E-15
IER3	14.69091713	38.84321829	1.402738274	7.75E-15	4.71E-14
GLYAT	31.29027123	10.68630063	-1.54995165	3.12E-16	2.42E-15
TMEM44	0.883613473	1.863458068	1.076495034	1.54E-16	1.29E-15
ZNF292	0.799530137	1.686044016	1.07641788	5.11E-19	7.24E-18
LDHB	7.711137835	18.41531368	1.255890311	0.002807275	0.0038321
NSD2	1.236739893	2.584843376	1.063534756	1.22E-23	6.16E-22
ABCA3	0.901105165	2.057605282	1.191198857	0.025219305	0.0308363
TGFA	0.555029552	2.286992275	2.042814999	6.84E-09	1.76E-08
MMP11	2.413420683	5.841909563	1.275360611	1.86E-10	5.84E-10
PKIB	1.471593012	3.641774763	1.307262967	4.71E-08	1.09E-07
CYP2A6	417.5544684	127.6948302	-1.70926429	7.48E-18	8.21E-17
CENPF	1.230017397	3.576550297	1.53989001	3.76E-21	8.90E-20
PDP1	0.846266066	1.950573298	1.204714989	1.24E-08	3.10E-08
NIBAN2	8.035694646	19.65502482	1.290403537	2.06E-14	1.16E-13
GYS2	17.26614447	7.441144493	-1.21434953	3.99E-13	1.82E-12
ASAH1	10.92761003	22.31292489	1.029901737	8.24E-11	2.72E-10
DMKN	0.836952572	2.578091463	1.623085671	0.000277882	0.0004256
LINC02381	1.209575361	3.476578574	1.523167539	3.45E-07	7.25E-07
KRT20	1.044289423	7.827202982	2.905975251	0.001525481	0.0021538
AP001783.1	13.51548822	3.625467447	-1.8983747	5.07E-11	1.73E-10
AC099850.3	0.936043601	3.280274104	1.809168736	6.45E-23	2.51E-21
SAMD5	0.729623137	1.545742343	1.083076475	0.000242962	0.0003741
PLAGL2	1.305376405	2.727839375	1.063292828	7.07E-19	9.79E-18
IKBKE	1.222921098	2.843840074	1.217509011	9.57E-18	1.02E-16
HMGB2	11.85112986	23.84253369	1.008512947	4.30E-18	5.02E-17
HOMER3	2.176931685	6.067612403	1.478832795	1.28E-14	7.52E-14
CDC25C	1.096483815	2.263780931	1.045849836	3.50E-13	1.61E-12
SH3PXD2B	1.234530979	2.622388318	1.086918293	3.07E-16	2.39E-15
CEP170	0.687202941	1.439594967	1.066854848	2.57E-21	6.34E-20
MYLIP	1.686398316	3.651657635	1.114606179	2.12E-14	1.19E-13
ADAM9	3.094173578	8.156478074	1.398392207	4.62E-15	2.90E-14
SLC6A13	2.334961034	1.118318622	-1.06206719	5.20E-12	2.02E-11
AFAP1-AS1	0.629904457	2.100292707	1.737385479	7.99E-05	0.0001293
DNMT1	2.771726365	6.095945087	1.13706507	2.84E-23	1.26E-21
SRC	3.485091293	7.442819484	1.094652797	2.50E-14	1.39E-13
UCHL1	2.15791425	13.23880687	2.617063665	5.32E-07	1.10E-06
PPM1H	0.935639643	2.646872467	1.500263788	2.84E-12	1.15E-11
RNU6-850P	0.710762104	1.579920475	1.152413275	1.78E-12	7.45E-12
MYOF	1.091664302	3.095820768	1.503792669	1.28E-07	2.82E-07
AC112206.2	1.694244047	0.665020782	-1.34917037	3.65E-08	8.58E-08
TRIM16L	3.983602125	8.613913401	1.112595259	0.000142203	0.0002241
TIMP2	11.96057606	28.98386677	1.276963203	0.000372059	0.0005623
ANXA4	13.00207078	28.86044419	1.150352092	5.00E-07	1.03E-06
MUC5B	0.9866622	6.852834003	2.796072597	1.87E-05	3.25E-05

(*continued on next page*)

Table 3 (*continued*)

gene	lowMean	highMean	logFC	pValue	fdr
RNF24	0.694810026	1.651814277	1.249361007	1.49E-23	7.32E-22
SPINT1	4.406293766	18.5597592	2.074540405	4.76E-08	1.10E-07
G6PD	5.127073376	22.64686307	2.143103779	4.57E-28	1.43E-25
HGFAC	36.68660018	15.47748709	-1.24508196	1.54E-07	3.37E-07
ECT2	1.347096838	4.239324846	1.653980955	3.55E-27	6.92E-25
FGFR3	11.53870451	23.87537433	1.049042095	2.52E-07	5.40E-07
SEMA6A	0.691647627	2.964373314	2.099618022	2.72E-08	6.50E-08
LINC01549	2.719826203	1.304912128	-1.05956181	0.002935599	0.0039972
AL035446.1	0.959154845	2.332977765	1.282336911	0.000549073	0.0008147
ZNF83	1.207418888	2.63247865	1.124495555	4.44E-09	1.17E-08
TM4SF1	21.84704512	49.80957376	1.188984901	5.70E-08	1.31E-07
GTSF1	1.443152259	3.966616397	1.458685366	1.30E-05	2.29E-05
TFF2	0.813748011	8.78795831	3.432874009	7.50E-06	1.36E-05
TRIM45	0.534058777	1.6695602	1.64439768	5.78E-23	2.27E-21
TESC	8.373724253	24.13972186	1.527467737	7.36E-08	1.67E-07
HTRA3	1.465823407	4.1126326	1.488350888	1.53E-06	3.00E-06
CKS2	20.60586523	41.47885629	1.009321072	7.48E-16	5.40E-15
WDR91	2.358778163	4.889640981	1.051688797	2.56E-17	2.49E-16
NUAK2	2.411727212	5.421907664	1.168733809	1.80E-10	5.67E-10
LIMK1	1.476797033	4.385565855	1.570291442	8.16E-28	2.16E-25
AC083809.1	1.322670419	4.106382519	1.634414406	3.24E-07	6.84E-07
SPHK1	2.495495983	8.284510697	1.731089909	4.52E-15	2.84E-14
MROH2A	1.913211068	0.511769408	-1.90243023	0.006630058	0.0086855
RAP1GAP	5.470403451	14.52306823	1.408627134	3.02E-15	1.97E-14
RHEX	0.700020292	1.997838334	1.512971195	0.000881652	0.0012798
TRAV30	0.769917323	1.596104527	1.051779698	0.000813167	0.001185
SPP2	91.93488936	36.12592556	-1.34757792	7.93E-15	4.81E-14
MT1CP	6.817395704	0.231762958	-4.87849882	6.06E-05	9.94E-05
SLC44A3	4.074064106	8.791460703	1.109634208	7.80E-10	2.25E-09
COL9A2	0.377370674	2.238401595	2.568414677	7.57E-17	6.77E-16
PMEPA1	1.652735971	7.939652003	2.264219507	0.000101899	0.0001631
ANXA5	39.56572746	81.97613026	1.050952605	2.08E-19	3.22E-18
SYT8	0.561914946	2.604639072	2.212659791	2.23E-08	5.40E-08
TMX2P1	0.793098194	1.702620777	1.102185737	2.31E-16	1.84E-15
PELI1	2.835953519	5.825879156	1.038641889	2.12E-15	1.42E-14
CDCA7	0.453413617	2.243204441	2.306661487	2.73E-11	9.66E-11
VTCN1	0.164212328	5.468735533	5.057572947	1.56E-06	3.06E-06
SMIM6	1.842730189	3.971668922	1.107900517	0.00114111	0.0016352
SLC7A8	0.674403788	1.830944678	1.440903657	9.42E-08	2.11E-07
FSCN1	5.859355989	15.62549882	1.415088237	4.58E-08	1.06E-07
EHF	1.14026879	3.075169282	1.431291886	2.86E-07	6.06E-07
AURKB	2.459040195	6.074374662	1.304640578	2.02E-17	2.02E-16
TEAD4	1.639197963	3.624541497	1.14480841	1.94E-06	3.76E-06
ADGRG1	1.912657804	5.170296002	1.434668095	6.06E-05	9.93E-05
ESRP1	0.971853733	2.742129269	1.49648548	0.013765555	0.0174338
RBBP8	1.999888448	4.043542169	1.015700127	6.42E-19	8.95E-18
GRAMD1A	5.57342807	11.4416061	1.037652713	1.22E-15	8.56E-15
ENO2	0.439070556	2.89879361	2.722927925	1.01E-18	1.35E-17
SLC2A1	1.012764415	4.209320461	2.055288728	1.60E-10	5.06E-10
UGT2B10	125.3522526	58.06017755	-1.11036703	2.48E-13	1.17E-12
CLIP3	0.907678849	2.054577202	1.178587698	4.90E-05	8.14E-05
NPNT	1.495150224	5.524254868	1.885489436	0.005893764	0.0077577
HMGA1	23.92692421	55.31608865	1.209064197	1.23E-19	2.00E-18
MTMR2	1.18672992	2.692358311	1.181878784	4.08E-24	2.54E-22
MYRF	3.792317853	8.95836084	1.24015489	5.46E-12	2.12E-11
MYO10	0.635324523	1.926339281	1.600296213	0.031594939	0.0382154
DKK1	4.594915934	14.09200111	1.616766122	4.40E-07	9.14E-07

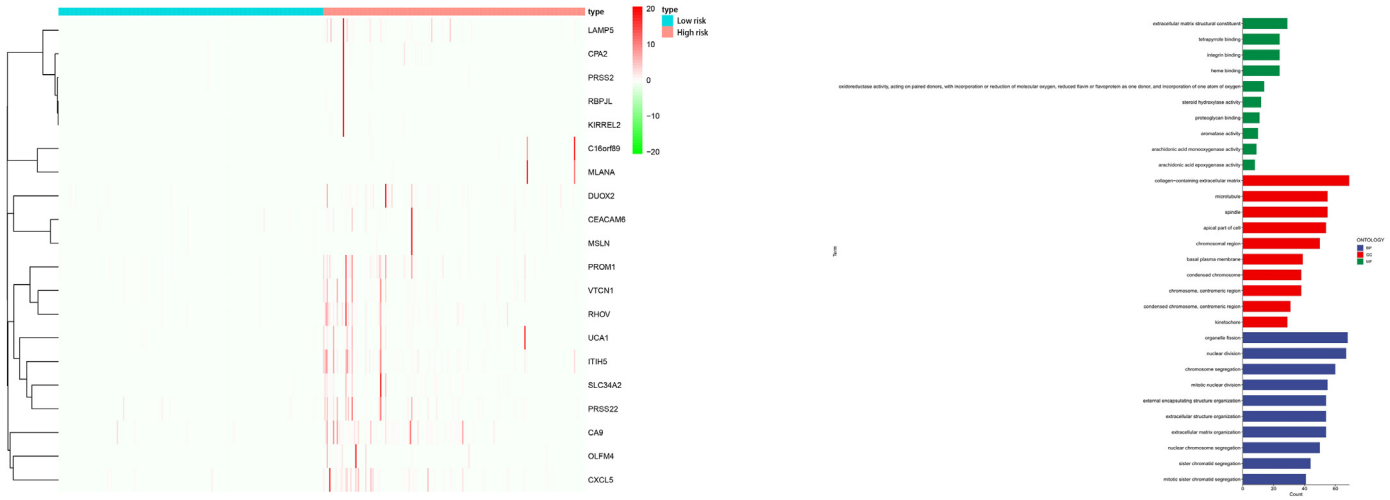

a b

Figure 11. a: Heatmap of differential genes between high-risk and low-risk groups. Differential genes are highly expressed in high-risk groups b: GO enrichment analysis of differential genes in high-risk and low-risk groups. The GO enrichment analysis of the differential genes showed that the differential genes were mainly located in the extracellular matrix and chromosomal regions, and may play regulatory roles in binding sites and catalytic enzymes, thereby affecting the chromosome division and cell proliferation. CC: cellular Component; BP: biological Process; MF: molecular Function.

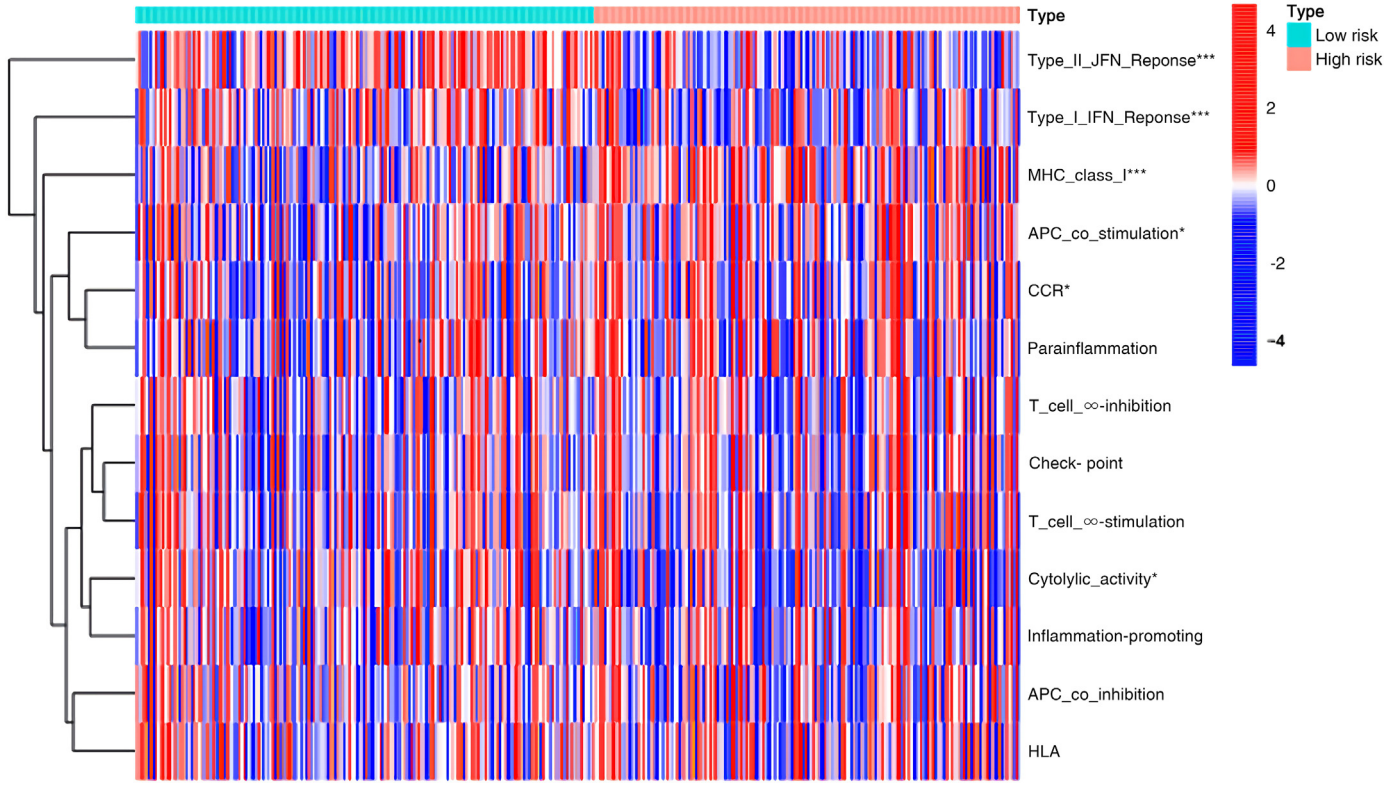

Figure 12. Analysis of differences in immune function between the high-risk group and low-risk group. Blue represents low-risk, red represents high-risk, "*" represents the difference in immune function between the two groups, and "***" represents the significant difference. The results of immune function analysis showed that, compared with the high-risk group and the low-risk group, the two immune functions of type II IFN response and type I IFN response were suppressed, and the function of major histocompatibility complex I (MHC I) was enhanced.

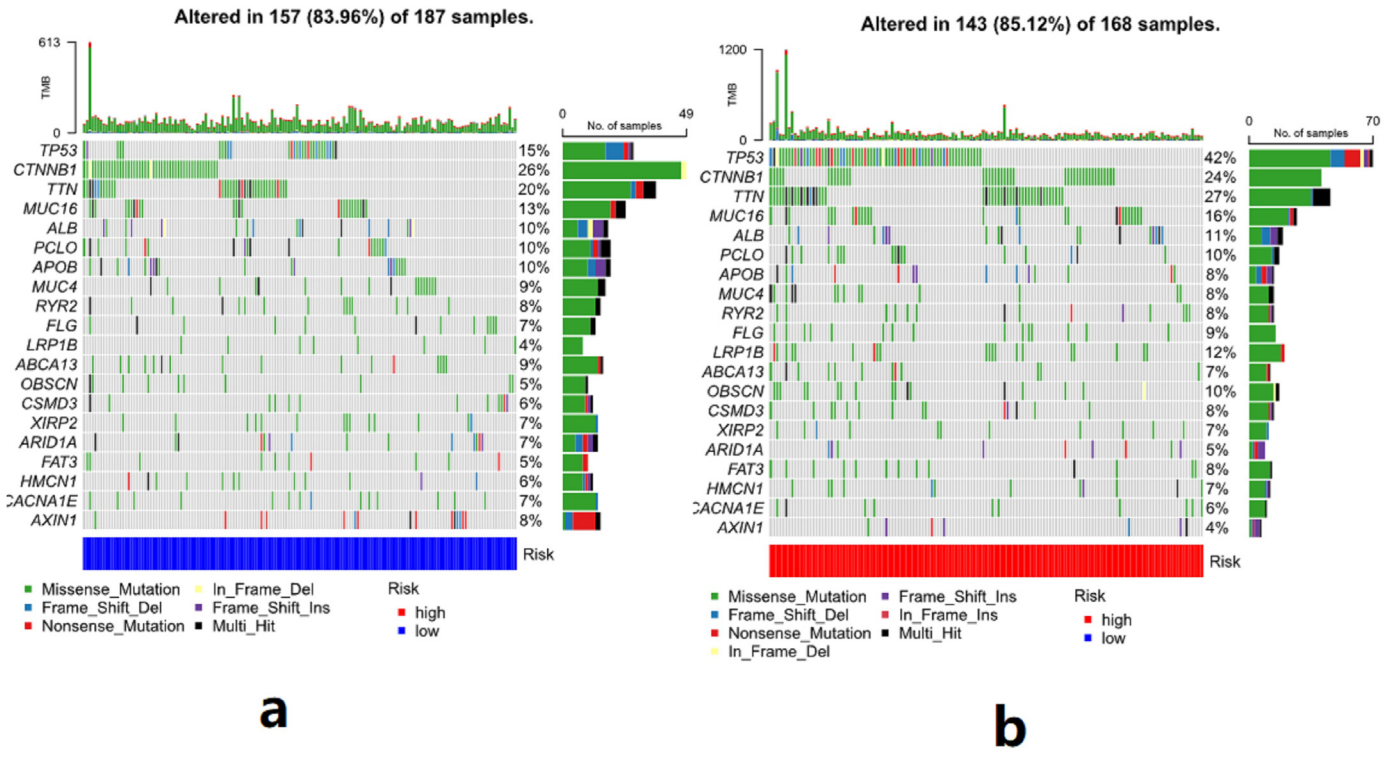

Figure 13. a: Frequency of mutations in the low-risk group, b: Frequency of mutations in the high-risk group. The high-risk group has a higher proportion of gene mutations, and the proportion of TP53 mutations in the high-risk group is significantly higher.

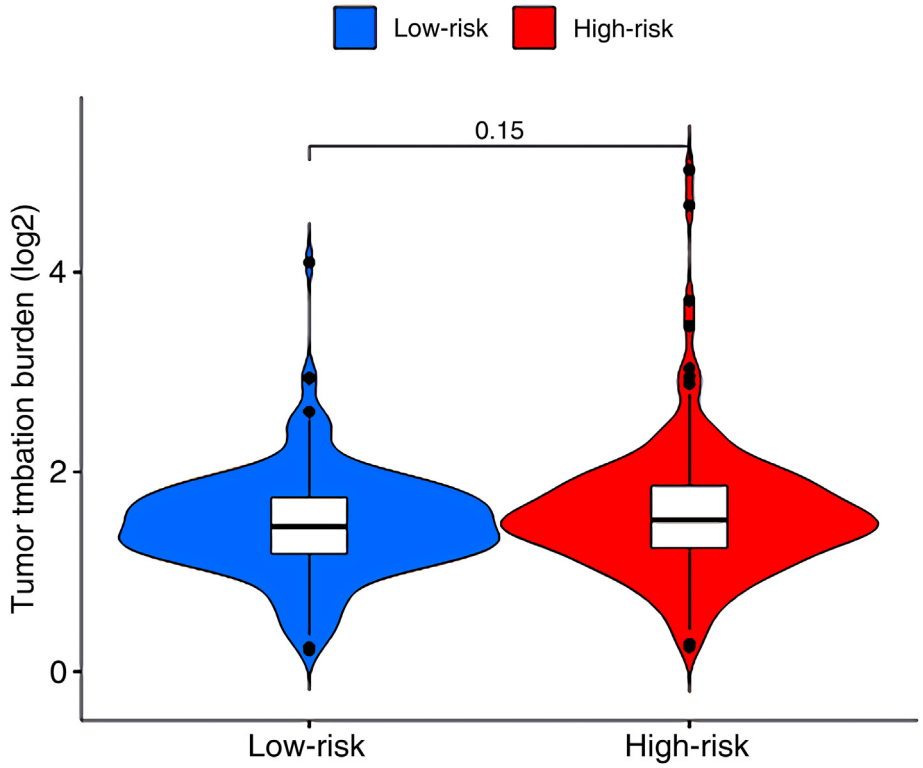

Figure 14. The comparison of TMB between the high-risk group and the low-risk group. There was no difference in TMB between the high-risk and low-risk groups.

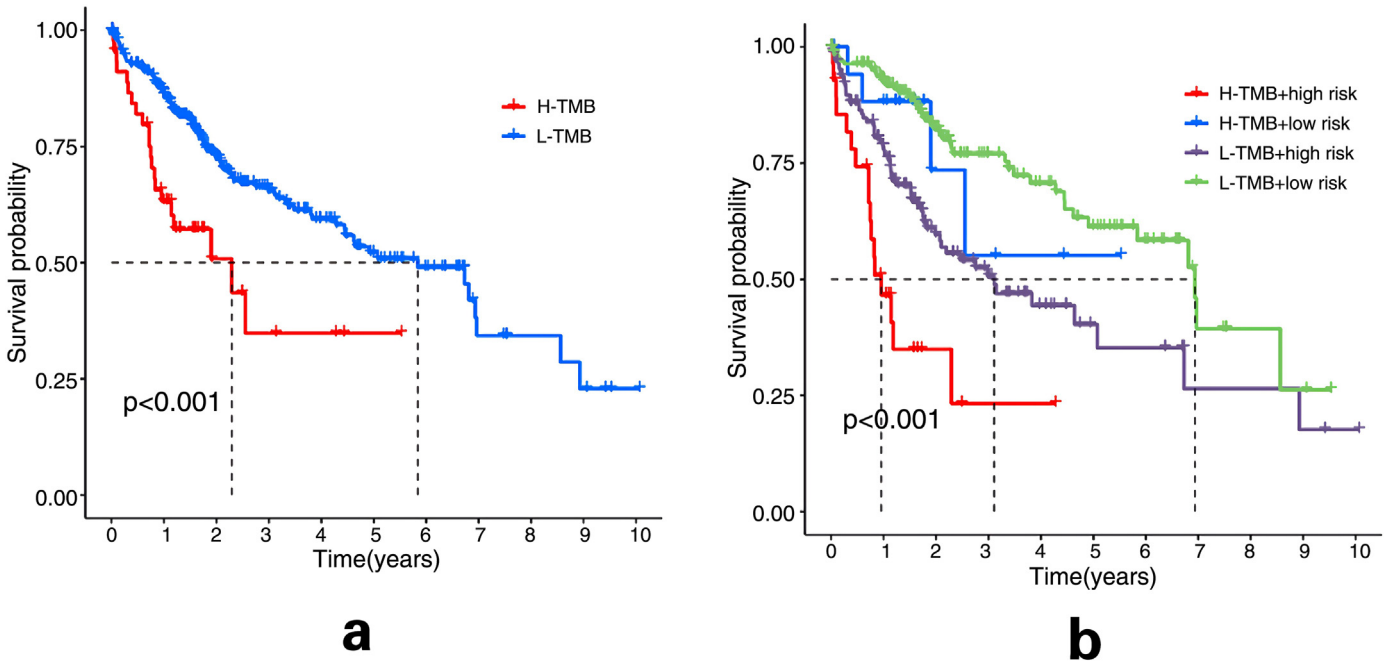

Figure 15. a: survival curves of the high TMB group and the low TMB group. The high TMB group had a worse prognosis and shorter survival than the low TMB group; b: Comparison of survival curves of TBM combined with the risk score for HCC patients.

4.5. Immune function analysis

Type II IFN response, type I IFN response, and MHC class I were significantly different between the high-risk group and low-risk group. Type II IFN response and type I IFN Response were highly expressed in the low-risk group, while MHC class I was highly expressed in the high-risk group. Besides that, APC co-stimulation, CCR, and Cytolytic activity were different, APC co-stimulation and CCR had high expression in the high-risk group, while Cytolytic activity had high expression in the low-risk group (Figure 12). The results suggest that changes in immune function in the high-risk group may contribute to the progression of HCC.

4.6. TMB analysis

Mutations in the high-risk group and low-risk group were analyzed, with the higher frequency of mutations in the high-risk group, as shown in Figure 13. But the comparison of TMB between the high-risk group and the low-risk group found no difference (P = 0.15) (Figure 14). The overall survival of the low TMB group was better than that of the high TMB group (Figure 15 a). When the TMB was the same, the high-risk group had a worse prognosis, and when the risk score was the same, the high TMB had a worse prognosis. Furthermore, the results showed that, in HCC, patients with low TMB in the low-risk group had the best prognosis (Figure 15 b). However, the Low-risk group seems to converge around year 7. This may be due to the smaller sample size of the high-TMB group in the low-risk group, especially 7 years later, no samples were included in the low-risk-high TMB group.

4.7. Screening for potential drugs

Based on previous studies, we found a total of 14 potential drugs, including A.443654, A.770041, ABT.263 (Navitoclax), ABT.888 (Veliparib), AICAR (Acadesine), Akt. inhibitor, AMG-706 (Motesanib), AS601245, ATRA, AUY922 (Luminespib), Axitinib, AZ628, AZD.0530, Rucaparib. A.443654, ABT.888 (Veliparib), AS601245, ATRA, AUY922 (Luminespib), AZ628, and Rucaparib were more effective for the high-risk group, while A.770041, ABT.263 (Navitoclax), AICAR (Acadesine), Akt. inhibitor, AMG-706 (Motesanib), Axitinib and AZD.0530 were more effective in the low-risk group (Figure 16).

5. Discussion

In our research, we found that NRAV and AL031985.3 are the most closely related lncRNAs in HCC. NRAV is a negative regulator of antiviral response. There are still few studies on its function. Existing research shows that it mainly stimulates gene transcription of immune response by influencing IFITM3 and MxA [40]. Besides that, NRAV may promote the development of HCC by regulating immune cell infiltration and immune checkpoint blockade (ICB) immunotherapy-related molecules [41]. Recent studies have shown that NRAV is up-regulated in HCC samples and is associated with a poor prognosis [41, 42, 43, 44, 45]. Possible mechanisms include the involvement of NRAV in regulating acetyltransferase activity, mRNA binding, and transport of GLUT4 to plasma membrane [42]. Similar to NRAV, many studies have shown that AL031985.3 is associated with the prognosis of HCC and can be used to construct a prediction model for the prognosis of HCC [46, 47, 48]. The results of our study were also consistent with those of previous studies, indicating that NRAV and AL031985.3 were correlated with the prognosis of HCC.

Studies have shown that NRAV and AL031985.3 were highly expressed in HCC tissues, modified by m6A, and were associated with prognosis [49, 50]. However, the mechanism by which m6A modifies these two lncRNAs remains unclear. METTL3, an important m6A methyltransferase, is significantly upregulated in HCC and is involved in the proliferation, migration, and colony formation of HCC cells [51]. The study by Zuo et al [52]. also demonstrated that METTL3 can up-regulate some lncRNAs, which is associated with the poor prognosis in HCC. Our results also showed that METTL3 up-regulated NRAV and AL031985.3 in tumor tissues, which was associated with poor prognosis of HCC. Yang et al [53] found that METTL14 is associated with the occurrence and metastasis of colorectal cancer. However, we found that in HCC, METTL14 was not significantly associated with NRAV and AL031985.3. High expression of IGFBP1 can inhibit the development of liver disease [54, 55], and our study also found that IGFBP1 can negatively regulate two lncRNAs. The above studies have shown that m6A is an important

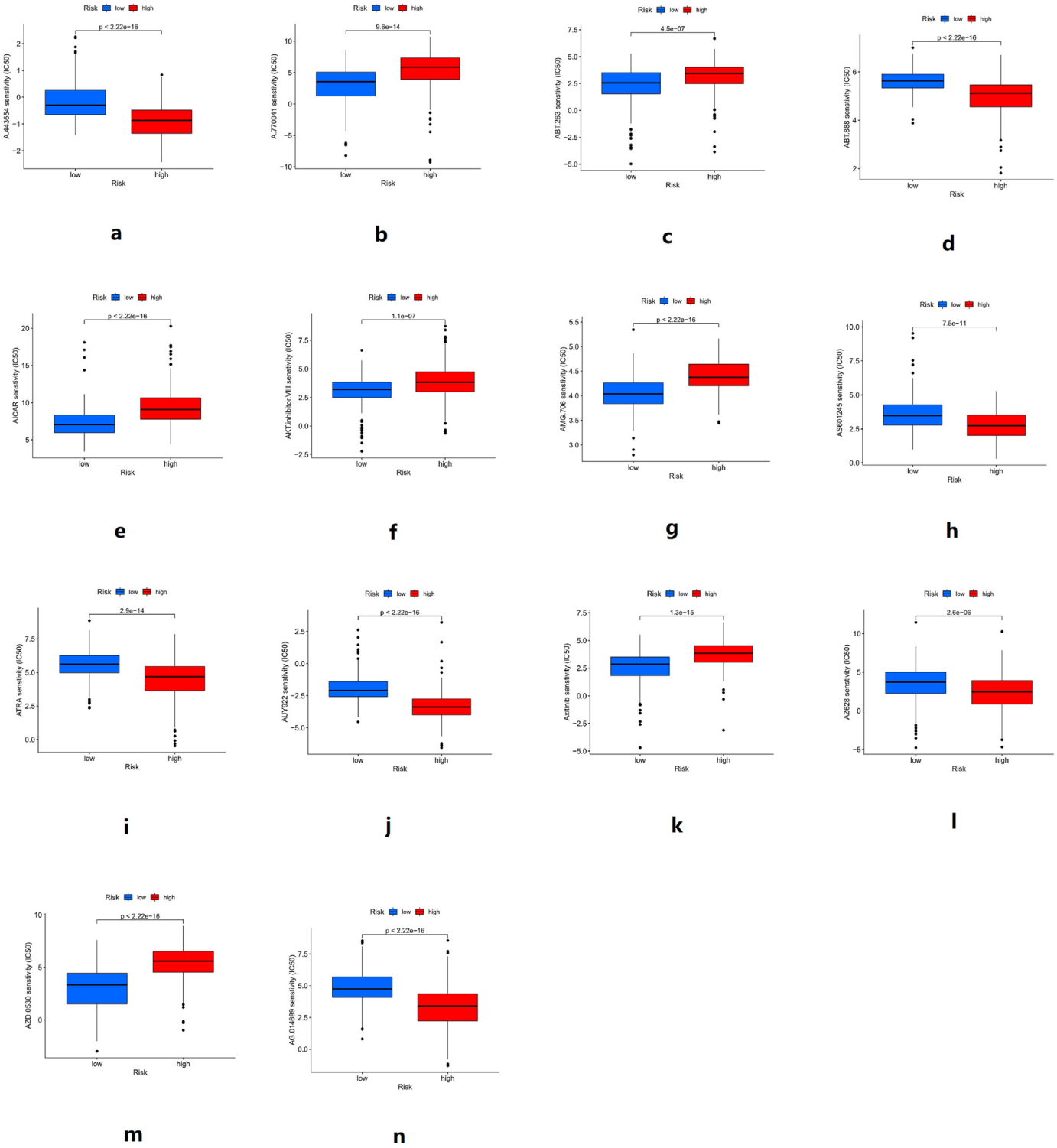

Figure 16. Drug sensitivity analysis of potential drugs for HCC. a: A.443654, b: A.770041, c: ABT.263 (Navitoclax), d: ABT.888 (Veliparib), e: AICAR (Acadesine), f: Akt. inhibitor, g: AMG-706 (Motesanib), h: AS601245, i: ATRA, j: AUY922 (Luminespib), k:Axitinib, l:AZ628, m: AZD.0530, n: Rucaparib.

regulatory mode of lncRNAs, which regulates the occurrence and progression of HCC by affecting the expression of lncRNAs.

Our research found that type II IFN response, type I IFN response, and MHC class I were the three most different functions in terms of immune function between the high-risk group and the low-risk group. Type II IFN response, type I IFN response was significantly down-regulated in the high-risk group, while MHC class I was up-regulated. Although it was believed that the main role of type I IFN was to play an antiviral immune role, existing studies have shown that type I IFN can directly act on tumors by blocking cell cycle progression and inducing apoptosis. They also have indirect antitumor activity, promoting clearance and preventing metastasis by priming immune cells [56, 57, 58]. It is worth noting that hepatitis virus infection is an important pathogenic factor for liver cancer. Compared with other tumors, the influencing factors of type I IFN

response in liver cancer are more complicated. Our results suggested that the type I IFN response is functionally enhanced in the low-risk group, which may be related to the involvement of type I IFN in the naturally occurring protective immune response of primary tumors [59]. Our results are also consistent with previous studies showing that down-regulation of type I IFN enhances tumor growth in a paracrine manner, reduces T lymphocyte cytotoxicity, and the ability of dendritic cells (DC) to process and present antigens [59, 60]. Type II IFN is mainly produced by immune cells (activated T cells, natural killer cells, and macrophages) and plays an important role in anti-tumor proliferation and cellular immunity [61, 62]. The low expression of type II IFN response and type I IFN response in the high-risk group may be due to an immunodeficiency of the tumor, which is present in a variety of tumors including breast cancer, melanoma, and gastrointestinal tumors [63]. Liver cancer cells all express MHC class I (MHC-I) antigens, but not in normal liver cells [64]. MHC-I plays an important role in controlling the phagocytosis of macrophages and can protect tumor cells from phagocytosis [65]. Differences in immune function create a favorable immune environment for cell proliferation and immune escape for HCC patients.

In our results, the GO enrichment analysis of the differential genes showed that the differential genes were mainly located in the extracellular matrix and chromosomal regions and may play regulatory roles in binding sites and catalytic enzymes, thereby affecting the chromosome division and cell proliferation of cells. In the high-risk group and the low-risk group, the most mutated genes were TP53, CTNNB1, TTN, and MUC16. About 11–41% of liver malignancies had CTNNB1 mutations, and 13–48% had TP53 mutations [66, 67]. CTNNB1 and TP53 mutations promoted glycolysis and cell proliferation through ALDOA phosphorylation [68]. It was worth noting that CTNNB1 and TP53 mutations were mutually exclusive, and the two mutations can cause different characteristics of HCC. HCC patients with CTNNB1 mutations had large tumors, well-differentiated, bile accumulation, and no inflammatory infiltration, while HCC patients with P53 mutations had poorly differentiated tumors, dense cells, and frequent vascular infiltration [69]. Our results also showed that in the high-risk group compared to the low-risk group, TP53 mutations increased and CTNNB1 decreased, which may mean that the patient's tumor cells had a worse differentiated and a higher risk of vascular invasion, which meant a worse prognosis.

We screened 14 potential therapeutic agents for HCC in our study. There were already some studies on these drugs. Navitoclax made liver cancer cells sensitive to sorafenib and regorafenib through a mitochondrial caspase-dependent mechanism [70]. However, the current problem was that due to the low binding affinity of Navitoclax and Mcl-1, the anti-cancer activity of Navitoclax was often weakened by the increased expression of Mcl-1 in HCC and other cancers [71]. In addition, the phase III clinical trials of veliparib combined with temozolomide in advanced HCC showed that it was well tolerated in patients with advanced HCC, but the patients did not show a significant survival benefit [72]. AICAR regulated the redox status of liver cancer cells through nuclear factor erythroid 2-related factor signaling pathway and AMP-activated protein kinase independent mechanism [73]. Akt inhibitor, as an ATP-competitive AKT kinase inhibitor, blocked the phosphorylation of downstream molecules of the AKT signaling pathway in a dose and time-dependent manner, inhibited the proliferation, and induces apoptosis of hepatoma cells [74, 75]. A-443654 was also an Akt inhibitor and has antitumor effects in various tumors [76, 77]. A-770041 was a potent Src family kinase (Lck and Src) inhibitor with antitumor activity in osteosarcoma [78]. The phase III, randomized clinical trial of motesanib in non-small cell lung cancer showed that its objective response rate was 60.1% [79]. In thyroid papilloma, the objective response rate was 14%. 67% of patients had stable disease [80]. AS601245 was a selective c-Jun-terminal kinase inhibitor, the strongly inhibits cell adhesion and migration, with antitumor potential [81, 82, 83]. All-trans retinoic acid (ATRA) was an active metabolite of vitamin A and played an important role in tumor cell proliferation, differentiation, and apoptosis [84]. AUY922, an inhibitor of heat shock protein 90, reduced the proliferation and viability of HCC cells in a dose-dependent manner [85]. Axitinib combined with radiotherapy for advanced HCC was well tolerated, with ORR of 66.7%, 1-year OS of 66.7%, and median PFS of 7.4 months [86]. AZ628 was a hydrophobic Raf-kinase inhibitor that may play a therapeutic role in breast cancer [87], adrenocortical carcinoma [88]. Saracatinib (AZD.0530) treatment abolished the activation of Fyn, down-regulated the Fyn/FAK/N-WASP signaling pathway in hepatic stellate cells, and significantly reduced the degree of CCl4-induced liver fibrosis in mice [89]. It was expected to be a therapeutic drug for liver fibrosis and HCC. Rucaparib, a poly (ADP-ribose) polymerase inhibitor, had been approved for the treatment of recurrent ovarian and prostate cancer, and clinical trial results had shown that moderate liver injury did not require dose adjustment [90]. Although many potential drugs for the treatment of HCC had been discovered through studies, we should also be aware that the mechanism of HCC development is very complex, and the effect of a single targeted drug was [91] not ideal. In the future, we should study the combination of different drugs to block the progression of HCC, to improve the overall survival of HCC patients.

There were also some limits in this study. Firstly, the samples of this study are from the TCGA database, the sample size of some groups may be small. For example, in Figure 15b, the Low-risk group seems to converge around year 7. This may be due to the smaller sample size of the high-TMB group in the low-risk group, especially 7 years later, no samples were included in the low-risk-high TMB group. Secondly, the risk score constructed by the study requires further validation by external validation and prospective studies. However, our study found the role of m6A-related lncRNAs in HCC prognosis and immunotherapy, established an effective risk score, and identified 14 potential therapeutic drugs for HCC, which is significant for further improving the prognosis of HCC patients.

6. Conclusion

The risk score constructed with NRAV and AL031985.3 had a good predictive effect on the Prognosis of HCC. Differences in genes and immune function between high-risk groups and low-risk groups promoted the occurrence and progression of HCC.

Declarations

Author contribution statement

Yan Xu: Conceived and designed the experiments; Performed the experiments; Analyzed and interpreted the data; Contributed reagents, materials, analysis tools or data; Wrote the paper.

Rong LIU: Conceived and designed the experiments; Contributed reagents, materials, analysis tools or data; Wrote the paper.

Funding statement

This research did not receive any specific grant from funding agencies in the public, commercial, or not-for-profit sectors.

Data availability statement

Data will be made available on request.

Declaration of interest's statement

The authors declare no conflict of interest.

Additional information

Data associated with this study has been deposited at Figshare under the URL https://doi.org/10.6084/m9.figshare.20575707.v1.

Acknowledgements

None.

References

[1] J. Ferlay, I. Soerjomataram, R. Dikshit, et al., Cancer incidence and mortality worldwide: sources, methods and major patterns in GLOBOCAN 2012, Int. J. Cancer 136 (5) (2015) E359–E386.
[2] F. Bray, J. Ferlay, I. Soerjomataram, et al., Global cancer statistics 2018: GLOBOCAN estimates of incidence and mortality worldwide for 36 cancers in 185 countries, CA A Cancer J. Clin. 68 (6) (2018) 394–424.
[3] M. Peck-Radosavljevic, S. Bota, F. Hucke, Time to stop using hepatic arterial infusion chemotherapy (HAIC) for advanced hepatocellular carcinoma?-the SCOOP-2 trial experience, Ann. Transl. Med. 8 (21) (2020) 1340.
[4] M. Tsurusaki, T. Murakami, Surgical and locoregional therapy of HCC: TACE, Liver Cancer 4 (3) (2015) 165–175.
[5] T. Couri, A. Pillai, Goals and targets for personalized therapy for HCC, Hepatol. Int. 13 (2) (2019) 125–137.
[6] E.G. Giannini, F. Farinati, F. Ciccarese, et al., Prognosis of untreated hepatocellular carcinoma, Hepatology 61 (1) (2015) 184–190.
[7] J.M. Llovet, S. Ricci, V. Mazzaferro, et al., Sorafenib in advanced hepatocellular carcinoma, N. Engl. J. Med. 359 (4) (2008) 378–390.
[8] A.L. Cheng, Y.K. Kang, D.Y. Lin, et al., Sunitinib versus sorafenib in advanced hepatocellular cancer: results of a randomized phase III trial, J. Clin. Oncol. 31 (32) (2013) 4067–4075.
[9] P.J. Johnson, S. Qin, J.W. Park, et al., Brivanib versus sorafenib as first-line therapy in patients with unresectable, advanced hepatocellular carcinoma: results from the randomized phase III BRISK-FL study, J. Clin. Oncol. 31 (28) (2013) 3517–3524.
[10] C. Cainap, S. Qin, W.T. Huang, et al., Linifanib versus Sorafenib in patients with advanced hepatocellular carcinoma: results of a randomized phase III trial, J. Clin. Oncol. 33 (2) (2015) 172–179.
[11] K. Ikeda, M. Kudo, S. Kawazoe, et al., Phase 2 study of lenvatinib in patients with advanced hepatocellular carcinoma, J. Gastroenterol. 52 (4) (2017) 512–519.
[12] M. Ikeda, C. Morizane, M. Ueno, et al., Chemotherapy for hepatocellular carcinoma: current status and future perspectives, Jpn. J. Clin. Oncol. 48 (2) (2018) 103–114.
[13] R. Desrosiers, K. Friderici, F. Rottman, Identification of methylated nucleosides in messenger RNA from Novikoff hepatoma cells, Proc. Natl. Acad. Sci. U. S. A. 71 (10) (1974) 3971–3975.
[14] C.R. Alarcon, H. Lee, H. Goodarzi, N. Halberg, S.F. Tavazoie, N6-methyladenosine marks primary microRNAs for processing, Nature 519 (7544) (2015) 482–485.
[15] D.P. Patil, C.K. Chen, B.F. Pickering, et al., m(6)A RNA methylation promotes XIST-mediated transcriptional repression, Nature 537 (7620) (2016) 369–373.
[16] U. Schumann, A. Shafik, T. Preiss, METTL3 gains R/W access to the epitranscriptome, Mol. Cell 62 (3) (2016) 323–324.
[17] S. Schwartz, M.R. Mumbach, M. Jovanovic, et al., Perturbation of m6A writers reveals two distinct classes of mRNA methylation at internal and 5' sites, Cell Rep. 8 (1) (2014) 284–296.
[18] J. Liu, Y. Yue, D. Han, et al., A METTL3-METTL14 complex mediates mammalian nuclear RNA N6-adenosine methylation, Nat. Chem. Biol. 10 (2) (2014) 93–95.
[19] K.D. Meyer, S.R. Jaffrey, Rethinking m(6)A readers, writers, and erasers, Annu. Rev. Cell Dev. Biol. 33 (2017) 319–342.
[20] X.L. Ping, B.F. Sun, L. Wang, et al., Mammalian WTAP is a regulatory subunit of the RNA N6-methyladenosine methyltransferase, Cell Res. 24 (2) (2014) 177–189.
[21] G. Zheng, J.A. Dahl, Y. Niu, et al., ALKBH5 is a mammalian RNA demethylase that impacts RNA metabolism and mouse fertility, Mol. Cell 49 (1) (2013) 18–29.
[22] G. Jia, Y. Fu, X. Zhao, et al., N6-methyladenosine in nuclear RNA is a major substrate of the obesity-associated FTO, Nat. Chem. Biol. 7 (12) (2011) 885–887.
[23] B.S. Zhao, I.A. Roundtree, C. He, Post-transcriptional gene regulation by mRNA modifications, Nat. Rev. Mol. Cell Biol. 18 (1) (2017) 31–42.
[24] S. Muller, M. Glass, A.K. Singh, et al., IGF2BP1 promotes SRF-dependent transcription in cancer in a m6A- and miRNA-dependent manner, Nucleic. Acids Res. 47 (1) (2019) 375–390.
[25] K.D. Meyer, S.R. Jaffrey, Rethinking m(6)A readers, writers, and erasers, Annu. Rev. Cell Dev. Biol. 33 (2017) 319–342.
[26] I.U. Haussmann, Z. Bodi, E. Sanchez-Moran, et al., m(6)A potentiates Sxl alternative pre-mRNA splicing for robust Drosophila sex determination, Nature 540 (7632) (2016) 301–304.
[27] S. Lin, J. Choe, P. Du, R. Triboulet, R.I. Gregory, The m(6)A methyltransferase METTL3 promotes translation in human cancer cells, Mol. Cell 62 (3) (2016) 335–345.
[28] J. Liu, M.A. Eckert, B.T. Harada, et al., m(6)A mRNA methylation regulates AKT activity to promote the proliferation and tumorigenicity of endometrial cancer, Nat. Cell Biol. 20 (9) (2018) 1074–1083.
[29] J.Z. Ma, F. Yang, C.C. Zhou, et al., METTL14 suppresses the metastatic potential of hepatocellular carcinoma by modulating N(6) -methyladenosine-dependent primary MicroRNA processing, Hepatology 65 (2) (2017) 529–543.
[30] M. Chen, L. Wei, C.T. Law, et al., RNA N6-methyladenosine methyltransferase-like 3 promotes liver cancer progression through YTHDF2-dependent posttranscriptional silencing of SOCS2, Hepatology 67 (6) (2018) 2254–2270.
[31] J.Z. Ma, F. Yang, C.C. Zhou, et al., METTL14 suppresses the metastatic potential of hepatocellular carcinoma by modulating N(6) -methyladenosine-dependent primary MicroRNA processing, Hepatology 65 (2) (2017) 529–543.
[32] F. Yang, J. Bi, X. Xue, et al., Up-regulated long non-coding RNA H19 contributes to proliferation of gastric cancer cells, FEBS J. 279 (17) (2012) 3159–3165.
[33] Z.Y. Xu, Q.M. Yu, Y.A. Du, et al., Knockdown of long non-coding RNA HOTAIR suppresses tumor invasion and reverses epithelial-mesenchymal transition in gastric cancer, Int. J. Biol. Sci. 9 (6) (2013) 587–597.
[34] W.J. Cao, H.L. Wu, B.S. He, Y.S. Zhang, Z.Y. Zhang, Analysis of long non-coding RNA expression profiles in gastric cancer, World J. Gastroenterol. 19 (23) (2013) 3658–3664.
[35] C. Xu, M. Yang, J. Tian, X. Wang, Z. Li, MALAT-1: a long non-coding RNA and its important 3' end functional motif in colorectal cancer metastasis, Int. J. Oncol. 39 (1) (2011) 169–175.
[36] X. Huang, Y. Gao, J. Qin, S. Lu, lncRNA MIAT promotes proliferation and invasion of HCC cells via sponging miR-214, Am. J. Physiol. Gastrointest. Liver Physiol. 314 (5) (2018) G559–G565.
[37] J. Chen, X. Huang, W. Wang, et al., LncRNA CDKN2BAS predicts poor prognosis in patients with hepatocellular carcinoma and promotes metastasis via the miR-153-5p/ARHGAP18 signaling axis, Aging (Albany NY) 10 (11) (2018) 3371–3381.
[38] J. Feng, G. Yang, Y. Liu, et al., LncRNA PCNAP1 modulates hepatitis B virus replication and enhances tumor growth of liver cancer, Theranostics 9 (18) (2019) 5227–5245.
[39] Y. Chao, D. Zhou, lncRNA-D16366 is a potential biomarker for diagnosis and prognosis of hepatocellular carcinoma, Med. Sci. Mon. Int. Med. J. Exp. Clin. Res. 25 (2019) 6581–6586.
[40] J. Ouyang, X. Zhu, Y. Chen, et al., NRAV, a long noncoding RNA, modulates antiviral responses through suppression of interferon-stimulated gene transcription, Cell Host Microbe. 16 (5) (2014) 616–626.
[41] Q. Xu, Y. Wang, W. Huang, Identification of immune-related lncRNA signature for predicting immune checkpoint blockade and prognosis in hepatocellular carcinoma, Int. Immunopharm. 92 (2021), 107333.
[42] Y. Feng, X. Hu, K. Ma, B. Zhang, C. Sun, Genome-wide screening identifies prognostic long noncoding RNAs in hepatocellular carcinoma, BioMed Res. Int. 2021 (2021), 6640652.
[43] Z.A. Chen, H. Tian, D.M. Yao, et al., Identification of a ferroptosis-related signature model including mRNAs and lncRNAs for predicting prognosis and immune activity in hepatocellular carcinoma, Front. Oncol. 11 (2021), 738477.
[44] Z.H. Wu, Z.W. Li, D.L. Yang, J. Liu, Development and validation of a pyroptosis-related long non-coding RNA signature for hepatocellular carcinoma, Front. Cell Dev. Biol. 9 (2021), 713925.
[45] P. Zhou, Y. Lu, Y. Zhang, L. Wang, Construction of an immune-related six-lncRNA signature to predict the outcomes, immune cell infiltration, and immunotherapy response in patients with hepatocellular carcinoma, Front. Oncol. 11 (2021), 661758.
[46] Y. Jia, Y. Chen, J. Liu, Prognosis-predictive signature and nomogram based on autophagy-related long non-coding RNAs for hepatocellular carcinoma, Front. Genet. 11 (2020), 608668.
[47] B. Deng, M. Yang, M. Wang, Z. Liu, Development and validation of 9-long Non-coding RNA signature to predicting survival in hepatocellular carcinoma, Medicine (Baltim.) 99 (21) (2020), e20422.
[48] W. Kong, X. Wang, X. Zuo, et al., Development and validation of an immune-related lncRNA signature for predicting the prognosis of hepatocellular carcinoma, Front. Genet. 11 (2020) 1037.
[49] L. Yin, L. Zhou, S. Gao, et al., Classification of hepatocellular carcinoma based on N6-methylandenosine-related lncRNAs profiling, Front. Mol. Biosci. 9 (2022), 807418.
[50] T. Dai, J. Li, L. Ye, et al., Prognostic role and potential mechanisms of N6-methyladenosine-related long noncoding RNAs in hepatocellular carcinoma, J. Clin. Transl. Hepatol. 10 (2) (2022) 308–320.
[51] M. Chen, L. Wei, C.T. Law, et al., RNA N6-methyladenosine methyltransferase-like 3 promotes liver cancer progression through YTHDF2-dependent posttranscriptional silencing of SOCS2, Hepatology 67 (6) (2018) 2254–2270.
[52] X. Zuo, Z. Chen, W. Gao, et al., M6A-mediated upregulation of LINC00958 increases lipogenesis and acts as a nanotherapeutic target in hepatocellular carcinoma, J. Hematol. Oncol. 13 (1) (2020) 5.
[53] X. Yang, S. Zhang, C. He, et al., METTL14 suppresses proliferation and metastasis of colorectal cancer by down-regulating oncogenic long non-coding RNA XIST, Mol. Cancer 19 (1) (2020) 46.
[54] L.J. Yang, Q. Tang, J. Wu, et al., Inter-regulation of IGFBP1 and FOXO3a unveils novel mechanism in ursolic acid-inhibited growth of hepatocellular carcinoma cells, J. Exp. Clin. Cancer Res. 35 (2016) 59.
[55] A. Adamek, A. Kasprzak, Insulin-like growth factor (IGF) system in liver diseases, Int. J. Mol. Sci. 19 (5) (2018).
[56] S. Booy, L. Hofland, C. van Eijck, Potentials of interferon therapy in the treatment of pancreatic cancer, J. Interferon Cytokine Res. 35 (5) (2015) 327–339.
[57] E.C. Borden, Interferons alpha and beta in cancer: therapeutic opportunities from new insights, Nat. Rev. Drug Discov. 18 (3) (2019) 219–234.
[58] H.M. Lazear, J.W. Schoggins, M.S. Diamond, Shared and distinct functions of type I and type III interferons, Immunity 50 (4) (2019) 907–923.
[59] G.P. Dunn, C.M. Koebel, R.D. Schreiber, Interferons, immunity and cancer immunoediting, Nat. Rev. Immunol. 6 (11) (2006) 836–848.
[60] A. Miar, E. Arnaiz, E. Bridges, et al., Hypoxia induces transcriptional and translational downregulation of the type I IFN pathway in multiple cancer cell types, Cancer Res. 80 (23) (2020) 5245–5256.
[61] M. Hagiwara, A. Fushimi, A. Bhattacharya, et al., MUC1-C integrates type II interferon and chromatin remodeling pathways in immunosuppression of prostate cancer, OncoImmunology 11 (1) (2022), 2029298.

[62] G.P. Dunn, C.M. Koebel, R.D. Schreiber, Interferons, immunity and cancer immunoediting, Nat. Rev. Immunol. 6 (11) (2006) 836–848.
[63] R.J. Critchley-Thorne, D.L. Simons, N. Yan, et al., Impaired interferon signaling is a common immune defect in human cancer, Proc. Natl. Acad. Sci. U. S. A. 106 (22) (2009) 9010–9015.
[64] C.H. Sung, C.P. Hu, H.C. Hsu, et al., Expression of class I and class II major histocompatibility antigens on human hepatocellular carcinoma, J. Clin. Invest. 83 (2) (1989) 421–429.
[65] A.A. Barkal, K. Weiskopf, K.S. Kao, et al., Engagement of MHC class I by the inhibitory receptor LILRB1 suppresses macrophages and is a target of cancer immunotherapy, Nat. Immunol. 19 (1) (2018) 76–84.
[66] C. Guichard, G. Amaddeo, S. Imbeaud, et al., Integrated analysis of somatic mutations and focal copy-number changes identifies key genes and pathways in hepatocellular carcinoma, Nat. Genet. 44 (6) (2012) 694–698.
[67] S.M. Ahn, S.J. Jang, J.H. Shim, et al., Genomic portrait of resectable hepatocellular carcinomas: implications of RB1 and FGF19 aberrations for patient stratification, Hepatology 60 (6) (2014) 1972–1982.
[68] Q. Gao, H. Zhu, L. Dong, et al., Integrated proteogenomic characterization of HBV-related hepatocellular carcinoma, Cell 179 (2) (2019) 561–577.
[69] J. Calderaro, G. Couchy, S. Imbeaud, et al., Histological subtypes of hepatocellular carcinoma are related to gene mutations and molecular tumour classification, J. Hepatol. 67 (4) (2017) 727–738.
[70] A. Tutusaus, M. Stefanovic, L. Boix, et al., Antiapoptotic BCL-2 proteins determine sorafenib/regorafenib resistance and BH3-mimetic efficacy in hepatocellular carcinoma, Oncotarget 9 (24) (2018) 16701–16717.
[71] G. Li, S. Zhang, H. Fang, et al., Aspirin overcomes Navitoclax-resistance in hepatocellular carcinoma cells through suppression of Mcl-1, Biochem. Biophys. Res. Commun. 434 (4) (2013) 809–814.
[72] A. Gabrielson, A.A. Tesfaye, J.L. Marshall, et al., Phase II study of temozolomide and veliparib combination therapy for sorafenib-refractory advanced hepatocellular carcinoma, Cancer Chemother. Pharmacol. 76 (5) (2015) 1073–1079.
[73] B. Sid, C. Glorieux, M. Valenzuela, et al., AICAR induces Nrf2 activation by an AMPK-independent mechanism in hepatocarcinoma cells, Biochem. Pharmacol. 91 (2) (2014) 168–180.
[74] F. Yang, R. Deng, X.J. Qian, et al., Feedback loops blockade potentiates apoptosis induction and antitumor activity of a novel AKT inhibitor DC120 in human liver cancer, Cell Death Dis. 5 (2014) e1114.
[75] M.C. Crouthamel, J.A. Kahana, S. Korenchuk, et al., Mechanism and management of AKT inhibitor-induced hyperglycemia, Clin. Cancer Res. 15 (1) (2009) 217–225.
[76] J. Zheng, A. Hudder, K. Zukowski, R.F. Novak, Rapamycin sensitizes Akt inhibition in malignant human breast epithelial cells, Cancer Lett. 296 (1) (2010) 74–87.
[77] M. de Frias, D. Iglesias-Serret, A.M. Cosialls, et al., Akt inhibitors induce apoptosis in chronic lymphocytic leukemia cells, Haematologica 94 (12) (2009) 1698–1707.
[78] Z. Duan, J. Zhang, S. Ye, et al., A-770041 reverses paclitaxel and doxorubicin resistance in osteosarcoma cells, BMC Cancer 14 (2014) 681.
[79] K. Kubota, H. Yoshioka, F. Oshita, et al., Phase III, randomized, placebo-controlled, double-blind trial of motesanib (AMG-706) in combination with paclitaxel and carboplatin in east asian patients with advanced nonsquamous non-small-cell lung cancer, J. Clin. Oncol. 35 (32) (2017) 3662–3670.
[80] S.I. Sherman, L.J. Wirth, J.P. Droz, et al., Motesanib diphosphate in progressive differentiated thyroid cancer, N. Engl. J. Med. 359 (1) (2008) 31–42.
[81] A. Cerbone, C. Toaldo, R. Minelli, et al., Rosiglitazone and AS601245 decrease cell adhesion and migration through modulation of specific gene expression in human colon cancer cells, PLoS One 7 (6) (2012), e40149.
[82] C. Bubici, S. Papa, JNK signalling in cancer: in need of new, smarter therapeutic targets, Br. J. Pharmacol. 171 (1) (2014) 24–37.
[83] Q. Wu, W. Wu, V. Jacevic, et al., Selective inhibitors for JNK signalling: a potential targeted therapy in cancer, J. Enzym. Inhib. Med. Chem. 35 (1) (2020) 574–583.
[84] X. Ni, G. Hu, X. Cai, The success and the challenge of all-trans retinoic acid in the treatment of cancer, Crit. Rev. Food Sci. Nutr. 59 (sup1) (2019) S71–S80.
[85] G. Augello, M.R. Emma, A. Cusimano, et al., Targeting HSP90 with the small molecule inhibitor AUY922 (luminespib) as a treatment strategy against hepatocellular carcinoma, Int. J. Cancer 144 (10) (2019) 2613–2624.
[86] K.L. Yang, M.S. Chi, H.L. Ko, et al., Axitinib in combination with radiotherapy for advanced hepatocellular carcinoma: a phase I clinical trial, Radiat. Oncol. 16 (1) (2021) 18.
[87] S.M. Hossain, J. Shetty, K.K. Tha, E.H. Chowdhury, Alpha-ketoglutaric acid-modified carbonate apatite enhances cellular uptake and cytotoxicity of a Raf-kinase inhibitor in breast cancer cells through inhibition of MAPK and PI-3 kinase pathways, Biomedicines 7 (1) (2019).
[88] C. Ma, J. Xiong, H. Su, H. Li, The underlying molecular mechanism and drugs for treatment in adrenal cortical carcinoma, Int. J. Med. Sci. 18 (13) (2021) 3026–3038.
[89] G. Du, J. Wang, T. Zhang, et al., Targeting Src family kinase member Fyn by Saracatinib attenuated liver fibrosis in vitro and in vivo, Cell Death Dis. 11 (2) (2020) 118.
[90] N. Grechko, V. Skarbova, M. Tomaszewska-Kiecana, et al., Pharmacokinetics and safety of rucaparib in patients with advanced solid tumors and hepatic impairment, Cancer Chemother. Pharmacol. 88 (2) (2021) 259–270.
[91] W. Cheng, A. Ainiwaer, L. Xiao, et al., Role of the novel HSP90 inhibitor AUY922 in hepatocellular carcinoma: potential for therapy, Mol. Med. Rep. 12 (2) (2015) 2451–2456.